International Conference
On

MECHANICAL AND INDUSTRIAL ENGINEERING

16th December, 2012
Nagpur

Editor-in-Chief
Dr. Rajendrakumar G Patil

Organized by:
INSTITUTE FOR RESEARCH AND DEVELOPMENT INDIA
IRD INDIA
Bhubaneswar, Odisha, India

Proceedings

Of

International Conference
On

Mechanical and Industrial Engineering

(ICMIE)

16th December, 2012
Nagpur

Editor-in-Chief
Dr. Rajendrakumar G Patil
Professor and Head of Department
Department of Mechanical Engineering
Atria Institute of Technology, Bangalore
Email- drrgp.atria@gmail.com

Organized By:

Institute for Research and Development India (IRD India)
Bhubaneswar, Odisha

About :: ICMIE

The main objective of International Conference on Mechanical and Industrial Engineering (ICMIE 2012) is to provide a platform for the researchers, engineers, academicians as well as industrial professionals from all over the world to present their research results and development activities in mechanical Engineering.

This conference provides opportunities for the delegates to exchange new ideas and application experiences face to face, to establish business or research relations and to find global partners for future collaboration.

Topics of interest for submission include, but are not limited to:

Mechanical Engineering
Acoustics and Noise Control
Aerodynamics
Applied Mechanics
Automation, Mechatronics and Robotics
Automobiles
Automotive Engineering
Ballistics
Biomechanics
Biomedical Engineering
CAD/CAM/CIM
CFD
Composite and Smart Materials
Compressible Flows
Computational Mechanics
Computational Techniques
Dynamics and Vibration
Energy Engineering and Management
Engineering Materials
Fatigue and Fracture
Fluid Dynamics
Fluid Mechanics and Machinery
Fracture
Fuels and Combustion
General mechanics
Geomechanics
Health and Safety
Heat and Mass Transfer
HVAC
Instrumentation and Control
Internal Combustion Engines
Machinery and Machine Design
Manufacturing and Production Processes
Marine System Design
Material Engineering
Material Science and Processing

Mechanical Design
Mechanical Power Engineering
Mechatronics
MEMS and Nano Technology
Multibody Dynamics
Nanomaterial Engineering
New and Renewable Energy
Noise and Vibration
Noise Control
Non-destructive Evaluation
Nonlinear Dynamics
Oil and Gas Exploration
Operations Management
PC guided design and manufacture
Plasticity Mechanics
Pollution and Environmental Engineering
Precision mechanics, mechatronics
Production Technology
Quality assurance and environment protection
Resistance and Propulsion
Robotic Automation and Control
Solid Mechanics
Structural Dynamics
System Dynamics and Simulation
Textile and Leather Technology
Transport Phenomena
Tribology
Turbulence
Vibrations

Organizing Committee

Chief Patron:

Prof. Pradeep Kumar Mallick
Chairman
Institute for Research and Development India
Bhubanesawr, India
Emai;: chairman.irdindia@gmail.com

Programme Chair

Dr. Rajendrakumar G Patil
Professor and Head of Department
Department of Mechanical Engineering
Atria Institute of Technology, Bangalore
Email- drrgp.atria@gmail.com

Programme Committee Members:

Prof. Dipti Prasad Mishra
(M.Tech., Ph.D, Thermal Engg. (IIT, Kharagpur))
Associate Professor & HOD
Institute of Technical Education & Research
Jagamohan Nagar, Khandagiri
Bhubaneswar – 751030, India
Email: diptimishra@iter.ac.in

Zaki Ahmad
Department of Mechanical Engineering,
KFUPM,Box # 1748, Dhaharan 31261 Saudi Arabia

Rajeev Ahuja
Physics Department,Uppsala University,
Box 530, 751 21 Uppsala Sweden

B.T.F. Chung
Department of Mechanical Engineering, University of Akron, Akron,
Ohio 44325 USA

S.Z. Kassab
Mechanical Engineering Department,
Faculty of Engineering, Alexandria
University, Alexandria, 21544 Egypt

Prof. Daniel Benevides da Costa
Federal University of Ceara (UFC)
Brazil

Prof. A.Cagatay Talay
Istanbul Technical University
Turky

Ashraf Shikdar
Department of Mechanical & Industrial Engineering,
S.Q. University,P.O Box 33, Al-Khod 123 Oman

Conference Coordinator

Er. Sushree Mohanty
Email:sushree.irdindia@gmaoil.com

Team IRD India

Mr. Bibhu Prasad Mohanty
Director, IRD India
Email: director.irdindia@gmail.com

Er. Puranjay Sahu
Secretary, IRD India
Email: secretary.irdindia@gmail.com
Mob: +91-9438737508

Er. Asish Patro
Head (System & Utilities), IRD India
Email: system.irdindia@gmail.com

Prof. Subhashree Rout
Technical Editor, IRD India
Email: subhashree.irdindia@gmail.com

Miss Pritika Mohanty
Email: icikm.bangalore@gmail.com

Miss Ujjayinee Swain
Miss Swagatika Satapathy
Er. Ratikant Maharana

Proceedings of International Conference On

MECHANICAL AND INDUSTRIAL ENGINEERING

DISCLAIMER

The authors are solely responsible for the contents of the papers complied in this volume. The publishers or editors do not take any responsibility for the same in any manner. Errors, if any, are purely unintentional and readers are requested to communicate such errors to the editors or publishers to avoid discrepancies in future.

ISBN Number : 978-93-81693-88-2

Published by :

INSTITUTE FOR RESEARCH AND DEVELOPMENT INDIA (IRD INDIA),
Plot No. : L/293, Rasulgarh, Bhubaneswar, Odisha

TABLE OF CONTENTS

Sl. No.	Title and Authors	Page No.
	Editor-in-Chief – *Dr. Rajendrakumar G Patil*	
1	**Design, Analysis and Simulation of a Composite Bulkhead** – *R.Arravind, M.Saravanan, R.Santhanakrishnan, R.Mohamed Rijuvan & D.Vadivel*	01-04
2	**Solar Stills with Condenser-Analytical Simulation Combined with Experimental and Thermal Performance Analysis** – *A. Maria Infant Tom & K. Vasanth*	05-10
3	**Case Depth Prediction by Dynamic Response Studies Using Laser Doppler Vibrometry** – *Husain Kanchwala, Mohan Misra & Bishakh Bhattacharya*	11-18
4	**Study on Effects of Heat Treatment on Grain Refined 319 Aluminum Alloy With Mg and Sr Addition** – *S. Gopi Krishna & Binu. C. Yeldose*	19-22
5	**Enterprise Resource Planning Implementation in Small and Medium Enterprises** – *M. S. Tufail & S. P. Untawale*	23-26
6	**Design and Improvement of Plant Layout** – *Ram D. Vaidya & Prashant N. Shende*	27-30
7	**A Suggested Stress Analysis Procedure for Nozzle to Head Shell Element Model – A Case Study** – *Sanket S. Chaudhari & D.N. Jadhav*	31-36
8	**FEA of Rectangular Cup Deep Drawing Process** – *Awad D.S., Poul A.D., Wankhede U.P. & V. M. Nandedkar*	37-40
9	**To Improve Productivity By Using Work Study & Design A Fixture In Small Scale Industry** – *Mayank Dev Singh, Shah Saurabh K, Patel Sachin B, Patel Rahul B & Pansuria Ankit P*	41-46
10	**Enhance Production Rate of Braiding Machine Using Speed Reduction Technique** – *Manoj A. Kumbhalkar, Sachin V. Mate, Sushama Dhote & Mudra Gondane*	47-51
11	**Optimization of Blank Holding Force in Deep Drawing Process Using Friction Property of Steel Blank** – *Prasad S. Pandhare, Vipul U. Mehunkar, Ashish S. Joshi, Amruta M. Kirde & V. M. Nandedkar*	52-56

12 **Passive Control Systems for Tall Structures** 57-61

– *Shreyas Kulkarni, Dattatray Jadhav & Pravin Khadke*

13 **Trouble Shooting in Vertical Fire Hydrant Pump by Vibration Analysis - A Case Study** 62-66

– *V. G. Arajpure & H. G. Patil*

14 **LEFM Analysis of Edged Crack Plate by Analytical and FEA Approach** 67-71

– *Swapnil Marwadi, Dattatray Jadhav & Nikhil Patil*

Editorial

In the Race of Scientific Civilization and Engineering Development Mechanical Engineering appears to be the oldest and broadest discipline. Till date it has accomplished many efficient mechanical systems using advanced practices of material science and Structural Analysis. As a matured academic discipline it has become an integrated component of Industrial Revolution. It has surpassed an odyssey of two centuries since its emergency in Europe. The basic philosophy although integrates two highlighting disciplines like Physics and Material Sciences but over the years it has developed its linkage with other domains like Composites, Mechatronics and Nanotechnology. Today's Mechanical Engineers uses the core principles with some sophisticated tools like Computer Aided Designing, and Product Life Cycle Management. These tools are also employed in Aerospace Engineering, Civil Engineering, Petroleum Engineering and Chemical Engineering, Aircraft, Watercraft, Robotics and Medical Devices.

In the advent of modern research there is a significant growth in Mechanical Engineering as Computer Aided Design has become instrumental in many industrialized nations like USA, European Countries, Scotland and GermOther CAE programs commonly used by mechanical engineers include product lifecycle management (PLM) tools and analysis tools used to perform complex simulations. Analysis tools may be used to predict product response to expected loads, including fatigue life and manufacturability. These tools include Finite Element Analysis (FEA), Computational Fluid Dynamics (CFD), and Computer-Aided Manufacturing (CAM). Using CAE programs, a mechanical design team can quickly and cheaply iterates the design process to develop a product that better meets cost, performance, and other constraints. No physical prototype need be created until the design nears completion, allowing hundreds or thousands of designs to be evaluated, instead of a relative few. In addition, CAE analysis programs can model complicated physical phenomena which cannot be solved by hand, such as viscoelasticity, complex contact between mating parts, or non-Newtonian flows.

As mechanical engineering begins to merge with other disciplines, as seen in mechatronics, multidisciplinary design optimization (MDO) is being used with other CAE programs to automate and improve the iterative design process. MDO tools wrap around existing CAE processes, allowing product evaluation to continue even after the analyst goes home for the day. They also utilize sophisticated optimization algorithms to more intelligently explore possible designs, often finding better, innovative solutions to difficult multidisciplinary design problems.

Apart from Industrial Development there is also an hourly need for creation of an influential professional body which can cater to the need of research and academic community. The current scenario says there existsd a handfull of bodies like American Society of Mechanical Engineers (ASME). Hence we must strive towards formation of a harmonious professional research forum committed towards discipline of Mechanical Engineering.

The conference is designed to stimulate the young minds including Research Scholars, Academicians, and Practitioners to contribute their ideas, thoughts and nobility in these two integrated disciplines. Even a fraction of active participation deeply influences the

magnanimity of this international event. I must acknowledge your response to this conference. I ought to convey that this conference is only a little step towards knowledge, network and relationship.

I congratulate the participants for getting selected at this conference. I extend heart full thanks to members of faculty from different institutions, research scholars, delegates, IRD Family members, members of the technical and organizing committee. Above all I note the salutation towards the almighty

Editor-in-Chief

Dr. Rajendrakumar G Patil
Professor and Head of Department
Department of Mechanical Engineering
Atria Institute of Technology, Bangalore
Email- drrgp.atria@gmail.com

Design, Analysis and Simulation of a Composite Bulkhead

R.Arravind[1], M.Saravanan[2], R.Santhanakrishnan[3], R.Mohamed Rijuvan[4] & D.Vadivel[5]

[1&4]Department of Aeronautical Engineering, Excel College of Engineering & Technology, Tamil Nadu, India
[2]SBM College of Engineering & Technology, Tamil Nadu, India
[3]Department of Aeronautical Engineering, SNS College of Technology, Coimbatore
[5]Aeronautical Engineering, Er.P.M.C Tech, Tamil Nadu, India
E-mail : arravind_r@rediffmail.com[1], drmsaravanan@yahoo.com[2], sanskrish@gmail.com[3], rijuvanaero09@gmail.com[4], vadivelaero@gmail.com[5]

Abstract – This paper presents an approach to "Design and Analysis of a composite Bulkhead for an aircraft "made out of advanced composites materials using advanced CAE tools and techniques. First, the property of material was obtained on the basis of some assumptions (i.e., Rule of Mixture and volume fraction). The model of the bulkhead structure is designed with the help of Catia V5R20 software and then the designed model is undergoing engineering simulation programmed which is based on the finite element method like Ansys or Nastran. In this analysis, problems with multiple laminated orientations are modeled by associating the geometry defining each component with the appropriate material model and specifying component interaction. Besides that, the load increments and convergence tolerance are continually adjusted to ensure an accurate solution is obtained. During the loading conditions like tensile load and compressive load, the maximum strain, stress and displacement were obtained.

Keywords – *bulkhead , pressurization , stress, strain, failure modes , composite materials*

I. INTRODUCTION

A bulkhead is an upright wall within the hull of the fuselage of an airplane. Other kinds of partition elements within a ship are decks and deck heads. The basic fuselage structure is essentially a single cell thin walled tube with many transverse frames called bulkhead and longitudinal stringers to provide a combined structure which can absorb and transmit the many concentrated and distributed applied forces safely and efficiently. The present study focusing on the optimizing the natural orientation for bulkhead which is made up of composite materials by using Finite Element Method (FEM). The study also includes the deformation, stress, failure criteria for different applied loads. Designing an aircraft can be an overwhelming task for a new designer. The designer must determine where the wing goes, how big to make the fuselage, and how to put all the pieces together. A sound choice of the general arrangement of a new aircraft design should be based on a proper investigation into and interpretation of the transport function and a translation of the most pertinent requirements into a suitable positioning of the major parts in relation to each other. No clear-cut design procedure can be followed and the task of devising the configuration is therefore a highly challenging one to the resourceful designer [1][2]. Several researches of fuselage structure have been conducted to get a good configuration of the aircraft. Marco et al. [3] showed a design and analysis of composite fuselage structure in order to reduce the weight of the fuselage. It presented a new methodology developed for an analytical model of a composite fuselage. It also presented finite element analysis of a simplified model and comparisons with more complete model. This comparison assesses the weight reduction obtained with the use of composite materials for designing fuselage. Further, From the study, we concluded that various loads will be applied to be carried out for the present study model.

A. Semi Monocoque Construction:

Semi monocoque fuselage design (Fig. 1) usually uses combination of longerons, stringers, bulkheads, and frames to reinforce the skin and maintain the cross sectional shape of the fuselage. The skin of the fuselage is fastened to all this members in order to resists shear load and together with the longitudinal members, the tension and bending load. In this design structure, fuselage bending load are taken by longerons which are supplemented by other longitudinal members known as stringers. Stringers are smaller and lighter than longerons. They provide rigidity to the fuselage in order to give shape and attachment to the skin. Stringer and longerons are essential to prevent tension and compression stress from bending the fuselage. The

fuselage skin thickness varies with the load carried and the stresses sustain at particular location. Moreover, bulkheads are used where concentrated loads are introduced into the fuselage, such as those at wing, landing gear, and tail surface attach points. Frames are used primarily to maintain the shape of the fuselage and improve the stability of the stringers in compression. The benefits of semi monocoque design is it overcome the strength to weight problem occurred in monocoque construction.

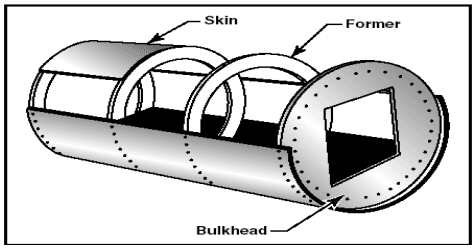

Fig. 1 : Semi-monocoque construction

II. LITERATURE SURVEY

Benjamin F. Ruffner [1] made an investigation to determine the possibility of using the photo elastic method for the stress analysis of bulkhead in monocoque structures. Tests of circular ring models were made to determine the effect of the skin thickness on the model results. The skin effects are eliminated for the study. The results indicate that the photoelastic method is quite accurate. The method is recommended for use where bulkheads with a large number of redundancies are present.

Ferhun C. Caner et al.,[3] made a study about the size effect on strength of laminate-foam sandwich plates using Finite element analysis with interface fracture. Zero-thickness interface elements with a softening cohesive law are used to model fractures at the skin–foam interface, in the fiber composite skins, and in the foam. The fracture energy and fracture process zone length of a shear crack in foam near the interface are deduced by fitting an analytical expression for size effect to the test data. Numerical simulations reveal that small-size specimens with notches just under the top skin develop plastic zones in the foam core near the edges of the loading platen, and that small-size specimens with notches just above the bottom skin develop distributed quasi brittle fracture in the foam core under tension. Both phenomena, though, are found to reduce the maximum load by less than 6%. Further it is shown that, in notch-less beams, the interface shear fracture is coupled with compression crushing of the fiber–polymer composite skin. For small specimens this mechanism is important because, when it is blocked in simulations, the maximum load increases. The size effect law for notch-less beams is calibrated such that beams of all sizes fail solely by interface shear fracture.

Seth S. Kessler et al.,[8] focused on the Design, Analysis and Testing of a High-g Composite Fuselage Structure. The aft section of the vehicle is not only subjected to high impulsive inertial loads, but its weight has a substantial effect on the controllability of the vehicle. Finite element models of this section as well as hand lay-up test specimens were produced to optimize the design. These specimens were tested statically as well as in a dynamic environment.

Priyadarsini.R.S. et al.,[7] carried out the Numerical and Experimental Study of Buckling of Advanced Fiber Composite Cylinders under axial compression. The thin-walled structures are susceptible to buckling when subjected to static and dynamic compressive stresses. In this study the details of a numerical (FEM) and an experimental study on buckling of carbon fiber reinforced plastics (CFRP) layered composite cylinders under displacement and load controlled static and dynamic axial compression are reported. The effects of different types of loadings, geometric properties, lamina lay-up and amplitudes of imperfection on the strength of the cylinders under compression are studied. It is shown that the buckling behavior of thin composite cylindrical shells can be evaluated accurately by modeling measured imperfections and material properties in FEM.

III. FLOW CHART

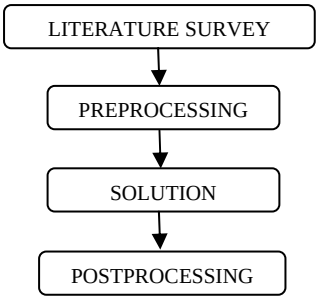

Fig.1 : Flow Chat

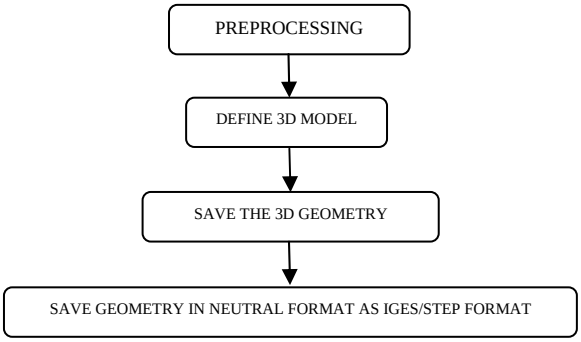

Fig. 1.1: Flow Chat

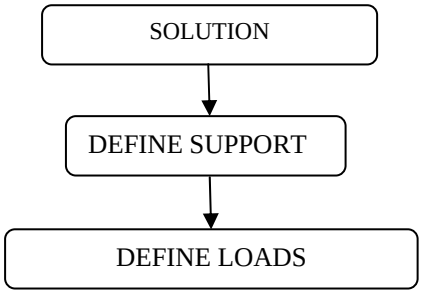

Fig.1.2 : Flow Chat

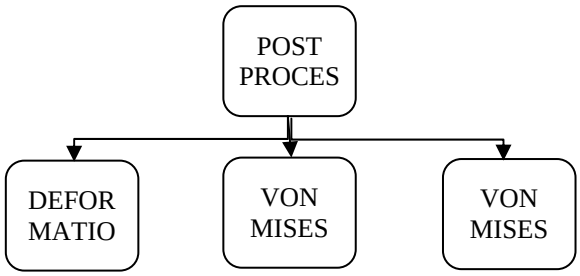

Fig.1.3 : Flow Chart

IV. DESIGN METHODOLOGY

1. Define Geometry : First of all, we have to define the geometry and dimension for the bulkhead. With the help of obtained geometry, we have to design 3D model of the fuselage bulkhead with the help of CAD Package softwares like Pro/E, Catia and NX CAD. After model has been designed, we have to save the modeled design in the common format like IGES or STEP.
2. For Analysis of bulkhead, here we are using Ansys Workbench V12.0.1, this analysis can be also done with the help Nastran software too.
3. Meshing has been done for the designed model, here we used tetrahydral element type for dividing the model into small number of elements.

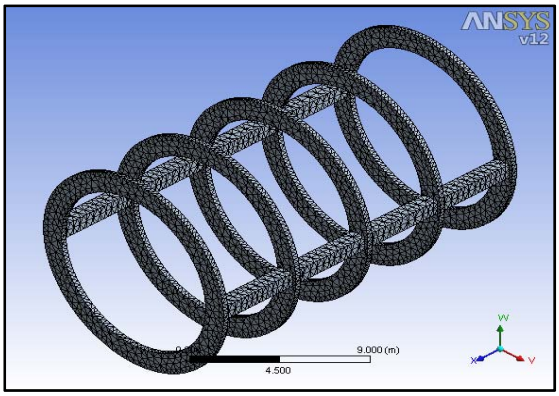

4. We have define the fixed support and pressure load acting on the bulkhead. Here we use pressure as 50N .

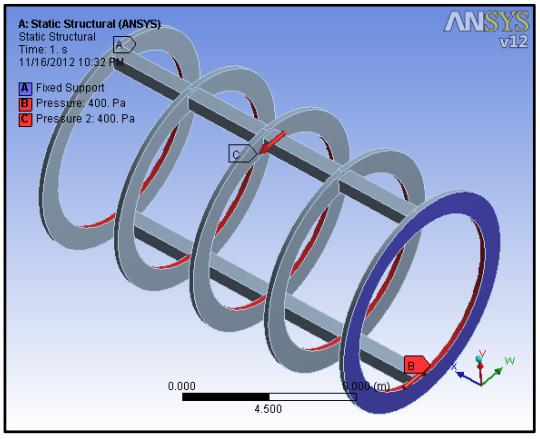

5. Then we have to select the result what are all we need for further studies like deformation, stress and strain

V. RESULTS AND DISCUSSION

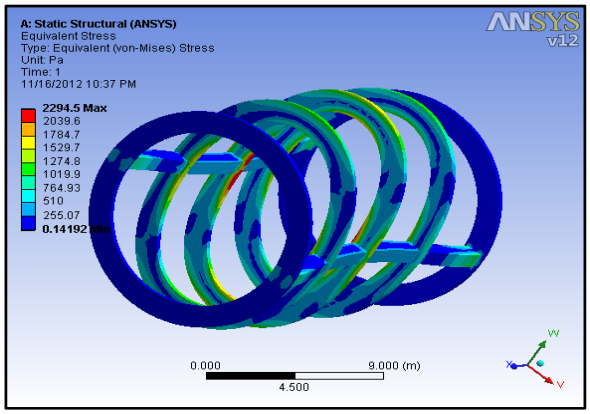

Fig. 2 : Von Mises Stress

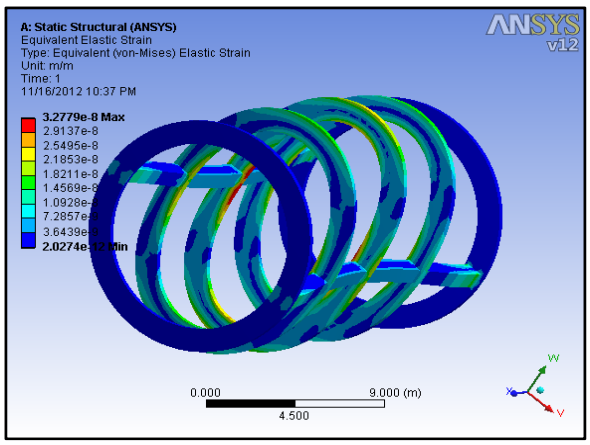

Fig.3 : Von Mises Strain

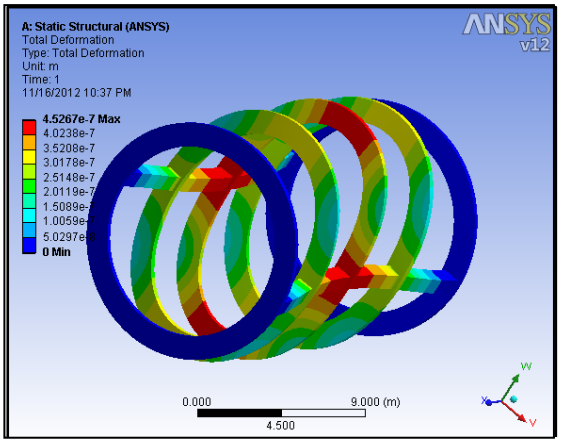

Fig.4 : Deformation

From the finite element analysis, the deformations and magnitudes of normal stresses meridional and circumferential) were obtained. The displacement contour is shown. The maximum displacement of 0.00045 mm was observed on the dome near the shoulder and cutout region. The stress contours were extracted for the composite parts. In the dome region, the maximum normal stresses in meridional and circumferential direction were nearly equal with a magnitude of 2294 MPa, showing a pure membrane action. The failure indices were calculated from the stress output of the analysis based on the Yamada-Sun failure criteria given below.

$$\sqrt{\left[\frac{\sigma_{11}}{S_L}\right]^2 + \left[\frac{\tau_{12}}{S}\right]^2} \leq 1.0$$

Where,

σ_{11} - Normal stress in lamina along fiber direction

S_L - Shear Stress in lamina

τ_{12} - Allowable stress in lamina along fiber direction

S - Allowable in-plane shear stress in lamina

The maximum failure index observed for the pressure bulkhead was 0.83. the failure index values were less than 1 for the various resions of the bulkhead, thus showing the adequacy of design from the strength point view. The analysis for the other load cases was carried through an integrated analysis with the fuselage of the aircraft. Safety of the composite bulkhead was ensured through these analyses prior to the detailed design and fabrication of the part.

VI. CONCLUSION

The primary goal of this research work to identify the action initiatives that make up and the implementation of existing bulkhead design and the initiation of new bulkhead design and procedures. The aim of this project is to design an advanced for future aviation, no more drills need to take power supply from cockpit. Whereas in this methodology we can take output where ever we needed. If the proposal gets admitted surely this method will be more reliable for bulkhead design as well as aircraft wiring system. In the occasion of this work reported to future aviation development. At end of this project we can able to safe thousands of hearts without any injury and much research has been done on the subject of bulkhead design. Some of more publicized techniques are not achieved design in bulkheads. Still lacking with combination of aircraft electrical wiring and bulkhead but this proposal will get succeed. End of this proposal will get admitted. Surely this method will be more reliable for bulkhead design as well as aircraft wiring system.

REFERENCE

[1] Benjamin F. Ruffner, “Stress Analysis of Monocoque Fuselage Bulkheads by the Photoelastic Method”, Oregon State College, December 1942(870)

[2] Bauchau et al., “Torsional Buckling Analysis and Damage Tolerance of Graphite/Epoxy Shafts” Journal of Composite Materials, vol. 22 – March 1988.

[3] C.Cerulli et al.,”Parametric Modeling of Aircraft Families for Load Calculation Support”, American Institute of Aeronautics and Astronautics

[4] Bruhn.E.F., ”Analysis and Design of Flight Vehicle Structures”,

[5] Hu.H.T., “ Buckling Optimization of fiber-composite Laminate shells with Large Deformation” National Center for Composite Materials Research, University of Illinois.

[6] Hu.H.T., “ Buckling Optimization of fiber-composite Laminate shells considering in-plane shear nonlinearity” Springer- verlag 1994, Structural Optimization 8, 168-173.

◈◈◈

Solar Stills with Condenser-Analytical Simulation Combined with Experimental and Thermal Performance Analysis

A. Maria Infant Tom & K. Vasanth

Mechanical Dept., Thiagarajar College of Engineering, Madurai
E-mail : avemariamit@gmail.com, vasanthleyo@gmail.com

Abstract – The increasing need for fresh water for domestic and industrial use triggered the need for new techniques to produce potable water at reduced cost. Solar thermal energy being renewable and eco-friendly source of energy is being utilized for the process. A single slope solar still is used to convert brackish water into pure form making use of solar irradiance. Various experiments are being done to increase the production rate of the still and here a modification from basic construction of the still were a condenser is attached behind the basin was fabricated and its performance was studied. Experiments were carried out from 9 hrs to 17 hrs on June 12,2012 in two single slope solar stills of various heights with condenser, fabricated and the water depth was maintained at 1 cm and also constant replacement of the evaporated water was maintained. Desalinated water production was measured for every hour and also cumulative calculations were done. Output from experiments revealed that the production rate and thus the efficiency of the system had increased as more condensation occurs in the condenser surface due to purging of water vapour. The output parameters were compared with theoretical simulation done using MatLab and thermal analysis using CFD and found to have close resemblance. Also water in the condenser can be used as preheated water in the basin and hence production rate can be increased. Hence use of condenser increases the productivity of the still.

Keywords – *Desalination, purging, preheat.*

I. INTRODUCTION

Most of these countries which are characterized by a high intensity of solar radiation make the direct use of solar energy a promising option for their arid communities to reduce the major operating cost for the distillation plant. Solar distillation is one of the available methods to produce potable water.

The sun's energy heats water to the point of evaporation. As the water evaporates, water vapor rises, condensing on the glass surface for collection. This process removes impurities such as salts and heavy metals, and destroys microbiological organisms. The end result is water cleaner than the purest rainwater. The use of solar energy is more economical than the use of fossil fuels in remote areas having low population densities, low rainfall and abundant available solar energy. The productivity of fresh water by solar distillation depends drastically on the intensity of solar radiation, the sunshine hours and the type of the still.

Single slope solar stills are considered one of the cheapest solutions for fresh water production. However, the amount of distilled water produced per unit area is somewhat low which makes the single-basin solar still unacceptable in some instances. Hence many steps are being made to enhance the productivity of the still.

II. THEORETICAL MODELING:

The energy available for utilization by the still is given by the amount of transmitted energy inside the glass cover. Kalidasa and Srithar [1] made theoretical study on the performance of solar still and the theoretical modeling was studied.

Transmittance (τ):

$$\tau = 0.859 + [2.417\times10^{-7}\times(90-\theta)^2] - [5.204\times10^{-3}\times K_d \times d] + (0.095\times K_d^2) + (0.029\times K_d) + [3.837\times10^{-4}(90-\theta)\times d] - (3.299\times10^{-3}\times d^2) - (0.028\times d) + [9.117\times10^{-4}\times(90-\theta)] + [1.005\times10^{-4}\times(90-\theta)\times K_d] \quad (1)$$

where θ can be found from the following equation :

$$\mathrm{Cos}\,\theta = Sin\,\delta Sin(\varphi - \beta) + Cos\,\delta Cos(\varphi - \beta)Cos\,\omega \quad (2)$$

From the above equations the transmittance of the glass was found to be between 0.86 to 0.96 at different times of a day.

For the given shallow stills, the basin bottom surface and water temperatures were similar. The basin water surfaces continuously absorb the solar radiation and part of it is transferred to the glass surface due to convection and radiation due to temperature difference. The remaining is transferred to the glass by evaporation due to the partial vapour pressure difference.

The transient energy balance equation for the basin water using [1] is:

$$(m_w C_{p,w} + m_{wm} C_{p,wm}) dT_w/dt = Q_t \alpha_{b,w} - Q_{c,w-g} - Q_{r,w-g} - Q_{e,w-g} - Q_b \quad (3)$$

The convective heat transfer from the basin to the cover plate is calculated using[1]

$$Q_{c,w-g} = h_{c,w-g} A_b (T_w - T_g) \quad (4)$$

Where $h_{c,w-g} = 0.884[(T_w - T_g) + \frac{(p_w - p_g)(T_w + 273.15)}{268900 - p_w}$ (5)

The partial pressure of water vapour in air in N/m^2 , is estimated for a given temperature (^oC)by

$$p = 7235 - 431.43T + 10.76\ T^2 \quad (6)$$

The evaporative heat transfer from the basin water to the cover plate is found using [1]

$$Q_{e,w-g} = h_{e,w-g} A_b (p_w - p_g) \quad (7)$$

Where the evaporative heat transfer coefficient is given by[1]

$$h_{e,w-g} = \frac{M_w h_{fg} p_r}{M_a C_{pa} (p_T - p_w)(p_T - p_g)} h_{c,w-g} \quad (8)$$

The latent heat of evaporation of water in J/kg at a given basin water temperature (^oC) is found by [1]

$$h_{fg} = (2503.3 - 2.398 \times T) \times 1000 \quad (9)$$

The specific heat capacity of the air inside the still is in J/kgK is calculated using the following equation in terms of average temperature between glass cover and water surface is given by [1]

$$C_{p.a} = 999.2 + 0.14339 \times T_{av} + 0.0001101\ T_{av}^2 \quad (10)$$

The radiation heat transfer from the basin to glass cover is found by[1]

$$Q_{r,w-g} = \sigma \in_{w,g} A_b [(T_w + 273.15)^4 - (T_g + 273.15)^4] \quad (11)$$

The heat loss from the basin to the surrounding is given by [1]

$$Q_b = U A_s (T_w - T_a) \quad (12)$$

The convective heat transfer occurs when the evaporated water vapour condenses and transfers it to the glass cover and is given by [1]

$$Q_{g,c-a} = h_{g,c-a} A_g (T_g - T_a) \quad (13)$$

$$\text{where } h_{g,c-a} = 5.7 + 3.8\ V \quad (14)$$

The instantaneous water production of the still is given by[1]

$$m_e = Q_{e,w-g} / h_{fg} \quad (15)$$

The overall production of the still

$$= \sum m_e(t) \Delta t \quad (16)$$

III. EXPERIMENTAL SETUP:

System 1:

A basin type single slope solar still fabricated with aluminium with overall size of 1.2 m × 1 m.All the sides of the basin was covered with glass wool, a good insulator to minimize the heat loss from the basin.The system was placed at a height in the steel frames designed and fabricated to prevent the still from damage during rain and other factors. The top surface was covered with 4mm thick glass, with 14^o inclination with the horizontal.The major modification is the use of condenser attached to the basin. Condensation takes place in the sloping surface and major occurs in the attached condenser due to transfer (purging) of vapour from solar still chamber to condensing chamber. Since most of the condensation takes place in the condensing chamber, the temperature difference between glass cover and water is more which causes faster evaporation and the condensed water is collected in channels kept in front of the slope as well as in the condenser surface. Fig 2.1 shows the view of solar still with condenser taken from (Faith et.al,1998)

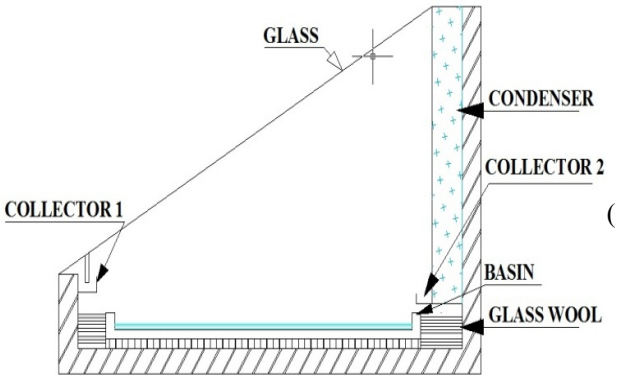

Fig.2.1 Sectional view of the system

Fig. 2.2 : Photograph of System 1 fabricated

System 2:

A basin type single slope solar still fabricated with steel similar to the first system with a condenser attached behind the basin. Glass with 4 mm thickness was used placed at 23^{o} with the horizontal and two outlets for fresh water was kept,one in front of the slope and other in the condenser surface.

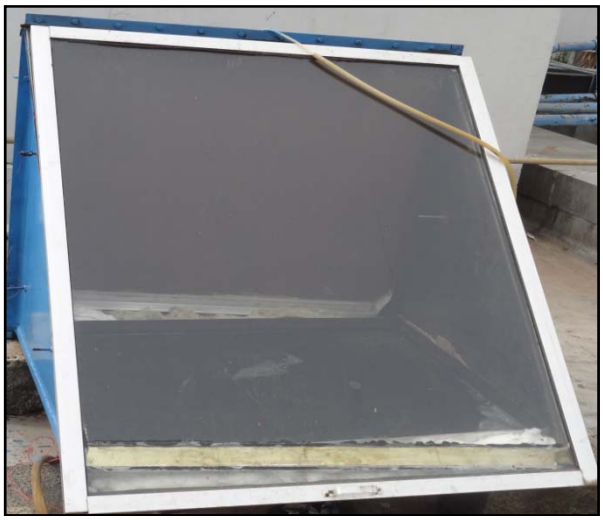

Fig. 2.3 : Photograph of System 2 fabricated

The use of condenser has also another advantage: The water used in the condenser exchanges its heat with the hot vapour inside the still and hence becomes hot. Periodical transfer of this water from the condenser into the basin helps in acquiring preheated water in the basin and hence more heating and more evaporation of water occurs and the condenser is filled with water at ambient temperature.

2.3 Experiment:

The solar incidence angles were calculated using the Eq(2).The energy transmitted through the covers was calculated using the equations .The transmittances of the cover plates were calculated using Eq(1).Calculations were made to study the performance of the still with minimum depth of water in the basin and also the level of water being maintained constant. The theoretical performance of the still was known using the heat balance equations and instantaneous and overall production of the still was known.

Initially the basin water temperature was assumed to be at ambient temperature and then measurement of various temperatures like vapour, basin,condenser were found using the thermocouples attached and read through multimeter.The multimeter was at first calibrated by repeatedly checking its accuracy by taking readings of water vapour at 100^{o}C.

The experiments were carried out from 9hrs to 17hrs with readings taken for every one hour and also the instantaneous production of fresh water was also measured. The water in the condenser periodically transferred into the basin and was filled with water at ambient temperature.

IV. RESULTS AND DISCUSSION:

Based on the measurements obtained from the experiment conducted the obtained results were plotted and their inference was understood.

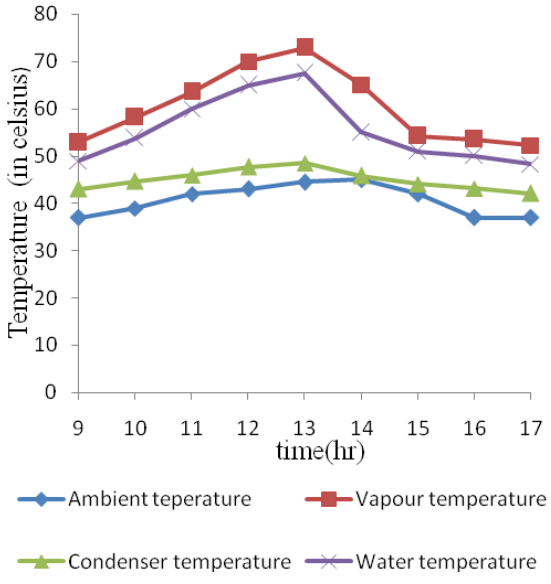

Fig.2.4 : Variation of tempearatures at different time intervals

The above Fig.2.4 shows the variation of ambient, vapour, condenser and water temperatures during the experiment period. All these temperatures we could see are at their maximum at around 1 PM**.**

It shows that the ambient temperature varied from 37^0C to 41^0C.Also the vapour temperature was maximum around 1PM.

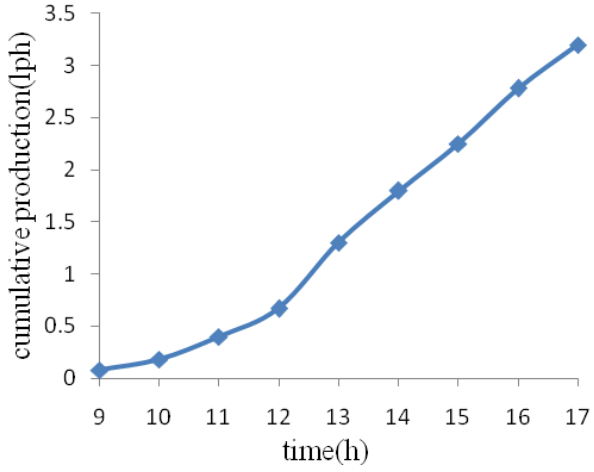

Fig.2.5 : Variation of cumulative production of system 1 for a day

Fig.2.5 shows the cumulative production of desalinated water of system 1 over a day.The productivity was measured at regular intervals and the cumulative production was calculated for a day.The maximum production rate was 3.2 litres per day measured form 9hrs and 17 hrs.

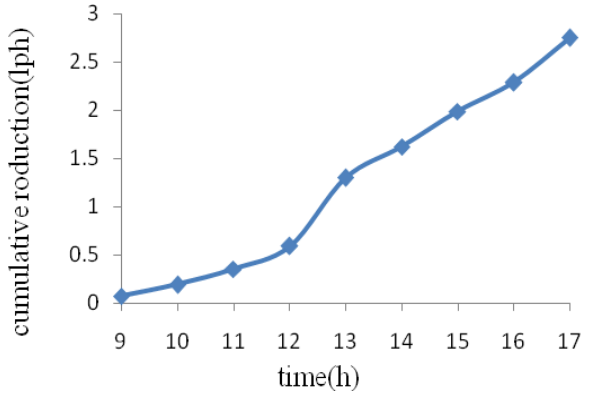

Fig. 2.6 : Variation of cumulative production of system 2 for a day

Fig.2.6 shows the cumulative production of desalinated water of system 2 over a day.The productivity was measured at regular intervals and the cumulative production was calculated for a day.The maximum production rate was 2.8 litres per day measured form 9hrs and 17 hrs.

V. THEORETICAL ANALYSIS:

The heat transfer equations and the required parameters were applied for system 1 using Matlab. The basin,water,glass temperatures and water output were obtained using the iterative procedure.

t(h)	T_b(°C)	T_w(°C)	T_g(°C)	m_e(l)
9- 10	43.18	41.2608	37.04	0.02
10-11	47.27	45.0239	40.86	0.06
11-12	54.39	51.6457	47.34	0.12
12-13	60.49	58.02	53.76	0.21
13-14	61.81	59.6374	55.5302	0.26
14-15	63.34	61.3873	57.371	0.30
15-16	61.86	61.0003	57.0720	0.36
16-17	53.53	53.04	49.33	0.42

VI. THERMAL ANALYSIS:

The above shown system 1 was modelled using gambit and ambient boundary condition was set for side walls and the basin and condenser were set as pressure outlet and glass layer as pressure inlet.The solar intensity was calculated for modelling using solar calculator in Fluent.

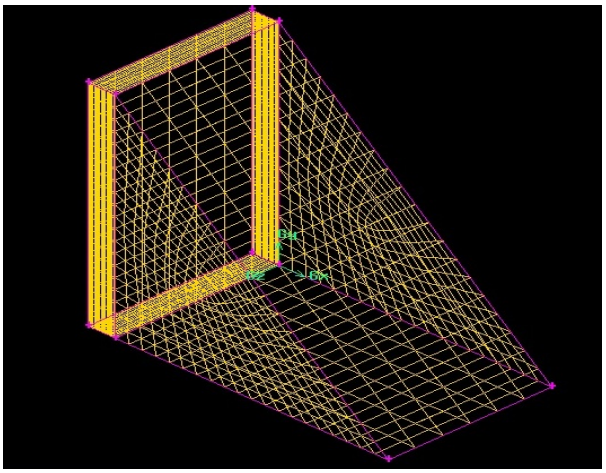

Fig.2.7 : Grid generation of still with condenser

Thermal analysis using the experimental conditions yielded better results.

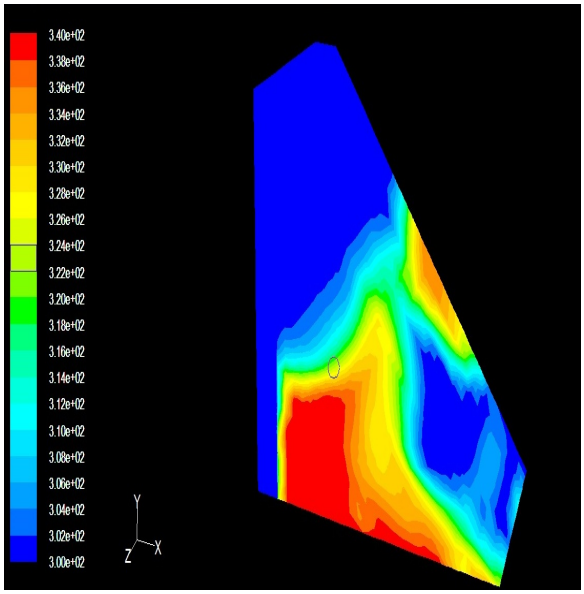

Fig.2.8 : Vapour temperature(K) contour obtained using Fluent

VII. COMPARISON OF RESULTS:

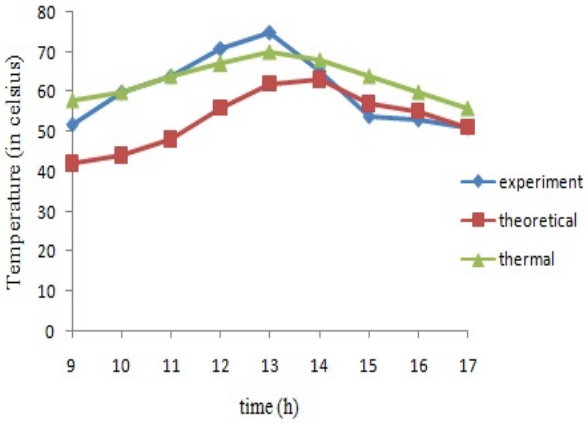

Fig.2.9 : Comparison of vapour temperatures

Fig.2.9 shows the different values of vapour temperature obtained using the 3 methods. It is observed that all the values converge at last and the mean error is 12% which occurs due to the different errors in iterations, boundary conditions and meteorological parameters.

VIII. CONCLUSION:

Thus two basin type single slope solar stills were fabricated with a modification of condenser attached to the basin. In both the systems the water brackish water level was maintained at 1 cm.The performance of the system was studied and variation of various parameters were studied and plotted. The estimated production rate of the models using theoretical and thermal analysis closely agreed to the experimental values obtained. The efficiency of the System 1 was high as less scattering of solar irradiation and high temperature difference occur in it when compared to System 2.The production rate was increased by using the condenser along with the basin and hence the efficiency of the system was increased.

IX. NOMENCLATURE:

a – area (m^2),C_p- specific heat capacit (J/kg K)

d- glass thickness (mm),

h- heat transfer coefficient (W/m^2K)

I- total radiation (W/m^2),

K_d-diffused radiation fraction

m- mass (kg),Q- heat transfer,energy (W)

t- time (s),T- temperature (^oC),

V- velocity of air (m/s)

U- overall heat transfer coefficient (W/m^2K)

p- partial pressure of water vapour (N/m^2)

M- molecular weight

Greek letters:

β - inclination of glass cover with horizontal ,degree

δ - sun declination angle ,degree,

φ - latitude,degree,

ω - hour angle ,degree,

$\in$ - emissivity,

α_b – absorptivity,

Δt - time step,s,

τ - transmittance,

σ - Stefen-Boltzmann constant

θ - solar incidence angle ,degree

Subscripts:

a-air,ambient,

av-average, b –basin

fw- feed water, r- radiation,

g- glass ,s-south

REFERENCES:

[1] K.Kalidasa Murugavel,K.Srithar 'Performance study on basin type double slope solar still with different wick materials and minimum mass of water'.Int J.Renewable Energy.Vol 36 pp 612-620 ,(2010).

[2] Tripathi Rajesh,Tiwari GN. 'Thermal modeling of passive and active solar stills for different depths of water by using the concept of solar fraction'. Int J.Solar Energy.Vol 80 pp 956-967, (2006).

[3] Naser K. Nawayseh , Mohammed Mehdi Farld,Abdul Aziz Omar ,Said Mohd.Al-Hallaj Abdul Rahman Tamimi. 'A simulation study to improve the performance ofsolar humidification-dehumidification desalination unit constructed in Jordan' Int.J Desalination.Vol 109 pp 277-284, (1997).

[4] Said al Hallaj;J.R.Selman,Sandeep. 'Solar desalination with Humidification and Dehumidification cycle. Review of Economics'. Int.J. Desalination .Vol 185 pp 169-186, (2005).

[5] Kalidasa Muragavel KTheoretical and experimental analysis on a single basin double slope solar still'. Ph.D Thesis ,Anna University, (2009).

[6] Kothandaraman CP,Subramanyan S.'Heat and mass transfer data book.India:New Age InternationaPublishers',(1999).

◈◈◈

Case Depth Prediction by Dynamic Response Studies Using Laser Doppler Vibrometry

Husain Kanchwala, Mohan Misra & Bishakh Bhattacharya

Indian Institute of Technology Kanpur
E-mail : husaink@iitk.ac.in, emkay@iitk.ac.in, bishakh@iitk.ac.in

Abstract – Surface hardening operations are carried out in order to develop a wear resistant surface while maintaining the overall toughness of a component. There are a number of surface hardening processes available today. One of the energy efficient approaches is to obtain required hardening by the use of Induction hardening. This process leads to a transition of lattice structure and causes the distortion of the crystal lattice. Any such distortion is known to initiate change in the elastic constants of the material. Consequently, dynamic response of a hardened steel plate gets modified due to the changes in the system properties. The eigen parameters, namely, natural frequencies, damping factor and the mode shapes associated reflect this change with the change in system properties. By determining these changes precisely using Laser Doppler Vibrometry (LDV), a neural network model has been developed to predict the case depth of the hardened layer.

I. INTRODUCTION

The hardened surface improves the wear resistance as well as the fatigue strength of steel components under dynamic and/or thermal stress condition. Surface hardness and the effective hardness depth are considered as pivotal characteristics of hardened parts [1].

Electromagnetic Induction hardening (Fig. 1) is an energy-efficient, in-line, heat-treating process widely used in automotive industry to surface-harden automotive parts at the lowest possible cost. The substitution of induction hardening for furnace hardening may lead to savings of up to 95% of the energy used in the heat-treating operations [2]. Also, such process would lead to significant weight saving in automotive power-train components, further saving energy and reduction in the manufacturing cost.

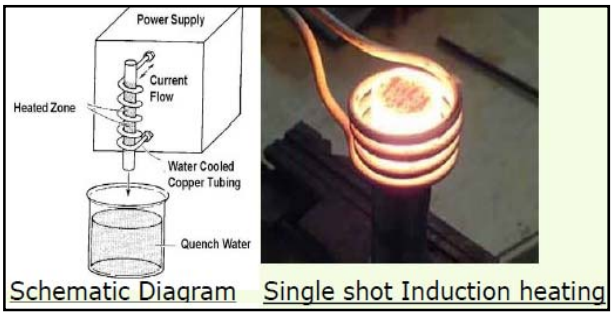

Fig. 1 : Induction Hardening Process

It is generally observed that Induction hardening process enhances the strength and wear resistance of the surface layer of the components at the cost of ductility and toughness [2]. Therefore, it is essential to evaluate the mechanical properties of hardening layer from the micro structural condition in the subsurface region of the hardened component and not merely from the surface hardness value. Hence, it is imperative to devise a non-destructive evaluation technique which can sense the finer microstructure variations.

Case depth or the thickness of the hardened layer is an essential quality parameter of the case hardening process, the darker periphery of a typical round plate as shown in Fig [1] shows the of case depth of a hardened sample. The methods employed for measuring such case depth are chemical, mechanical, visual (with an acid etch) and nondestructive techniques [3].

In order to evaluate the characteristics of the hardened surface, it is advantageous to use a nondestructive method for measuring the case depth. Different solutions towards this direction have been proposed in the open citations [5] including

(a). Using the magnetic and magneto-electrical characteristics of this layer [6],

(b). Using the sound velocity of ultrasonic waves [7, 8] and

(c). Using the backscatter of ultrasonic waves [9].

(d). Other techniques [e.g. potential drop measurement, etc.]

II. DYNAMIC RESPONSE OF HARDENED PLATE

It is noted that medium carbon steel [C-0.45%] when undergone induction hardening process, at temperatures above 730°C, steel atoms are arranged according to a crystal lattice form known as austenite. As steel slowly cools, austenite changes into ferrite, which has a different lattice structure. To validate this conjecture, modal analysis of EN-8 samples were carried out on Polytech scanning vibrometer PSV-3D and vibration signature as well as damping analysis for Un-hardened and hardened samples was recorded.

Following Figure [2] shows a typical frequency response in pre and post hardening stage.

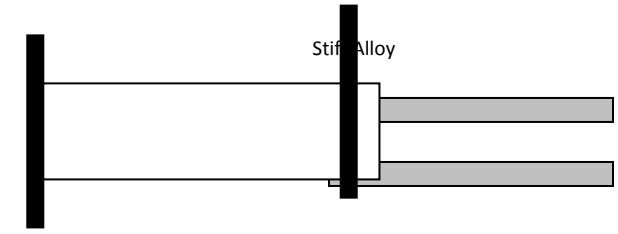

Unhardened Component **Hardened Component**

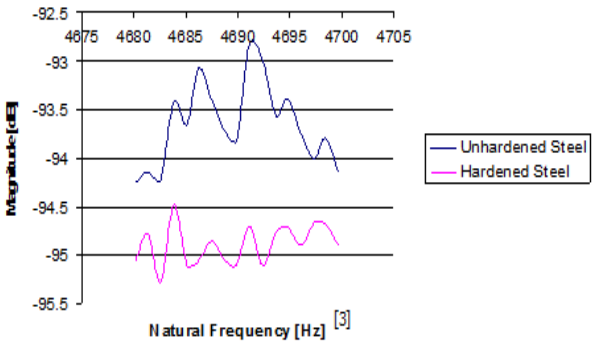

[3]

Fig. 2 : Wave response due to hardening of Steel Sample

Change in dynamic response in a hardened sample is characterized by changes in eigen parameters, i.e., natural frequency, damping factor and the mode shapes associated with each natural frequency. Experimental modal analysis of En-8 Steel sample is performed using Laser Doppler Scanning Vibrometer. The experimental modal analysis is conducted on frequency domain in fixed-free boundary condition using dynamic excitation at the center of the sample by an electro-dynamic shaker. The hardened specimen show distinct decrease in the natural frequencies in comparison to the un-hardened sample. Damping losses for different modes are also determined. Applicability of experimental modal analysis for predicting in-process case depth is discussed in the present paper.

2.1 Experimental Dynamic Response

2.1.1 Sample preparation

En-8 Steel samples of diameter 38 x 32mm were hardened under varying process parameters on Inductotherm make 250KW, 3-10 KHz Induction heater model UP-12 to obtain effective case depth of 4mm and 12mm with hardness value of 60-62 HRC. To achieve better vibration response at Laser Doppler vibrometer, a very thin slice of 2.5~2.6 mm were cut with copper electrode in EDM machine so that no apparent changes in case depth or hardness value happened. Steel samples were coated with developer so that laser signals could easily reflect from the surface to achieve accurate results.

rameters for Inductotherm Make 250KW, KHz Induction Heater, Model UP-12

S.No.	Process Parameter	Values to Obtain 4mm Case Depth	Values to Obtain 12 mm Case Depth
1	Frequency	10KHz	2 KHz
2	Power	65 KW	65 KW
3	Current	105 A@415 V	105 A@415 V
4	Scanning Speed	1300 mm/min	550 mm/min
5	Quench flow	40 LPM@22psi	40 LPM@22psi
6	Quench Temperature	32° C	32° C
7	Surface Hardness	60-62 HRC	60-62 HRC

Table1: Process parameter to obtained desired case depth

2.2 PSV 3D measurement method- Laser Doppler Vibrometry

Laser Doppler Vibrometer (LDV) is a Laser based non-contact vibration measurement system. It consists of three measuring scan heads which are capable of measuring the movements in all the three orthogonal directions yielding full information of the three dimensional movements [Figure 2.] The system works on the principle of Doppler Effect and interferometry for vibration measurement.

The minimum detectable vibration speed using this system is 5 µm/s at 1Hz resolutions while the maximum speed is of 10 m/s. The LDV system software controls the entire measurement process with graphical user interface. The PSV system also has the provision for input channels which can be used for simultaneous acquisition of data from accelerometers, load cells etc. Transfer function between any of the input channels connected to the system can be obtained. Signal generator card (NI-671x) contained in the system is used for generating excitation signals in the frequency range of 0-80 kHz. LDVs can measure vibrations up to 30 MHz range with very linear phase response and high accuracy. Applications of LDV include modal analysis of automotive parts, car bodies and aircraft panels etc.

Fig. 3: 3D Laser Doppler Vibrometer

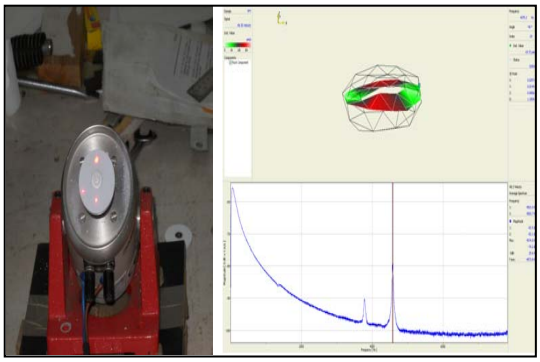

Fig. 4: Sample & Experimental set up

The Laser Doppler Vibrometer works on the basis of optical interference requiring two coherent light beams. The interference term relates to the path difference between both the beams.

Excitation Signal	Pseudo random
Frequency Range	0-7500 Hz
FFT Lines	1600
Window	Rectangle
Averages	10 (complex)
Velocity decoder	VD-09 Digital decoder (velocity range 0-10 mm/sec)

Table 2 : Details of excitation signal used for testing

In the present analysis, 21 scan points were defined due to smaller size of EN-8 Sample and it took about 2 minutes to complete the scan. Response plots, mode shapes animations were visualized after the scan.

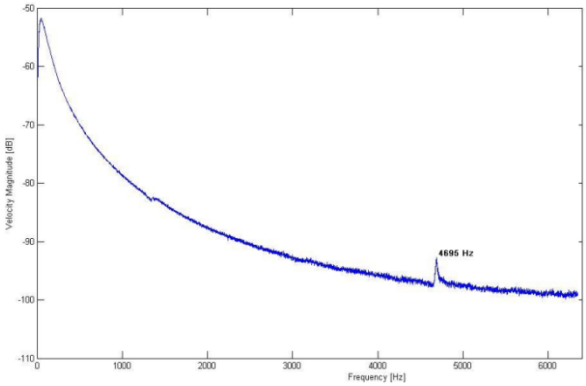

Fig. 5 : Natural frequency ω_n for Unhardened sample

From fig.5, the natural frequency obtained, for first bending mode, is 4695 Hz and the velocity amplitude of -93.38 dB .

Figure 6. En-8 Sample mounted on Electro-Dynamic shaker

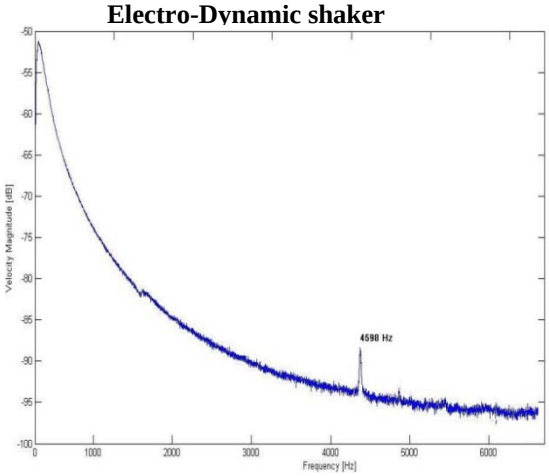

Fig. 6 : Natural frequency ωn obtained in Hardened sample with 12mm case depth from modal Analysis

Figure 6 shows the dynamic response of hardened plate with 12mm case depth. In this case, the dynamic response has changed significantly. The fundamental frequency in bending mode is reduced to 4598 Hz with velocity amplitude of -93.22 dB. The similar drop in natural frequency of bending mode for hardened plate with 4mm case depth is also observed. A drop of 2% in natural frequency is observed due to hardening of steel plate. This observation is quite remarkable in terms of predicting the case depth.

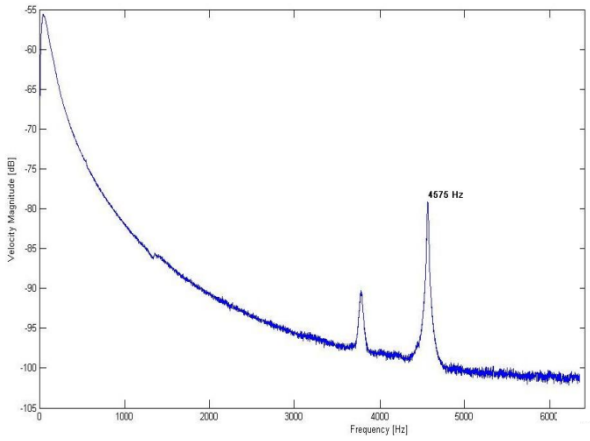

Fig.7 : Natural frequency ω_n obtained in Hardened sample with 4mm case depth from modal Analysis

2.2.6 Measurement of damping

A quantitative measure of damping ratio ζ is obtained by using the half-power bandwidth method shown graphically in Figure 12.

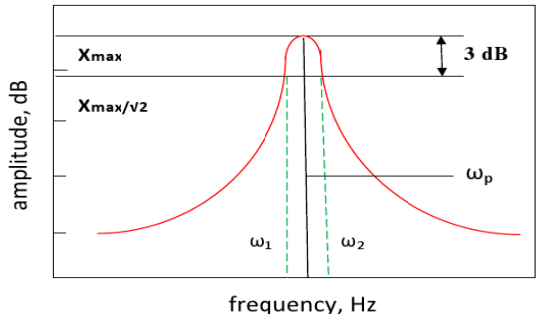

Fig. 8: Measuring Damping using 3dB method

The damping ratio, ζ can be determined by

$$\zeta = \frac{\Delta \omega}{2 \omega p}$$

$\Delta\omega$ is determined from the half power points down from the resonant peak value, *Xmax*. On a decibel scale, this corresponds to –3dB down from the peak value. Hence, is also referred as 3 dB method.

S.No.	Sample Description	Natural Frequency [Hz]	Damping Ratio [ζ]	Loss Factor
1	Un hardened sample	4695	0.024	0.012
2.	Sample with 4mm Case depth	4575	0.0088	0.0044
3.	Sample with 12mm Case depth	4598	0.014	0.007

Table 3 : Experimental results for Hardened and Un-hardened Steel Samples

III. FE ANALYSIS OF FREE VIBRATION OF HARDENED PLATE

A standard FEM Package 'ABAQUS' is used for modal analysis of En-8 samples to verify the results of experimental modal analysis. A good agreement in natural frequencies for different modes is seen.

Following were the parameters for this analysis:

- Element type: Liner hexahedral [C3D8R]
- Mesh size: from 0.001~0.002

However, a good convergence was observed for mesh size 0.0014, with the experimental values of natural frequency.

S No.	Sample Type	Mesh Size	Element Type	No. of Element	No. of Node	Natural Frequency [Hz]
1	Unhardened	0.0014	C3D8R	968	1584	4952
2.	Case depth 4mm	0.0014	C3D8R	1080	1755	4976
3.	Case Depth 12mm	0.0014	C3D8R	660	1080	5031

One of the Actual Test Samples

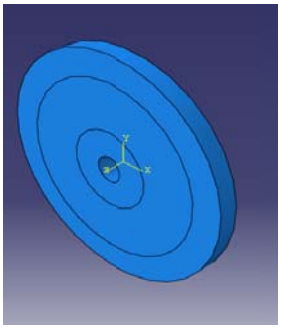

FE model with 4mm case depth

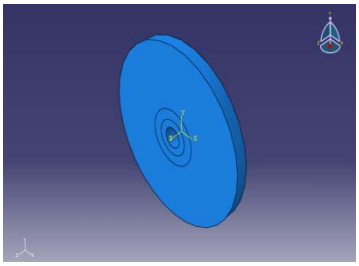

Sample description
EN-8 Steel round plate
Section : Ø 35 x 2.6 mm

Hardened Sample with 12 mm Case depth

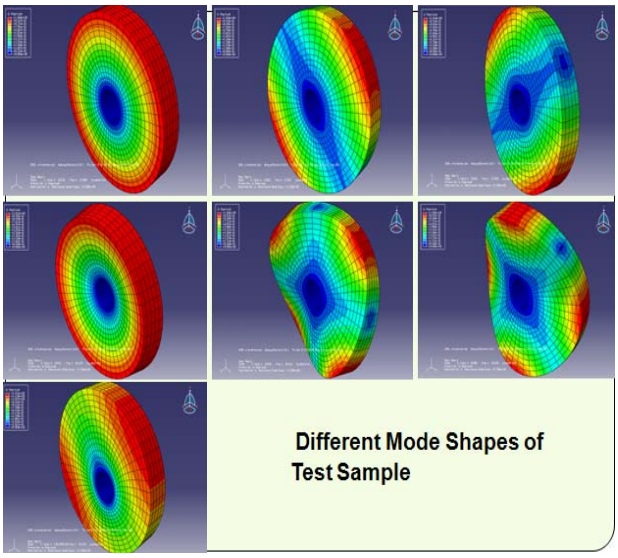

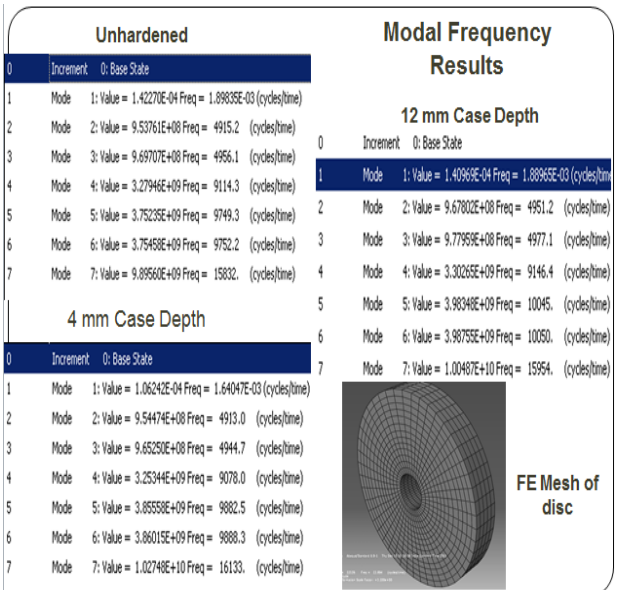

Fig. 9: F.E. Models of sample for free vibration showing natural frequencies & Corresponding Mode shapes

IV. TESTING

4.1 Micro hardening Testing

An induction hardened sample is said to be conformed if the hardness value is with in specified limits in case depth zone. The experimental samples in this case, were qualified for a hardness values 60±2 HRC. The standard testing procedure for Rockwell hardness test method was adopted. After placing the sample on flat bed platform, diamond indenter is forced into the sample with preliminary load F_o of 10 kgf, dial indicator is set to a datum on testing machine dial after the equilibrium is reached. After additional major load of 140 kgf was applied on the sample, there was an increase in penetration. Once the equilibrium is again established after release of major load, the dial indicator gives direct hardness value in C scale. Figure 10 shows the experimental setup.

Fig.10 : Rockwell hardness testing machine at IITK

4.2 Microstructure Analysis

After induction hardening of the samples, the microstructures were seen at various level of magnification in order to ensure that the phase transformation is been properly achieved. It is expected that the core should be Pearlite and the outermost layer Martensite which has been revealed by the microstructures (see Fig. 11).

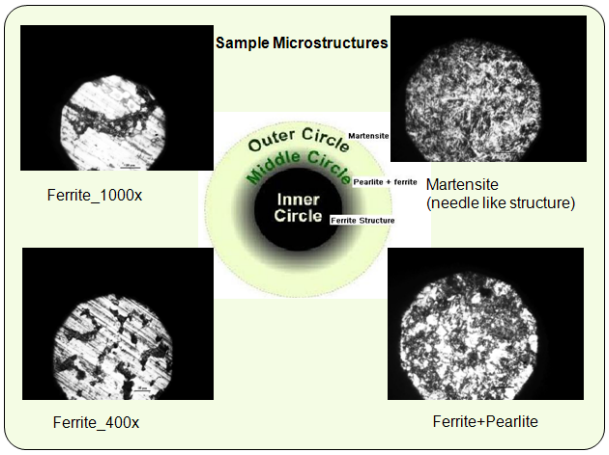

Fig. 11: Microstructures at 1000x magnification

V. DATA FUSION USING WEKA WITH MULTILAYER PERCEPTRON ALGORITHM

Weka is a collection of machine learning algorithms for data mining tasks developed by Machine Learning Group at University of Waikato, New Zealand. Data mining, as it describes, a process of finding correlations or patterns among various parameters in large relational databases. These methods enable a computer program to automatically analyze a large collection of data for deciding on what information is most relevant. Artificial Neural Network shows a good promise to provide a comprehensive solution for predicting case depth of desired hardness value. Mutlilayer perceptron algorithm is an efficient and powerful universal approximation technique. It is very useful in predicting the output behavior based on even limited number of input variables. It is a feed forward neural network, with one or more layer between input and output layer, which maps number of input variables to output very efficiently. The data is processed based on Back propagation training algorithm which determines the weighing functions.

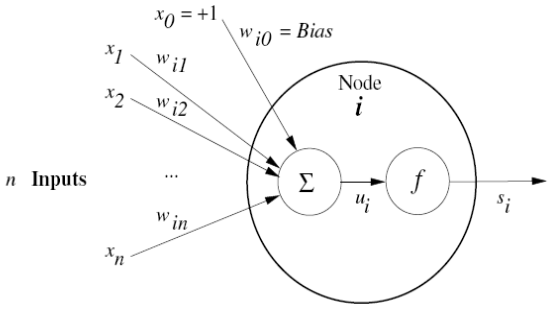

Fig.12. Conventional representation for ANN (Artificial Neural Network)

The FE model for unhardened and hardened disk has been built up in Abaqus. As the material properties change because of hardening process, it is taken as a basis to determine the case depth by measuring the dynamic response parameters.

For identification of case depth a number of frequency response parameters have been selected namely Natural frequency and Loss factor which changes as a function of the case depth. After obtaining these parameters from the FE code a physical correlation has been done by comparing the obtained response characteristics with the physical test setup using LDV.

After this FE model updating has been done so that the response from the finite element model closely matches the experimental results. Once the FE model is mature enough a number of similar models of varying case depths have been made to generate the database for training the Multi-layer perceptron model for identification of case depth of an unknown sample on the basis of these parameters.

We have also formulated a full scale elaborative model in which the parameters obtained from non-destructive tests and other destructive test parameters have been considered (namely the hardness measures at various points along the radial direction). This has been developed by the means of actual test samples.

Parameters supplied to Elaborated model:

Micro Hardness				
hardeness_4mm	hardeness_8mm	hardeness_12mm	hardeness_16mm	

Dynamic Response			Frequency Domain response	
loss_factor_hardened	nat_freq_hardened	Damping ratio	Max response	Rms Value

The output predicted after training :

Case Depth

VI. RESULTS AND DISCUSSION

In an attempt to study a relation between case depth of hardened layer in a steel sample and dynamic response under free vibration, 35 steel samples have been studied. 10 nos each of 12mm and 4 mm case depth and 5 nos of unhardened steel samples were taken. Following attributes were measured

1. Micro hardness measurement at 4mm, 8mm, 12mm and 16mm plane from center.
2. 2nd Modal frequency for all the samples under clamped center condition with PSL 3D laser Doppler vibrometer.

3. Damping ratio and loss factor with the help of 3dB method in FFT model of modal analysis.

These results obtained are as follows:

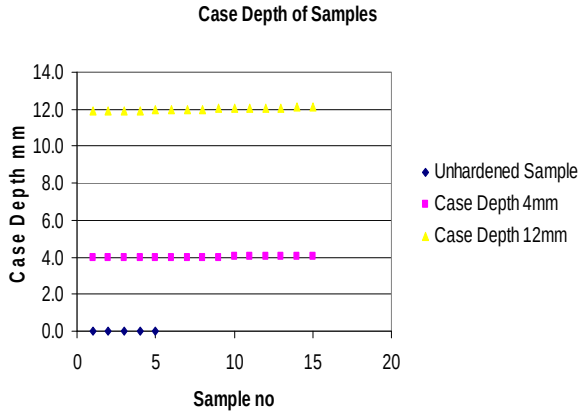

Fig.13 : Case depth vs. Sample no.

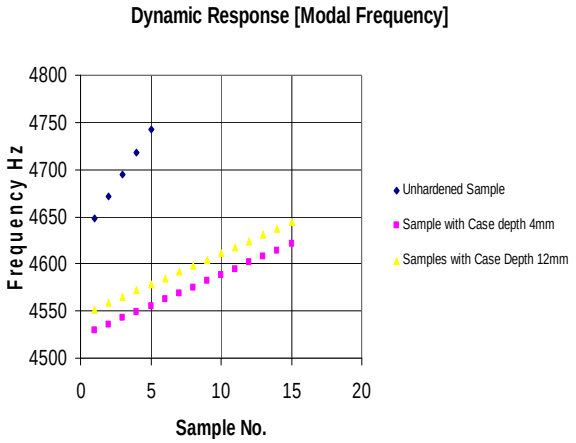

Fig. 14 : Frequency vs. Sample no.

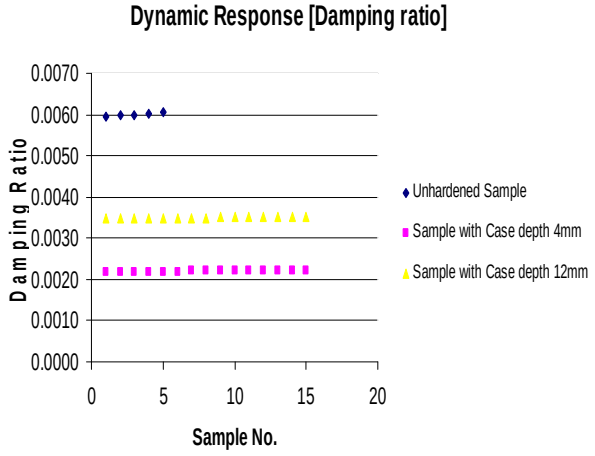

Fig. 15: Damping Ratio vs. Sample no.

To accurately predict the case depth of unknown samples, Weka software was used with mutilayer perceptron algorithm.

A trial run of 35 unknown samples was performed through Weka. Following were the results obtained:

- Correlation Coefficient: 0.84
- Root Mean square error: 11.36 %

The results indicate that accurate model prediction is possible and this can be used as a measure of predicting case depth after further training with a large number of samples.

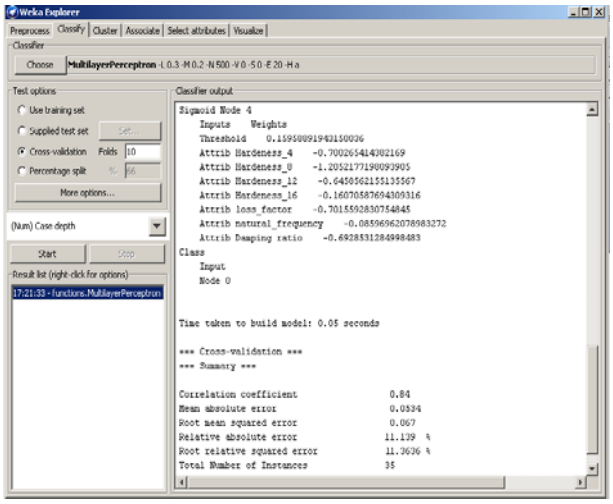

Fig. 14 : WEKA interface showing summary of results for Case depth prediction of 35 steel samples

VII. CONCLUSION

The following are the brief conclusions from this study.

- The Vibration analysis is quite sensitive towards change in micro structure of material. Therefore, it is very useful to establish quality parameter of an output of heat treatment process such as induction hardening.
- The study of dynamic response for unhardened and hardened plate shows the effectiveness in predicting the case depth of hardened layer.
- This model can be generalized to predict the case depth during the hardening process itself.
- By using the ANN model a knowledge bank has been developed which can be used for developing an Adaptive feedback controller for real-time induction hardening process.

REFERENCES:

[1] ASTM A941 - 10a Standard Terminology Relating to Steel, Stainless Steel,Related Alloys, and Ferroalloys, ASTM International, www.astm.org.

[2] ASM International Nov. 2002, Surface Hardeneing of Steel-Understanding the Basics.

[3] SAE Standard J423(1998), Methods of Measuring Case Depth, SAE International, www.sae.org.

[4] Moorthy V, Shaw B A, and Hopkins P, Surface and subsurface stress evaluation in case-carburized steel using high and low frequency magnetic Barkhausen emission measurements, J. Magn. Magn. Mater.Apr2006;299(2):362–375.

[5] Honarvar F, Zeighami M, Application of signal processing techniques to case depth measurements by ultrasonic method, 17th World Conference on Nondestructive Testing, 25-28 Oct 2008, Shanghai, China

[6] Morganer W, Michel F, Some New Results in the Field of Non-Destructive Case Depth Measurement, 9th European NDT Conference (ECNDT2006), Berlin, Germany, September, 25-29, 2006.

[7] Singh S, Fuquen R, Leeper D R, Process for measuring the case depth of case- carburized steel, United States Patent 5648611, 1997.

[8] Honarvar F, Sheikhzadeh H, Moles M, Sinclair A N, Improving the time resolution and signal-to-noise- ratio of ultrasonic NDE signals, Ultrasonics 2004;41:755-763.

[9] Baqeri R, Honarvar F, Mehdizad R, Case Depth Profile Measurement of Hardened Components Using Ultrasonic Backscattering Method, 18th World Conference on Nondestructive Testing, Durban South Africa, April,16-20, 2012

[10] Wilson John W, Tian Gui Yun, Moorthy Vaidhianathasamy, and Shaw Brian A, Magneto-Acoustic Emission and Magnetic Barkhausen Emission for Case Depth Measurement in En36 Gear Steel, IEEE TRANS ON MAGNETICS Jan 2009;45(1):177-183.

[11] Moorthy V, Shaw B A, and Evans JT, Evaluation of tempering induced changes in the hardness profile of case-carburized EN36 steel using magnetic Barkhausen noise analysis, NDT & E Int. Jan2003;36(1): 43–49.

[12] Theiner W, Kern R, Stroh M, Process Integrated Nondestructive Testing of Ground and Case Depth Hardened Parts, European Conference on Non-Destructive Testing (ECNDT2002), Barcelona, Spain, June, 17-21, 2002.

[13] Good MS, Schuster GJ, and Skorpik JR, Ultrasonic Material Hardness Depth Measurement, United States Patent, Patent No. 5646351, 1997.

[14] Medved A I, Bryukhanov A E, The variation of Young's Modulus and the hardness with tempering of some quenched chromium steels, UDC 669.15'26-194:539.32

◈◈◈

Study on Effects of Heat Treatment on Grain Refined 319 Aluminum Alloy With Mg and Sr Addition

S. Gopi Krishna & Binu. C. Yeldose

Mar Athanasius College Of Engineering, Kothamangalam
E-mail : gopsmech@yahoo.in, binucyeldose@yahoo.com

Abstract – The effect of heat treatment on A319 alloy with 0.45%wt Magnesium, 0.02%wt Strontium and grain refinement using Titanium has been investigated by hardness measurement and tensile testing. Experiments have been conducted at ageing temperatures 150°C, 160°C and 170°C. Hardness has been estimated up to 24 hours aged samples. The results indicate that hardness of 319 alloy increases with Sr addition and grain refinement. When Mg is added hardness is again found to be increasing progressively up to a maximum value and then varying non – uniformly. The tensile strength and microstructure after Mg modification and heat treatment have been discussed.

Index Terms*— ageing, grain refinement, heat treatment.*

I. INTRODUCTION

The use of aluminum castings in aerospace, automotive and general engineering industry has increased dramatically over the past three decades. Automotive industry strives to achieve light weight components to reduce fuel consumption, to improve overall performance and to meet environmental requirements. Weight reduction can be achieved by replacing steel and cast iron products by aluminum [1-2]. Aluminum readily forms alloys with many elements such as copper, zinc, magnesium, manganese and silicon. The alloy known as A319 (Al-6.5%Si-3.5%CU) is a commercially popular alloy used in various applications due to their excellent combination of properties such as fluidity, low coefficient of thermal expansion, high wear resistance, high strength to weight ratio, good corrosion resistance etc. In the 319 alloy silicon and copper are the major alloying elements and magnesium is added for improving mechanical properties. The presence of magnesium improves strain hardenabilty and enhances material strength by solid solution [3-5]. Presence of Ti enhances grain refinement [4].

In order to improve mechanical properties of cast components 319 alloy can be heat treated [5]. The typical heat treatment for 319 alloy is T6 heat treatment. T6 heat treatment comprises of solution treatment followed by quenching and age hardening [6].

II. EXPERIMENTAL DETAILS

A. Casting preparation

The 319 ingots before melting were cleaned using acetone to make castings free from defects caused by impurities in the metal and to make it free from moisture. Cast iron moulds are used through out the experiments. Graphite coatings are provided inside the moulds for easy separation of the castings from the mould after solidification. The moulds are then preheated to a temperature of 250°C

B. Sequence of casting operation

10kg of 319 alloy is weighed using a weight balance. The pit furnace is heated to 700°C to become red hot and the alloy is charged in the crucible. Coverall flux of 100gm is also added in to the crucible while charging the 319 alloy. Hexa chloro ethane tablets were added to degas the melt after 319 ingots gets completely melted. 0.45%wt Mg is added in to the melt after degassing followed by 0.02%wt Sr and TiB addition. After all the additions are over the melt is subjected to nitrogen degassing for 1hour.

After degassing the molten metal is poured in to the pre heated moulds. While pouring the temperature of melt should be at 720°C. Then the moulds are allowed to solidify as shown in Fig.1. After solidification, the castings are removed from the mould.

C. Specimen preparation

Samples are cut from random portions of castings for hardness as well as microstructure study and also for tensile testing as per the ASTM standards.

D. Heat treatment

T6 heat treatment includes 3 main steps. Solution treatment at 500°C for 8 hours in an air circulated furnace as per ASTM standards. Next step is quenching. Quenching is done in water at 60°C and then natural aging for 12 hours. Last step is the artificial ageing. 3 sets of samples were taken and aged at 3 different temperatures at 150°C, 160°C and 170°C for 24 hours.

E. Hardness samples

Hardness samples were prepared according to ASTM standard. Hardness samples were cut from different portions of casting and then machined as per the ASTM standard dimensions.

F. Tensile testing

Tensile testing is carried out using computer controlled universal testing machine. The ends of specimen were gripped in the UTM and load is applied till it fractures. The tensile samples were also prepared according to the ASTM standards.

Fig. 1 Cast iron moulds allowed for solidification after the melt is poured. Moulds should be pre heated before the molten metal is poured otherwise shrinkage will occur in castings.

G. Metallographic testing

Samples are cut and machined from casting for micro-structural study. Mechanical grinding is performed in successive steps using abrasive emery papers of different grit sizes. Paper polishing was followed by machine polishing using diamond pastes.

III. RESULTS & DISCUSSIONS

A. Microstructure

Fig.2 shows microstructure of unmodified 319 alloy which consists of aluminum network and eutectic silicon. The morphology of silicon is plate like structure (acicular structure). This needle like structure acts as stress raisers in the microstructure making the material to fracture. Fig.3 shows microstructure of unmodified 319 alloy after heat treatment. The structure of silicon is changed to round structure after heat treatment.

Fig.4 shows microstructure of 319 alloy with 0.02%wt strontium modification and heat treatment. In the unmodified alloy the silicon particles had a coarse plate like form. Microstructure reveals that addition of strontium modifies the coarse, acicular silicon to finer fibrous structure

B. Hardness

Hardness of 319 alloy increases with Sr addition and grain refinement. When Mg is added hardness is again found to be increasing. Hardness values plotted at 150°C of strontium modified and grain refined alloy is shown in fig. 5. At each ageing temperature hardness increases with ageing time, reaches a maximum value and thereafter decreases as shown in fig.6. Top hardness is found at 170°C for 8 hours. At this time and temperature hardness is 125 BHN.

The size, morphology and the distribution of silicon particles could affect the hardness of the eutectic mixture. Modified and grain refined 319 alloy without Mg shows a maximum hardness of 102 BHN at 150°C. Increase in hardness is due to the cooperative precipitation of Al_2Cu and Mg_2Si precipitates. So a solutionisng temperature of 500°C is appropriate for the alloy. Below this temperature solutionisation is insufficient, whereas coarsening of silicon particles and melting of Al_2Cu may occur at higher temperatures.

C. Tensile Strength

Fig 7, 8 and 9 shows the ultimate tensile strength, yield strength and elongation of as cast as well as heat treated samples of base alloy and modified alloy.

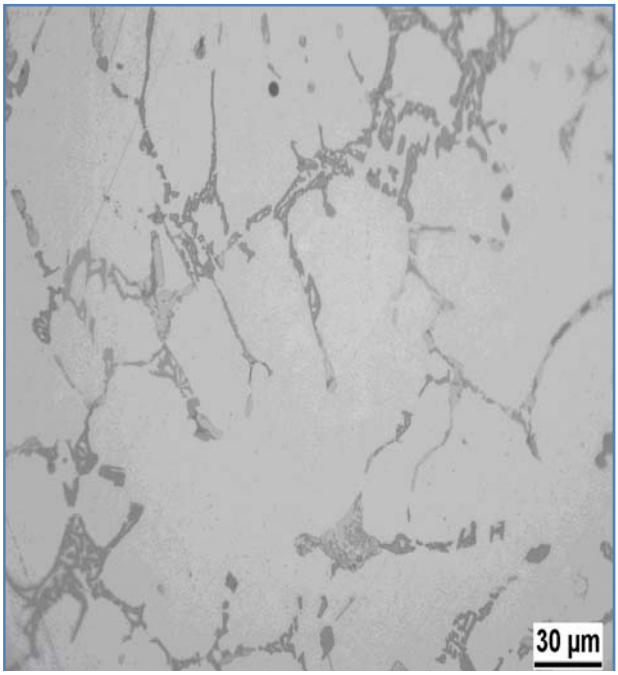

Fig. 2 Microstructure of unmodified 319 alloy. Silicon particles are having needle shape structure which acts as stress raisers.

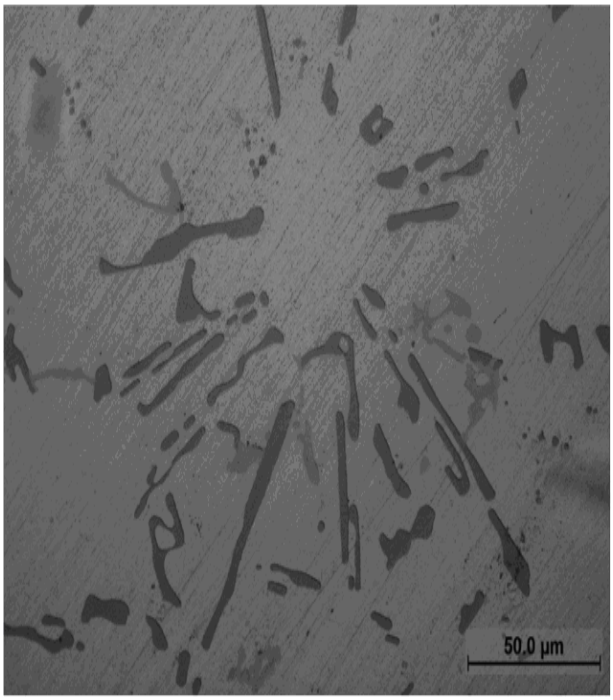

Fig. 3 Microstructure of unmodified 319 alloy after heat treatment. Needle shaped silicon structure is transformed to round shaped structure.

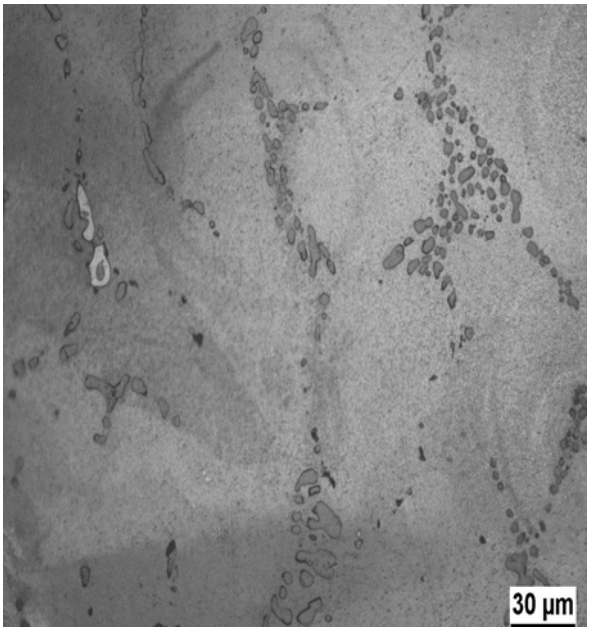

Fig. 4 Microstructure of strontium modified 319 alloy after heat treatment. Coarse structural silicon changes to fine round shaped silicon.

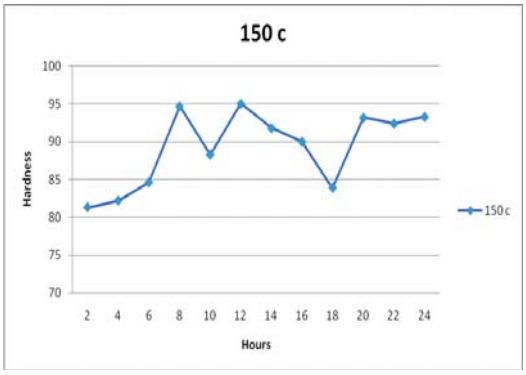

Fig. 5 Hardness of strontium modified and grain refined alloy at 150°C

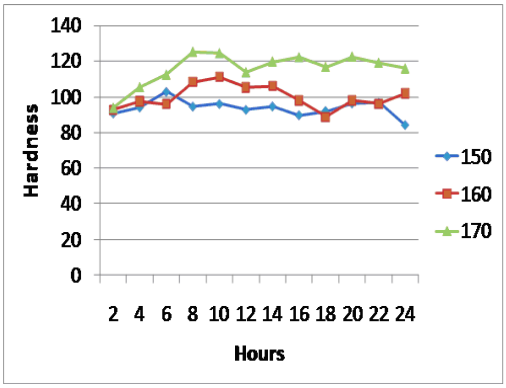

Fig. 6 Artificial aging curve of Al 319 + 0.45% Mg

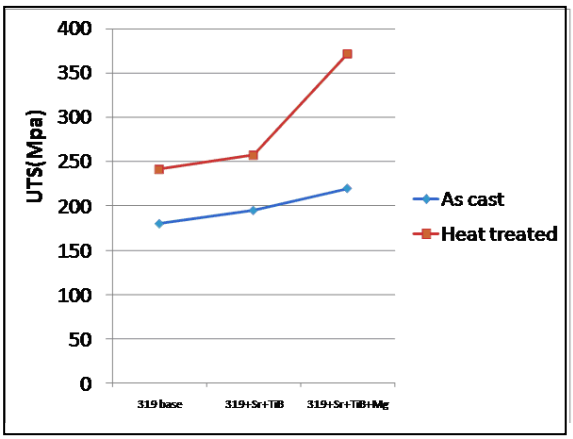

Fig. 7 Ultimate tensile strength of as cast and heat treated samples

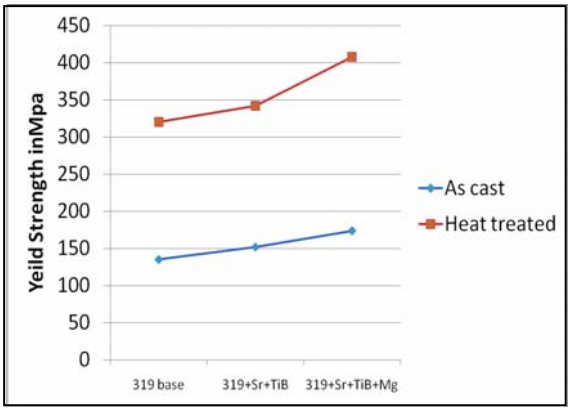

Fig. 8 Yield tensile strength of as cast and heat treated samples

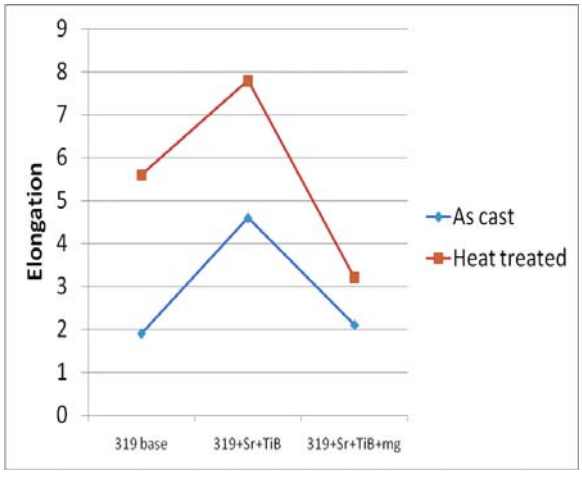

Fig. 9 Elongation of as cast and heat treated samples

IV. CONCLUSION

The work is mainly focused on effect of T6 heat treatment on Mg added 319 alloy. Heat treatment is done at different ageing temperatures for 24 hours. Base alloys show optimum mechanical property at 150°C for 12 hours of ageing. Base alloy with Mg is heat treated at different ageing temperatures. From the ageing curve it can be seen that hardness values increases, reaches a maximum value and then varying non- uniformly. Increase in hardness is due to an additional phase called Q- $Al_5Mg_8Si_6Cu_2$ with the increase in percentage addition of magnesium. Alloy with Mg shows optimum mechanical property at 170°C for 8 hours of ageing. The tensile test shows that with the addition of Mg, the ultimate tensile strength and yield strength increases. The Mg added 319 alloy with heat treatment shows highest tensile strength and yield strength. Mg added 319 alloy with heat treatment shows highest tensile strength of 372Mpa at 170°C for 8 hours of ageing. The magnesium addition decreases elongation due to the formation of brittle phases.

ACKNOWLEDGMENT

Thanks to M.C.Shaji, Scientist, NIIST, Trivandrum for his technical assistance. Technical support got from NIIST, Trivandrum is gratefully acknowledged.

REFERENCES

[1] E. HATCH, in "Aluminium, Properties and Physical Metallurgy" (American Society for Metals, USA, 1993) p. 232

[2] P. OUELLET and F. H. SAMUEL, *J. Mater. Sci.* **34** (1999) 4671

[3] R. M. GOMES, T. SATO and H. TEZUKA, *Mater. Sci. Forum Vols.* **217–222** (1996) 793

[4] M. MURAYAMA, K. HONO, M. SAGA and M. KIKUSHI, *Mater. Sci. and Eng. A* **250** (1998) 132.

[5] Z. LI, A. M. SAMUEL, F. H. SAMUEL, C. RAVINDRAN and S . VALTIERRA, *J. Mater. Sci.* **38** (2003)

[6] F. H. SAMUEL, *J. Mater. Sci.* **33** (1998) 2284

[7] P. S . WANG, S . L. LEE and J . C. LIN, *J. Mater. Res.* **15** (2000) 2035

[8] L. LASA and J . M. RODRIGUEZ-IBABE, *Mater. Charact.* **48** (2002) 371

[9] Ouellet P, Samuel FH. Effect of Mg on the ageing behavior of Al–Si– Cu 319 type aluminum casting alloys. J Mater Sci 1999;34:4671–97.

◈◈◈

Enterprise Resource Planning Implementation in Small and Medium Enterprises

M. S. Tufail & S. P. Untawale

Department of Mechanical Engineering, Y.C.C.E, Nagpur, India
E-mail : mstufail@rediffmail.com,untawale@gmail.com

Abstract – To improve productivity and overall performance, Enterprise Resource Planning (ERP) is one of the solutions for the Small and Medium Enterprises (SMEs) in order to face the global challenges. Though ERP systems, which evolved from Manufacturing Resource Planning (MRP II) systems, have many advantages, there are some failure stories also. The successful implementation of ERP systems is a challenging task. Evidence shows that the number of failing ERP projects is increasing. This means that a model is necessary to help companies avoid previous mistakes and provide them with understanding of how ERP implementation can be effectively carried out and what its essential success components are. This paper review the several issues that one has to contend with when implementing an ERP system in the SME segment like awareness, perception, earlier implementation, cost change management, HRP, and top management commitment etc.

Keywords – *Enterprise Resource Planning, Small and Medium Enterprises, Implementation.*

I. INTRODUCTION

With the globalization of economy and trade, competition among enterprises has become intensive. Enterprise informatization has been developing from large-scale enterprises to small and medium enterprises. Enterprise Resources Planning (ERP) systems are commercial software packages that enable information flow throughout companies and organizations. They improve the organizational performance and enhance the competitive advantages Nowadays SMEs have been faced with a complex and changeful business environment. Along with the process of economic globalization, on one hand that is the good opportunity of development, on the other hand SMEs are faced with the challenge foreign competitor joined. Hence, it is urgent that SMEs carry out construction of informatization and implement ERP to raise the level of management. Although SMEs have been increasingly embracing ERP in recent years, research indicates that many of them fail to reach their goals. The poor achievement can be attributed to, for example, wrong choice of ERP vendor, poor Management after ERP implementation, high cost of supporting and maintaining ERP systems.

In the post liberalization and opening up of the economy business era, ease in international trade barriers, economic liberalization, globalization, privatization, disinvestments and deregulation have thrown several challenges to Small and Medium-Sized Enterprises (SMEs) in the fast developing economies like India. Compressed product development cycles, cut throat domestic and global competition, economic downturns, rapidly changing customer demands and volatile financial markets have all increased the pressure on SMEs to come up with effective and competitive capabilities to survive and succeed. Enterprise Resource Planning is often considered as one of the solutions for their survival.

II. ERP OVERVIEW

ERP system is an IT solution that helps organizations to achieve enterprise wide integration which results in faster access to accurate information required for decision making. ERP has its roots in manufacturing as the name is an extension of Manufacturing Resource Planning (MRP II) . Today, an ERP system is considered as the price of entry for running a business and for being connected to other businesses, which allows for business-to-business electronic commerce. Many multinationals restrict their business to only those companies that use the same ERP As SMEs have MNCs as their clients, they have to consider ERP systems as a requirement to allow for tighter integration with their larger counterparts.

ERP combines all the business functions together into one single integrated system with a single central

database as shown in figure-1. This system serves the information needs of all the departments across geographies, while allowing them to communicate with each other. As illustrated in fig-1, a typical ERP system consists of modules for manufacturing, Production Planning, Quality Management, Financial Management, Human Resource, Manufacturing and Logistics and Sales and Distribution.

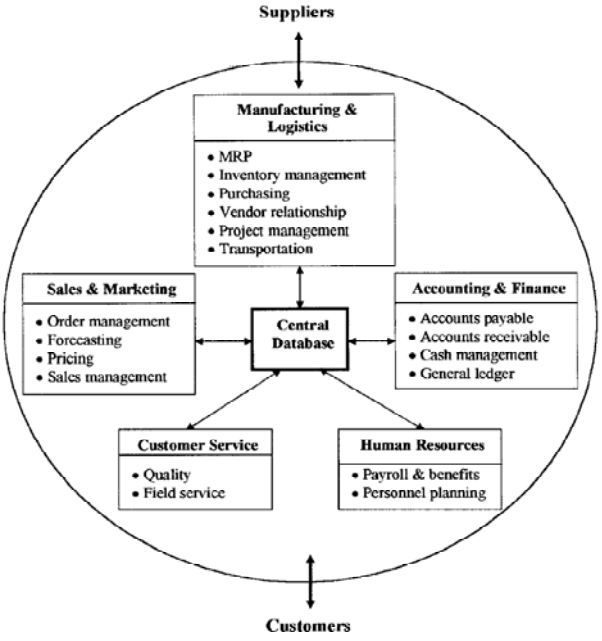

Fig. 1 : An overview of ERP system

Once an enterprise wide implementation is in place, operating managers are relieved of routine decisions and they thus have the time to plan and execute long-term decisions that are vital for the growth of an organization. It leads to significant cost savings as the health of the organization is continuously being monitored. Though the cost of an ERP system is very high, it becomes insignificant in the face of the benefits a proper ERP implementation provides in the long run.

III. IMPLEMENTATION

ERP systems affect both the internal and external operations of an organization. Hence successful implementation and use are critical to organizational performance and survival.

ERP implementation brings with it tremendous organizational change, both cultural and structural. This is on account of the best practice business processes that ERP systems are based on. This calls for ERP implementations to be looked at from strategic, organizational and technical dimensions. The implementation thus involves a mix of business process change and software configuration to align the software and the business processes.

There are two strategic approaches to ERP system implementation. The first approach is where a company goes for the plain vanilla version of ERP. Here the organization has to reengineer the business process to fit the functionality of the ERP system which brings with it major changes in the working of the organization. This approach will take advantage of future upgrades, and allow organizations to benefit from best business processes. The second approach is where the ERP system is customized to fit the business processes of the organization. This will not only slow down the implementation but also will introduce new bugs into the system and make upgrades difficult and costly. ERP vendors' advice organizations to take the first approach and focus on process changes. One third of ERP implementations worldwide fail owing to various factors. One major factor for failure is considering ERP implementation to be a mere automation project instead of a project involving change management. It is a business solution rather than an IT solution, as is perceived by most organizations. Yet another reason for failure is over customization of the ERP system. Therefore, organizations need to very carefully go about their ERP implementations, if they are to be successful.

Most large companies have either implemented ERP or are in the process of doing so. Several large companies in India, both in the public and private sectors, have successfully implemented ERP and are reaping the benefits. Some of them are Godrej, HLL, Mahindra & Mahindra and IOC. With the near saturation in the large enterprise market, ERP vendors are looking to tap the potential in the SME segment. The spending on ERP systems worldwide is increasing and is poised for growth in the next decade. Some of the reasons for this are:

- Vendors are continuously increasing the capabilities of their ERP system by adding additional functionality like Business Intelligence, Supply Chain, and CRM, etc.
- Vendors have shifted to web-based ERP.
- The demand for web-based ERP will increase due to the perceived benefits of e-commerce.
- There are several markets that are yet unexplored.

IV. REASONS OF ADOPTING ERP IN SME's:

Following are the reasons to adopt the ERP.

- Pressure from larger counterparts: Due to globalization, SMEs today operate in a wider arena.

Majority of them have MNCs as their clients. These MNCs require SMEs to implement the same ERP system as them to allow for tighter integration in their

supply chain, which permits them to design and plan the production and delivery so as to reduce the turnaround time.

- Peer pressure: Considering the growth in ERP implementation in the SME segment, several SMEs are adopting ERP systems as their peers have done so.
- To gain competitive advantage and respond quickly to the dynamic market scenario.

An ERP system would allow SMEs to integrate their business functions. It would provide for a transactional system, which provides for a disciplined way of doing business. Thus SMEs would be able to increase their efficiency and productivity by implementing a suitable ERP system.

V. ISSUES AND CHALLENGES:

Though the market for ERP seems to be growing, there are several issues and challenges one has to contend with when implementing an ERP system in the SME segment. Some of these are:

- Awareness: There is a low level of awareness amongst SMEs for ERP vendors, applications etc.Most of the time they do not even know what ERP systems are and what they can do. They consider ERP systems to be a magic wand, which will help solve all their business problems, be it in terms of quality, or process defects. ERP brings in a more disciplined execution of business process giving more transparency and visibility to the working of the organization.
- Perception: SMEs have the perception that ERP is meant only for large firms mainly owing to the high costs of acquisition, implementation and maintenance as also the complexity. Some of the SMEs even feel they do not need ERP.
- Earlier Implementations: SMEs have heard of the much-publicized failures in ERP implementation, which have led firms to bankruptcy. Some SMEs who have implemented ERP earlier have failed. This has led SMEs to believe that ERP implementations are a waste of time and effort and can even lead to the demise of company.
- Approach to implementation: ERP vendors' advice SMEs to mould the business to ERP's way of working, considering that ERP systems bring with it best business practices. This is the plain vanilla approach that was mentioned earlier, which would bring down the cost of implementation. But most SMEs have processes that they have evolved over time and hold very dear to their hearts.

As a result, SMEs are having the entire ERP system customized to meet their requirements. This would increase the overall cost of implementation. A good approach would be to keep the customization to a minimum.

- Cost: SMEs have less of capital than their larger counterparts.
- Change management: One of the major reasons why ERP implementations nationwide have been known to fail is due to the implementation being considered as an automation project instead of one that involves change management. This results in the system being put in place but not being used effectively due to people not ready to accept the change.
- Limited resources: Most SMEs do not have an in-house IT team. Due to this they have to rely on external agencies to help them and this adds to the implementation costs.

Before embarking on an ERP system journey, organizations have to ask themselves whether they are ERP ready. Some of the factors to be considered before starting an ERP system implementation are:

- Infrastructure resource planning
- Education about ERP
- Human resource planning
- Top management commitment Training facilities
- Commitment to release the right people for the implementation

These factors help organizations to understand their level of preparedness for an ERP implementation.

VI. CONCLUSION

ERP systems put in place a disciplined way of working and provide better visibility to the working of the organization. In India, SMEs are the backbone of the economy and are today faced with global competition. Therefore it becomes imperative for them to look for means of responding to the dynamic markets. ERP Systems have become the most common IT strategy for most large companies. SMEs too are moving towards ERP systems. They need to adopt a proactive approach towards ERP.

Though the ERP market is growing and ERP vendors have shifted their focus to the SME segment, there are several issues to be resolved. Firstly, SMEs need to be made 'ERP aware'. Vendors need to micro verticalise the ERP solution to better meet the requirements of SMEs. Since the financial resources of

SMEs are limited, the cost of ERP system needs to be further reduced. SMEs on their part need to carefully evaluate their current IT systems and document its shortcomings while creating a wish list of what they want to achieve. While these are some of the issues to be considered there are certainly many more which the authors hope to find in their further study. The conceptual model of ERP implementation in SMEs shown in Fig-2 is the procedure to adopt by them for successful implementation.

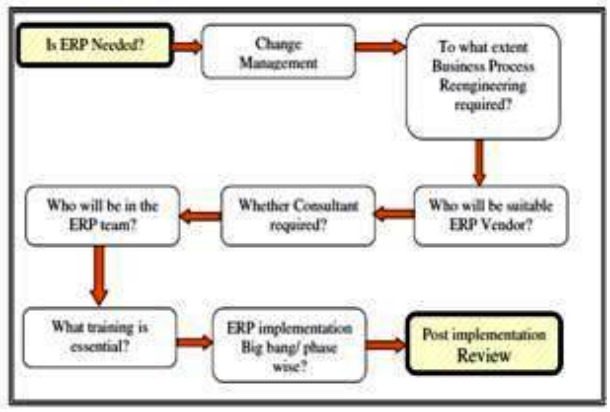

Fig. 2 : Conceptual model Of an ERP Implementation in SME's

REFERENCES

[1] Pandian T. K., (2006), "Big issues in ERP for small units", Business Line.

[2] Shehab E. M., Sharp M. W., Supramaniam L., Spedding T. A., (2004) "ERP: An integrative review", Business Process Management Journal, Vol. 10 (4), pp 359-86.

[3] Kale P. T., Banwait S. S., Laroiya S. C., (2007)" Enterprise Resource Planning Implementation".

[4] Davenport Thomas, (2000), "Mission Critical", Harvard Business Press.

[5] Garg Venkitakrishnan, (2006). "ERP Concepts and Practice", Prentice Hall India.

[6] Gupta A., (2000), "Enterprise resource planning: The emerging organizational value systems", Industrial Management & Data Systems, Vol. 100 (3), pp. 114-18.

[7] Kale P. T., Banwait S. S., Laroiya S. C., (2007), "Review of Key Performance Indicators of Evaluation of Enterprise Resource Planning System in Small and Medium Enterprises", XI Annual International Conference of Society of Operation Management, India.

[8] Leon A., (1999), "Enterprise Resource Planning", Tata McGraw-Hill.

[9] Levy Margi, Powell Philip, (2006), "Strategies for growth in SMEs: The role of Information and Information Systems", Information Processing and Management: an International Journal. Vol 42.

◈◈◈

Design and Improvement of Plant Layout

Ram D. Vaidya & Prashant N. Shende

Mech. Dept., YCCE, Nagpur
E-mail : ramdvaidya@gmail.com, prashant_sn1@yahoo.co.in

Abstract – This research aims to improve the plant layout of pipe shell and travelling roller manufacturing industry to make optimum space utilization, eliminate obstructions in material flow and thus obtain maximum productivity. The present layout and operation process of each section (i.e. material storage, cutting, welding, machining shop , fabrication shop, assembly and inspection section and finish product storage) have been investigated. The problem in the space utilization and material flow pattern was identified. The result showed that raw material section, cutting section and fabrication shops should be allocated to make the good material flow. The suitable of new plant layout can decrease the distance of material flow, which rises production.

Keywords – *Material Flow, Plant Layout, Production.*

I. INTRODUCTION

In industry sectors, it is important to manufacture the products which have good quality products and meet customers' demand. This action could be conducted under existing resources such as employees, machines and other facilities. However, plant layout improvement, could be one of the tools to response to increasing industrial productivities. Plant layout design has become a fundamental basis of today's industrial plants which can influence parts of work efficiency. It is needed to appropriately plan and position employees, materials, machines, equipments, and other manufacturing supports and facilities to create the most effective plant layout.

II. LITERATURE SURVEY

Anucha Watanapa [1], proposed an improve the plant layout of pulley's factory to eliminate obstructions in material flow and thus obtain maximum productivity. The present plant layout and the operation process of each section have been investigated. The problem in term of material flow of each operation section was indentified. The result showed that disassembly surface finishing and inspection sections should be allocated to make the good material flow. The suitable of new plant layout can decrease the distance of material flow, which rises production.

W.Wiyaratn and A. Watanapa [2], study plant layout of iron manufacturing based on the systematic layout planning pattern theory (SLP) for increased productivity. The detailed study of the plant layout such as operation process chart, flow of material and activity relationship chart has been investigated. The new plant layout has been designed and compared with the present plant layout. The SLP method showed that new plant layout significantly decrease the distance of material flow from billet cutting process until keeping in ware house.

R. Jayachitra and P. S. S. Prasad [3], study the suitability of a virtual cellular layout (VCL) along with an existing functional layout (FL) of an industry and a classical cellular layout (CL), if considered for implementation. A Genetic algorithm (GA) based intra-cell formation procedure is used in the cellular layout design. To identify the suitability of a particular layout in a given environment, a typical manufacturing system is modeled using the WITNESS 2006 simulation software. Design of experiments (DOE) is used to plan the simulation experiments.

Uttapol Smutkupt, and Sakapoj Wimonkasame [4], gives the simulation technique to plant layout design to show more information about the design such as total time in system, waiting time, and utilization. To add the simulation to a plant layout design, Microsoft Visual Basic is used to develop a design system based on CRAFT model.

III. PLANT LAYOUT PLANNING

A. Procedure for Plant Layout Design

The sequences of procedure following three steps were described.

1. The fundamental of plant layout was studied.
2. Machines are collected
3. The process for product production has been used in analysis.
4. The present plant layout was analyzed to identify the problem under flow material and operation.
5. The suggestions were collected to write the report and were proposed to authorize to make decision for rearrangement the plant layout

B. Company Details

Name-: Prasoon Industries
Location-: Sewagram MIDC, Wardha (Maharashtra)
Product-: Travelling Roller and Pipe Shell

Area statement-:
Plot area =10,805 SQMT
Build up area 50% = 5,402 SQMT
Factory shed area = 832.08 SQMT

Build up area-:
Ground floor = (12.92x8.69) + (3.23x5.86)
Total build up area =1540.68 SQMT

C. Analysis of Existing Layout

This case is based on the travelling roller manufacturing industry. The original layout of company is shown in figure 1. The details of each section were described as follows. In additional the size and number of equipments was relational to area as shown in Table 1.

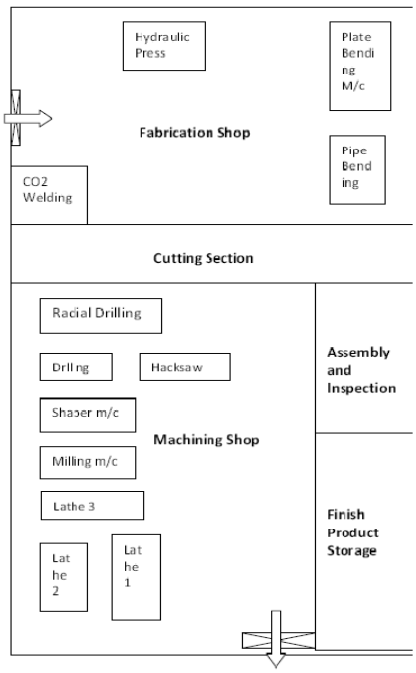

Fig. 1 : Existing Layout

Table1. Relationship between machine size and area

Machines	**Area**
Lathe m/c 1	(6.55×1.5) m^2
Lathe m/c 2	(3.3×0.8) m^2
Lathe m/c 3	(4.6×1.1) m^2
Shaper m/c	(2.1×1.2) m^2
Drilling m/c	(4.6×1.1) m^2
Power Saw m/c	(1.5×0.8) m^2
Radial drilling m/c	(2.5×1.2) m^2
Plate Bending m/c	(4.1×1.3) m^2
Pipe Bending m/c	(4.1×1.1) m^2

IV. ANALYSIS PLANT LAYOUT

According to the study of the manufacturing process, the details for flow of material, raw material storage, fabrication shop, machining shop, surface finishing, inspection sections, and material handling equipment were described as follows.

Flow of material from raw material storage to shipping is in irregular pattern and covers the indirect path, which results into more travelling distance.

Raw material storage is at outskirt area of plant, which creates problem in material handling and each time worker go outside to bring raw material.

Fabrication shop is the section approximated within (33.56×12.52) m2 area. Pipe shell is manufactured in these section.

Machining shop is section approximated within (33.56×12.52) m2 area. Travelling roller is manufactured in this section.

Assembly and inspection section for machining and fabrication shops are separate, which acquire more space and creates obstacle in flow of material.

CO2 welding machine is located in fabrication section which is useful for assembly. Existing position of CO2 welding machine creates an indirect path for machining shop and assembly section.

Cutting section is approximated with (12.52×7.96) m2 area. This section consists of arc welding, torch cutting (O2 Welding) and plug cutting machine (LPG welding).

Assembly and inspection section is approximated with (14.27×4.31) m2 area.

Finish product storage section is approximated with (18.40×4.31) m2 area.

After studying on the mentioned information, the new plant layout design is created by shifting raw

material storage area and fabrication shop (Fig. 2). In addition, the assembly and inspection section is improved for optimum space utilization.

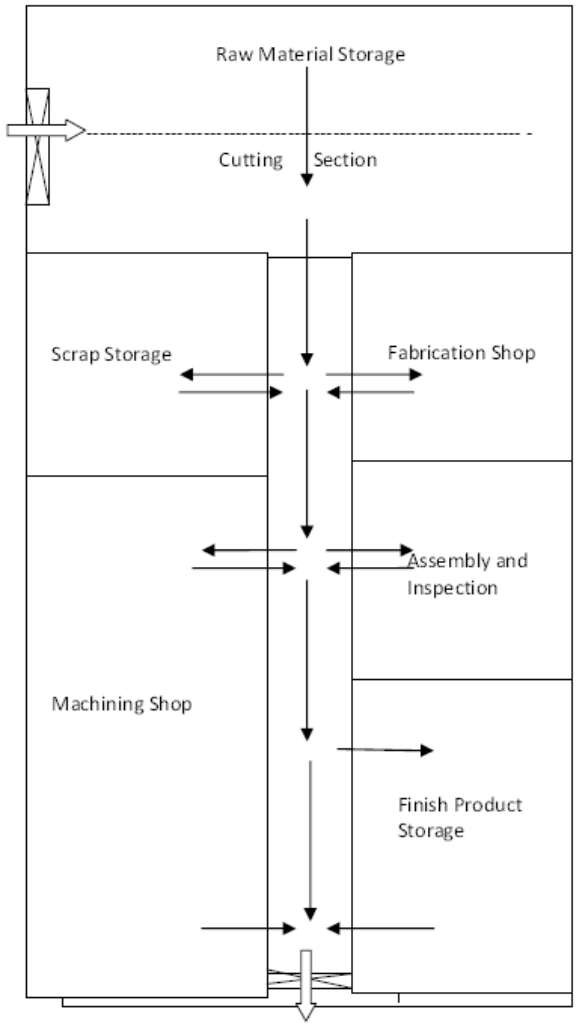

Fig. 2 : Propose layout

V. METHODOLOGY

In this research, proposed layout is design on the basis of operation process chart (fig. 3 & 4) of products pipe shell and travelling roller.

Load distance score method is quantitative technique for layout analysis use for optimum space utilization and reduced the travelling distance.

In this method, first load/Frequency matrix made based on department/machines.

Secondly, Distance matrix is made based on proposed layout.

Finally, total Distance Matrix is form, for analysis of layout. Load distance score method applied for both products pipe shell and travelling roller on the basis of their operation process chart (fig. 3 & 4).

Travelling Roller					
Operations	○	⇨	□	▽	Distance meter
Store					
Gas cutting					16.13
Hack saw cutting					40.07
Lathe1(machining)					
Lathe 2					30.57
Lathe 3					
Shaper(slots)					
Drilling					26.07
Radial Drilling(boring, drilling)					
Slotting					
Assembly & Inspection					15.17
Storage					
	Total				129.01

Fig. 3 : Operation process chart of Travelling Roller

Pipe Shell					
Operations	○	⇨	□	▽	Distance meter
Store					
Gas cutting					16.13
Hack saw cutting					36.92
Plate Bending					
Pipe Bending					
Hydraulic Press					28.89
CO2 Welding(Assembly)					23.43
Inspection					15.17
Storage					
	Total				120.54

Fig. 4 : Operation process chart of Pipe Shell

Operation process chart for pipe shell and travelling roller is investigated. In existing layout, indirect path is observed from storage area to cutting section. Total distance travel from raw material to finish product storage for pipe shell and travelling roller are 129.01 meter and 120.54 meter.

VI. CONCLUSION

According to the analysis of the workflow for the pipe shell and travelling roller, it was found that raw material storage, cutting section and fabrication sections should be modified for the layout for convenient workflow. The distance of workflow from the modified plant layout of their sections can be reduced. Not only improving workflow but also the accidents from objects which were not in order during material transportation can be decreased. Finally, rearranging layout decreased distance and time consumption in flow of material and accidents, resulting in an increase in productivity.

REFERENCES

[1] Anucha Watanapa, Phi chit Kajondecha, Patcharee Duangpitakwong , and Wisitsree Wiyaratn, "Analysis Plant Layout Design for Effective Production", International Multiconference of Engineers and Computer scientists (IMECS 2011) Vol II, Hong Kong.

[2] W. Wiyaratn, and A. Watanapa, "Improvement Plant Layout Using Systematic Layout Planning (SLP) for Increased Productivity", World Academy of Science, Engineering and Technology 72 2010.

[3] R. Jayachitra and P. S. S. Prasad, "Design and selection of facility layout using simulation and design of experiments", Indian Journal of Science and Technology, Vol. 3 No. 4 (Apr. 2010), 437-446.

[4] Uttapol Smutkupt, and Sakapoj Wimonkasame, "Plant Layout Design with Simulation", Proceedings of the International MultiConference of Engineers and Computer Scientists 2009 Vol II, IMECS 2009, March 18 - 20, 2009, Hong Kong.

[5] Dhamodharan Raman, "Towards measuring the effectiveness of a facilities layout", Robotics and Computer-Integrated Manufacturing 25 (2009) 191–203.

[6] Eida Nadirah Roslin and Ong Gee Seang, "A Study on Facility Layout in Manufacturing Production Line Using WITNESS", The 9th Asia Pasific Industrial Engineering & Management Systems Conference,(APIEMS 2008) 412-421.

[7] Kevin so, "Facility layout improvement", The university of British Columbia (2008), 1-37.

[8] Taho Yang, "Multiple-attribute decision making methods for plant layout design problem", Robotics and Computer-Integrated Manufacturing 23 (2007) 126–137.

[9] Stefan Bock, Kai Hoberg, "Detailed layout planning for irregularly-shaped machines with transportation path design", Elsevier, European Journal of Operational Research 177 (2007) 693–718.

[10] Amine Drira, Henri Pierreval,"Facility layout problems: A survey", Elsevier, Annual Reviews in Control 31 (2007) 255–267.

[11] Sukanto Bhattacharya, "Optimal Plant Layout Design for Process-focused Systems", School of Information Technology Bond University, Australia (2002) 1-13.

[12] Hamed Tarkesh, "FACILITY LAYOUT DESIGN USING VIRTUAL MULTI-AGENT SYSTEM" Proceedings of the Fifth Asia Pacific Industrial Engineering and Management Systems Conference (2004).

[13] Pedro M. Vilarinho, "A Facility Layout Design Support System", Departamento de Economia, Gest~ao e Engenharia Industrial, Universidade de Aveiro (2003).

[14] C.N. Potts and J.D. Whitehead, "Workload balancing and loop layout in the design of a flexible manufacturing system", European Journal of Operational Research 129 (2001) 326-336.

[15] Robin S. Liggett, "Automated facilities layout: past, present and future", Automation in Construction Elsevier 9,197–215, (2000).

[16] Saifallah Benjaafar and Mehdi Sheikhzadeh, "Design of Flexible Plant Layouts with Queueing Effects", Department of Mechanical Engineering University of Minnesota, Minneapolis (1997), MN 55455.

[17] Andrew KUSIAK and Sunderesh S. HERAGU, "The facility layout problem", European Journal of Operational Research 29, North-Holland (1987) , 229-251 .

◈◈◈

A Suggested Stress Analysis Procedure for Nozzle to Head Shell Element Model – A Case Study

Sanket S. Chaudhari & D.N. Jadhav

Sardar Patel College of Engineering
E-mail : mechanical.sanket@gmail.com, d_jadhav@spce.ac.in

Abstract – Stress analysis of pressure vessel has been always a serious and a critical analysis. The paper performs a standard procedure of pressure vessel analysis and validation based on previous papers. It also demonstrates the most critical part and how it affects entire structure. Relevant ASME (ASME, 2004, ASME Boiler and Pressure Vessel Code, Section VIII, Division 2, American Society of Mechanical Engineers, New York) norms are produced to explain analysis procedure. WRC (Welding research council) methodology is explained to validate finite element analysis work

Keywords – *Design by analysis, Finite element analysis, Membrane and bending stresses*

I. INTRODUCTION

This document summarizes and expands upon earlier papers by Hechmer and Hollinger [1]and incorporates the stress linearization concepts published by Kroenke [2] and Kroenke et al. [3]. Together, work explained here gives a demonstration of pressure vessel procedure for analysis by Porter [4] . The analysis of pressure vessel is generally done with 3D modeling and relevant elements. It needs to model welding attachment separately; stresses obtained from these elements are not membrane and bending stresses hence modeling and output calculations are required to give more attention. The suggested procedure reduces all efforts of modeling and post processing work. A case study presented in this paper is a project carried out on a hydrogen storage tank.

II. LITERATURE REVIEW

The spherical shells are widely used in chemical industry. Opening and nozzle on spherical shells are important for illustration, process and inspection [5]. They will not only weaken the strength of spherical shell but also generates boundary stress on the joint of vessel nozzle, leading to sever stress concentration [6] [7]. So the joint is most vulnerable part to failure. It's of great importance to study the influence of various parameters on stress distribution of the openings and nozzles. Many experts and scholars have done a lot of research with finite element technique [8] [9] [10]. Due to different loadings applied to these structures, a local stress state of the nozzle connection characterized by high stress concentrations occurs in the intersection region [11] The action of mechanical and thermal loads leads to high local stress in the intersection region, thus resulting in stress concentrations there. Additional difficulties can arise due to welding and this region thus becomes the weakest point and the source of failure of the entire structure [12]. Cylindrical shells with nozzles are commonly used in many industries. The significant stress concentration almost always occurs in the vicinity of the nozzle-to-shell junction due to the inherent structural discontinuity that is formed by the intersection. [13]

As to the cases of the cylindrical shells subjected to external branch pipe loads, Lekkerkerker [14] obtained the analytical solutions based on shallow shell equation, but no design method and data are presented. Based on Timoshenko's equation, Bijlaard [15] obtained a thin shell theoretical solution for a simply supported cylindrical shell without a nozzle or cutout, subjected to local loading.

Cottam and Gill [16] carried out 11 tests, to rupture, on mild steel cylindrical pressure vessels with flush nozzles. Two cylindrical vessels without nozzles were also tested to establish datum curves for the vessels with nozzles. Rodabaugh [17] summarized 31 available burst test data and failure locations on basic configuration pipe connections. The basic configuration was a pipe connection consisting of a run pipe with a uniform-wall branch pipe; there was no pad or any other type of reinforcement other than that provided by a fillet weld

on the outside surface of the intersection. Burst tests were conducted on two cylindrical shell intersections (90 deg intersections and 30 deg laterals) by Sang [18].

Nozzle to head attachment will not only weaken the strength of spherical shell but also generates boundary stress on the joint of vessel nozzle, leading to sever stress concentration [6] [7]. Many experts and scholars have done a lot of research with finite element technique [8] [9] [10].

Blachut and Vu [19] computed the burst pressure of shallow spherical caps and torispheres loaded by uniform pressure. Bursting was determined using the ABAQUS code with axisymmetric shell elements and defined using plastic strain criteria taken from one dimensional true stress and strain curves. Results were benchmarked against the experimental data. The use of nonlinear FEA to predict the failure pressure of real corrosion defects was investigated by Cronin [20] using the results from 25 burst tests of pipe sections removed from service due to the presence of such defects. The author concluded that the elastic-plastic FEA provided an accurate prediction of the burst pressure and the failure location for complex-shaped corrosion defects.

III. WHAT IS REQUIRED AND HOW?

It is required to identify and to pay more attention on critical region. Once it is defined then cause of failure i.e. stresses induced should be evaluated. It is very important to make a vessel which will work safely for predefined time period. Hence it is prime objective to find stresses induced in vessel. From the literature survey presented here it is very clear that intersection of nozzle to head junction is the most critical part.

Now how is this possible to determine actual stresses in the vessel? The most logical choice is to do experiment on the model. The choice is very costly, time consuming and sometimes not practical. Finite element analysis provides output close to that of experimental values. But it should be done very carefully to get accurate results. If wrong boundary conditions are applied at wrong place then analysis will not give real practical values. Hence it is very important to validate the Finite element analysis. To verify FEA output WRC (Welding research council) bulletin is used.

IV. A SUGGESTED METHOD OF ANALYSIS

The method of least effort, more accurate and reliable output becomes right approach; saving in time and giving desired results. To achieve such a goal a suggested method is to use shell element analysis with medium mesh carried out according to ASME (American society of mechanical engineers) section 8 Division 2 and, a WRC calculation.

Shell/Plate elements are specially developed to have membrane stresses and bending stresses as an output. [21] Ha has indicated that with a minimum of 96 elements around the periphery of a nozzle, convergence is assured.

It reduces effort to get membrane and bending stresses because stress linearization is not required to perform. To begin investigation ASME guidelines are very important. Some of the relevant norms are presented here.

V. ELASTIC STRESS ANALYSIS METHOD [22]

To evaluate protection against plastic collapse, the results from an elastic stress analysis of the component subject to defined loading conditions are categorized and compared to an associated limiting value. The basis of the categorization procedure is described below.

I. A quantity known as the equivalent stress is computed at locations in the component and compared to an allowable value of equivalent stress to determine if the component is suitable for the intended design conditions. The equivalent stress at a point in a component is a measure of stress, calculated from stress components utilizing a yield criterion, which is used for comparison with the mechanical strength properties of the material obtained in tests under uni-axial load.

II. The maximum distortion energy yield criterion shall be used to establish the equivalent stress. In this case, the equivalent stress is equal to the Von-Mises equivalent stress given in (1)

$$S_e = \sigma_e = \frac{1}{\sqrt{2}}[(\sigma_1 - \sigma_2) + (\sigma_2 - \sigma_3) + (\sigma_3 - \sigma_1)]$$

The outputs of the stresses are shown in results. The ASME section VIII Division 2 says the limit load is obtained using a numerical analysis technique (e.g. finite element method) by incorporating an elastic-perfectly-plastic material model and small displacement theory to obtain a solution [22].

Consider the case presented here has following loading

Pressure = 3.266 MPa

Table I Loading Condition

Force	Moment
F_X = - 6621.8 N	M_X = 9816500 N.mm
F_Y = 9811.1 N	M_Y = 7850500 N.mm
F_Z = 9811.1 N	M_Z = 5886500 N.mm

The model configuration is as follows

Table II Model configuration

Material Name	SA-387 12
Composition	1Cr-0.5Mo
UNS	K11757
Type / Grade	12
Material Density Kg/ cm^3	0.0077504
Allowable stress at design temperature N/ mm^2	132.94
Modulus of Elasticity N/mm^2	199270

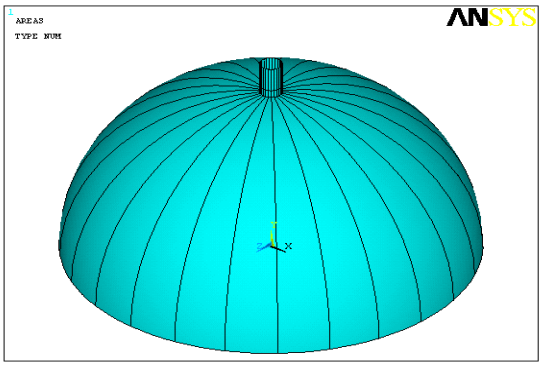

Fig. 1 : Nozzle to head model

The shell element is used for the analysis. The reason of selecting shell element is output from the element are linearized. Other elements' outputs are required to be linearized. If shell element is used then equivalent stresses form middle and top layers should be selected for membrane stresses and bending stresses respectively.

A detailed stress analysis performed using a numerical method such as finite element analysis typically provides a combination of $P_L + P_b$ and $P_L + P_b + Q + F$ directly [22] . Here Fatigue case is not induced. The output shown is of $P_L + P_b$.

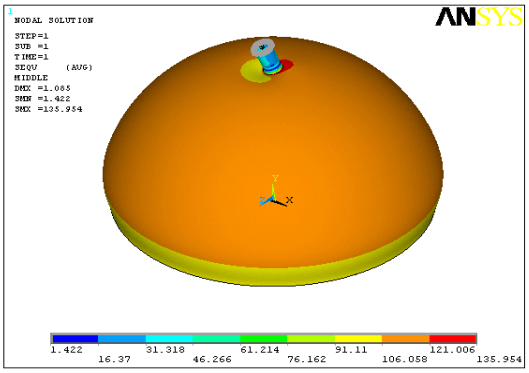

Fig. 2 : Membrane stress

Figure shows membrane stresses. The result is obtained from middle layer. According to ASME

Table III Membrane stress output

Nature	Primary membrane stresses N/mm^2	Allowable Stresses N/mm^2	Result
General	68	132.94	Pass
General and Local	135.954	199.41	Pass

Bending stresses from the top layer are found as follows

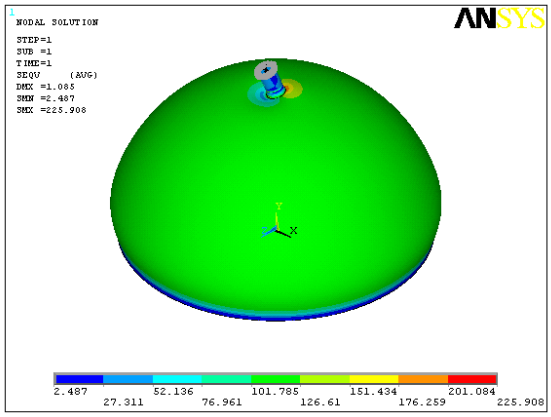

Fig. 3 : Bending stress

Table IV Bending stress result

Primary membrane + secondary stresses N/mm^2	Allowable Stresses N/mm^2	Result
225.908	398.82	Pass

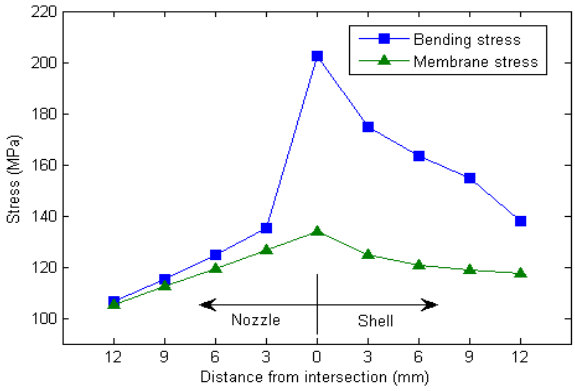

Fig. 4 : Stress distribution near attachment junction

VI. WRC

Welding research council has carried out number of analytical as well as experimental study of intersecting bodies. It has developed several charts, which provides experimental values of stresses induced near intersection as a dimensionless number. Hence it is very important to evaluate stress values by WRC to get experimental value. The analysis and experimental values should be close in order to validate the FEA work. The loading condition in WRC calculations are shown in fig. 4 (a) and (b).

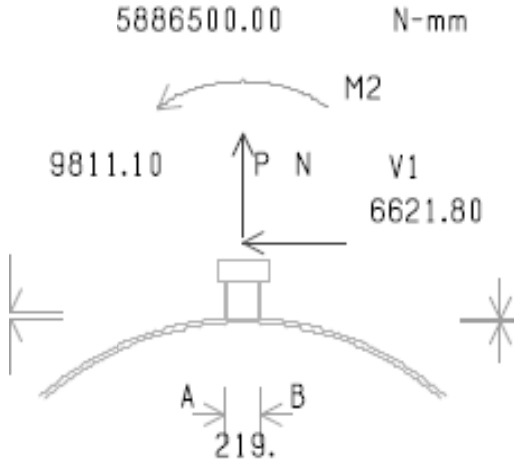

Fig. 5 : Loading condition in WRC (a)

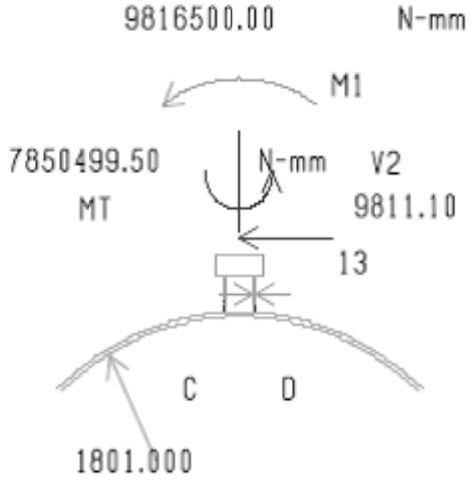

Fig. 5 : Loading condition in WRC (b)

WRC objects to calculate dimensionless parameter. With the help of these dimensionless parameters relevant chart is used and membrane and bending stresses are obtained. Following table shows values obtained from curve for the model considered.

Table V WRC dimensionless values

Curves read for 1979	Curve	Value	Location
$\left(\frac{N_x T}{P}\right)$	SP 4	0.07166	(A,B,C,D)
$\left(\frac{M_x}{P}\right)$	SP 4	0.02934	(A,B,C,D)
$\frac{N_x T\sqrt{R_m T}}{M_1}$	SM 4	0.23295	(A,B,C,D)
$\frac{M_x\sqrt{R_m T}}{M_1}$	SM 4	0.10384	(A,B,C,D)
$\frac{N_x T\sqrt{R_m T}}{M_2}$	SM 4	0.23295	(A,B,C,D)
$\frac{M_X\sqrt{R_m T}}{M_2}$	SM 4	0.10384	(A,B,C,D)
$\left(\frac{N_y T}{P}\right)$	SP 4	0.35112	(A,B,C,D)
$\left(\frac{M_y}{P}\right)$	SP 4	0.16223	(A,B,C,D)
$\frac{N_y T\sqrt{R_m T}}{M_1}$	SM 4	0.18854	(A,B,C,D)
$\frac{M_y\sqrt{R_m T}}{M_1}$	SM 4	0.67774	(A,B,C,D)
$\frac{N_y T\sqrt{R_m T}}{M_2}$	SM 4	0.18854	(A,B,C,D)
$\frac{M_y\sqrt{R_m T}}{M_2}$	SM 4	0.67774	(A,B,C,D)

On calculating stresses following result is obtained.

Table VI WRC Result

Type of Stress intensity	Max. S.I.	S.I. Allowable	Result
P_m (SUS)	60.1	132.94	Pass
$P_m + P_l$ (SUS)	133.6	199.41	Pass
$P_m + P_l + Q$ (SUS)	249.47	423.84	Pass

On comparing WRC and FEA results it can be concluded that analysis performed according to ASME section 8 Division 2 design by analysis by shell element found to be accurate.

Type of Stress intensity	WRC	FEA	S.I. Allowable	Result
P_m	60.1	68	132.94	Pass
$P_m + P_l$	133.6	135.954	199.41	Pass
$P_m + P_l + Q$	249.47	225.908	423.84	Pass

VII. RECOMMENDED ASSESSMENT PROCEDURE [4]

In order to assess the stress in a thin wall (r / *t* and *R*/*T* > 10) Nozzle/shell junction using FE and shell elements, the authors recommend that the following procedure be followed:

1. The nozzle should be modeled using shell elements with a minimum of 96 elements around the circumference of the nozzle. This assumes that linear plate elements are being employed. If higher order shell elements are used, a lesser number of elements may be required. A convergence analysis or some other verifiable check must be employed to assess the element behavior if fewer elements are employed.
2. The model should be constructed to ensure that a row of nodes is located at a distance of 1.5*t* from the junction on the shell side and P+t on the nozzle side.
3. The elements used should have a length-to-width aspect ratio less than 2.0.
4. No transition in element size should be made within the pad area and/or within $\sqrt{rt}$ or ten times the thickness, whichever is greater_ of the intersection on the nozzle and shell, respectively.
5. All operating loads, including gravity, pressure, thermal and external forces, and moments, should be applied to the model for the surface stress intensity (3*Sm*) check. The local membrane under combined loading should also be evaluated at the junction ring.
6. The computed stress intensity on the lines of elements 1.5t on the shell and P+t on the nozzle shall be compared with the 3*Sm* criterion. If the indicated stress intensities do not exceed the criterion level, the nozzle meets the code requirements.
7. Note: The $3S_m$ criterion is based on a range of stresses. In the case of thermal loading, it may be necessary to consider several loading conditions to evaluate the proper range.
8. The above procedure assumes that the engineer will employ the proper elements and verification methods to ensure the validity of the FE model used for the analysis

VIII. NOMENCLATURE

P = pad thickness

P_m = General membrane stress

P_L = local membrane stress

P_b = bending stress

Q = secondary stress

r = radius of nozzle (also used for generalized radius and radius of weld)

R = radius of shell

S_m = allowable stress

t = thickness of nozzle (also used for generalized thickness)

T = thickness of shell

REFERENCES

[1] J. L. Hechmer and G. L. Hollinger, "The ASME Code and 3D Stress," ASME Journal of Pressure Vessel Technology, vol. 113, pp. 481-487, 1991.

[2] W. C. Kroenke, "Classification of Finite Element Stresses According to," Pressure Vessels and Piping, Analysis and computers, pp. 107-140, 1974.

[3] W. C. Kroenke, G. W. Addicott, and B. M. Hinton, "Interpretation of Finite Element Stresses According to ASME Section III," ASME Paper No.75-PVP–63, pp. 1-12, 1975.

[4] M. A. Porter, D. H. Martens, and S. M. Caldwell, "A Suggested Shell/Plate Finite Element Nozzle Model Evaluation Procedure," Journal of Pressure Vessel Technology, vol. 130, Aug. 2008.

[5] C. J. Dekker and H. J. Brink, "Nozzle on spheres with outward weld area under internal pressure analyzed by FEM and thin shell theory," International Journal of Pressure vessel and Piping, pp. 399-415, 2000.

[6] S. Schindler and J. L. Zeman, "Stress concentration factors of nozzle-sphere connections," International Journal of Presseure vessel and Piping, vol. 80, pp. 87-95, 2003.

[7] J. S. Liu, G. T. Parks, and P. J. Clarkson, "Shape optimization of axisymmetric cylindrical nozzle in spherical pressure vessel subjected to stress constraints," International Journal Journal of Pressure vessel and technology, vol. 78, pp. 1-9, 2001.

[8] E. weib and J. Rudolph, "Finite element analyses concerning the fatigue strength of nozzle to spherical shell intersection," International Journal of Pressure vessel and Piping, vol. 64, pp. 101-109, 1995.

[9] J. Jayaraman and K. P. Rao, "Thermal stresses on spherical shell with a conical nozzle," Nuclear Eng. Des., vol. 48, pp. 367-375, 1978.

[10] Y. J. chao and M. A. Sutton, "stress concentration factors for nozzle and ellipsoidal pressure heads due to thrust loads," International journal of pressure vessel and piping, vol. 19, pp. 69-81, 1985.

[11] V. N. Skopinsky and A. B. Smetankin, "Modeling and stress analysis of nozzle connections in ellipsoidal heads of pressure vessels under external loading," International Journal of Applied Mechanics and Engineering, vol. 11, no. 4, pp. 965-979, 2006.

[12] L. Xue, G. E. O. Widera, and Z. Sang, "Parametric FEA Study of Burst Pressure of Cylindrical Shell Intersections," Journal of Pressure Vessel Technology, pp. 1-7, 2010.

[13] M.-D. Xue, Q.-H. Du, and K.-C. H. Z.-H. Xiang, "An Analytical Method for Cylindrical Shells With Nozzles Due to Internal Pressure and External Loads—Part I Theoretical Foundation," Journal of Pressure Vessel Technology, vol. 132, pp. 1-9, 2010.

[14] J. G. Lekkerkerker, "The Determination of Elastic Stresses Near Cylinder-to-Cylinder Intersection," Nuclear Eng. Des., vol. 20, pp. 57-84, 1972.

[15] P. P. Bijlaard, "Stresses From Local Loading in Cylindrical Pressure Vessels," Tran. ASME, pp. 805-812, 1955.

[16] W. J. Cottam and S. S. Gill, "Experimental Investigation of the Behavior Beyond the Elastic Limit of Flush Nozzle in Cylindrical Pressure Vessels," Journal of Mechanial Eng. Sci., pp. 330-354, 1966.

[17] E. C. Rodabaugh, "A Review of Area Replacement Rules for Pipe Connections in Pressure Vessels and Piping," Weld. Research Council Bull. No. 335., 1988.

[18] Z. F. Sang, L. Xue, Y. Lin, and G. E. O. Widera, "Limit Analysis and Burst Test for Large Diameter Intersections," Weld. Res. Counc. Bull., No. 451, 2000.

[19] J. Blachut and V. T. Vu, "Burst Pressures for Torispheres and Shallow Spherical Caps," Strain, vol. 43, pp. 26-36, 2007.

[20] D. S. Cronin, "Finite Element Analysis of Complex Corrosion Defects," Pressure Vessel and Piping, Computational Mechanics: Developments and Applications, vol. 441, pp. 55-61, 2002.

[21] J. L. S. B. C. ,. a. K. B. Ha, "Local Stress Factors of a Pipe-Nozzle Under Internal Pressure," Nuclear Engineering and Design, vol. 157, pp. 81-91, 1995.

[22] ASME, "ASME Boiler and Pressure Vessel Code," vol. Section VIII, Division 2, 2011.

[23] R. K. Wichman, A. G. Hopper, and J. L. Mershon, "Welding Research council Bulletin 107," 2002.

[24] K. Weicker, R. Salahifar, and M. Mohareb, "Shell analysis of thin-walled pipes-I.Field equations and solution.," International Journal of Pressure Vessel and Piping, vol. 87, pp. 402-13, 2010.

[25] S. Timoshenko, Theory of Plates and Shells. New York: McGraw-Hill, 1940.

[26] ASME, ASME Section II, Part D, Properties (Metric) Materials. New York: ASME, 2010.

◈◈◈

FEA of Rectangular Cup Deep Drawing Process

Awad D.S.[1], Poul A.D.[2], Wankhede U.P.[3] & V. M. Nandedkar[4]

[4]Professor in Production Engineering Department,
[1,2,3,4] Shri Guru GobindSinghji Institute of Engineering & Technology, Vishnupuri, Nanded, 431 606
E-mail : dsawad011@gmail.com, abhijitpoul@gmail.com, uw0160@gmail.com, vilas.nandedkar@gmail.com

Abstract – Deep drawing is a process for shaping flat sheets into cup shaped articles without fracture orexcessive localized thinning. The complex deep drawing of thin metallic sheets is widely used during industrial material forming applications. It allows production of thin walled parts with complicated shapes such as automotive panels or structural parts. The process consists of the plastic deformation of an initial at blank subjected to the action of a rigid punch and die while constrained on the periphery by a blank holder. Conventional design processes for sheet metal forming are usually based on a empirical approach. However, due to the requirement of high precision and reliability in shaped parts, these methods are far away from a final and reliable solution. Nowadays, Finite Element Method (FEM) is being gradually adopted by industry to envisage the formability properties of sheet metals.

The design and control of a deep drawing process depends not only onthe work piece material, but also on the condition at the tool work piece interface, the mechanics ofplastic deformation and the equipment used.

In this paper, rectangular cup component of EDDQ Steel and Mild Steel is simulated using HYPERMESH 11 by varying various process parameters

Keywords*: Finite Elements Analysis, Deep drawing, simulation*

I. INTRODUCTION

In deep drawing process final part is exactly defined by its dimensions, tolerances and mechanical properties. In order to achieve the production with low costs it is necessary to control the production in every single detail. We need a detailed understanding of the parameters affecting the production process and the final product.

Technology preparation phase of deep drawing process includes:

- prediction of fracture,
- prediction of wrinkling
- prediction of final sheet thickness,
- determination of optimal initial blank geometry,
- Evaluation of loads on the tool.
- Prediction of surface deflection.

The most used numerical method for numerical simulation of the forming process is finite elements method (FEM). The numerical simulations included the evaluation of the influence of various factors on the production process, the analysis of various test geometry, as well as the evaluation of loads on the production process. The problems of deep-drawing process are studied on the simple rectangular cup example. The method of using finite element softwareAltair HYPERMESH [1].

II. SIMULATION OF DEEP DRAWING PROCESS:

Finite element method used to simulate the rectangular cup deep drawing process. In this paper the finite element method software HYPERMESH, commercially available software for rectangular cup drawing process. The punch, die, blank and binder are discretized using finite element [2].

The material properties, punch speed, friction and blank holding pressure are provided as input for simulation. The strain and displacement are the outputs of simulation.

Geometry contains four components are

1. Die
2. Blank
3. Binder
4. Punch

Table- I : Geometry definition of model

Blank Size[mm^2]	540*614
Thickness of Blank[mm]	1
Blank Holder force[N]	50000
Die Size[mm^2]	282*366
Punch Size[mm^2]	280.95*364.955

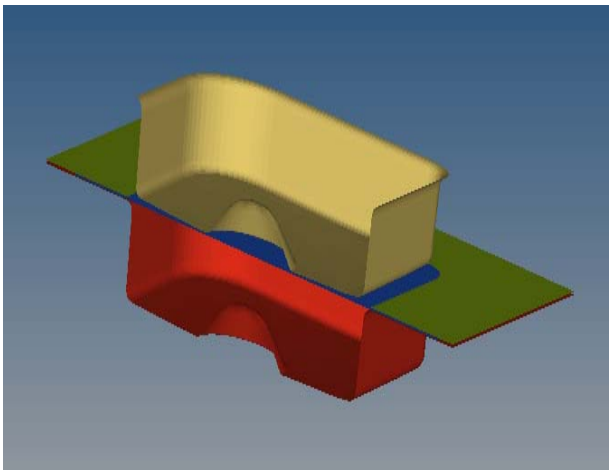

Fig. 1: Geometry of components

2.2 CONTACTS

Contact surfaces used here are:

- Top blank – bottom punch
- Top blank – bottom binder
- Bottom blank – top die

2.3 MESHING

Meshing is critical operation in FEA so it has done precisely and carefully.

Table II. Fine meshing size

Tool Meshing	
Minimum edge length[mm]	0.5
Maximum edge length[mm]	30
Fillet angle	15^0
Chordal deviation	0.1
Blank	
Average edge length[mm]	30

2.4 MATERIAL PROPERTIES

Tools are assumed as rigid, so there is no need to define material, but for blank it has to be defined

Table III. : Material Properties

Properties\Material	**EDDQ-STEEL**	**MILD STEEL**
Young Modulus(E)	210000	21000
Poission's Ratio(μ)	0.3	0.3
Density(rho)	7.8e-06	7.8e-6
Ultimate tensile strength(UTS)	309.57	311.4
Yield strength(YS)	154.44	173.1
Strain hardening exponent(n)	0.25	0.22
Plastic Strain ratio(r)	1.9	1.5

2.5 POSTPROCESSING

The important results obtained from this simulation are:

- Displacement
- % thinning of blank sheet
- Von mises Stresses
- Thickness distribution

III. RESULTS

1. FOR EDDQ STEEL

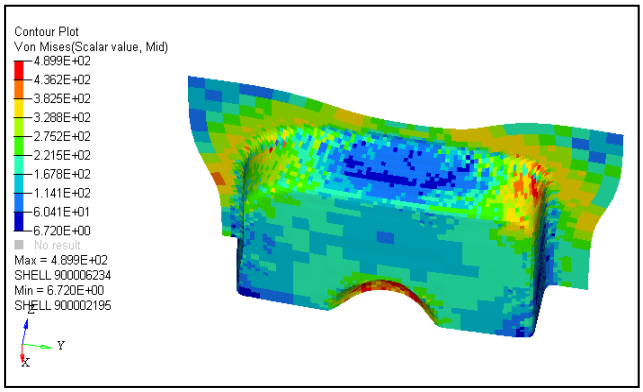

Fig 2. : Distribution of stresses (Von mises) after finished drawing operation for EDDQ Steel

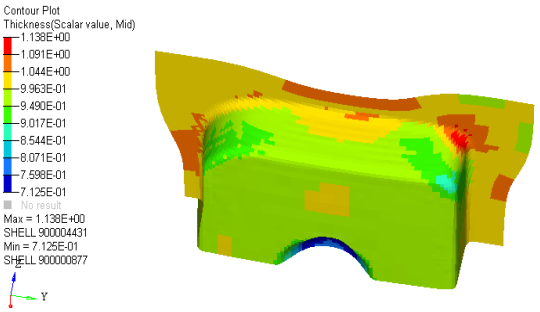

Fig. 3 : Distribution of thickness after finished drawing operation for EDDQ Steel

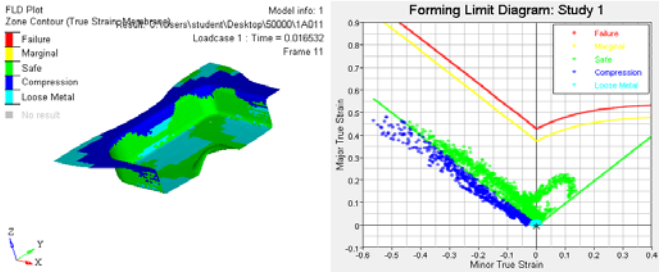

Fig. 4 : Forming limit Diagram for EDDQ

2. FOR MILD STEEL

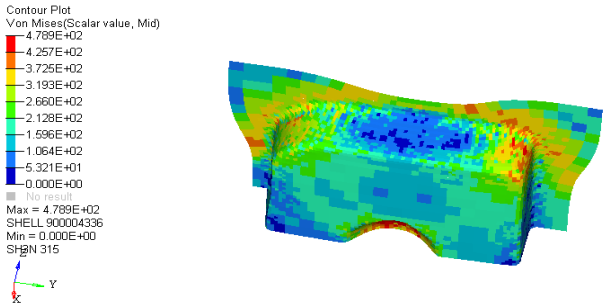

Fig. 5 : Distribution of stresses (Von mises) after finished drawing operation for MILD Steel

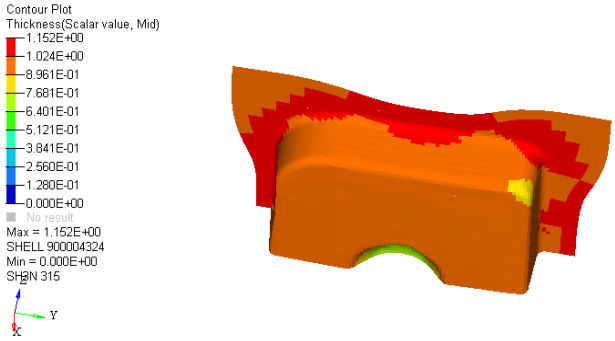

Fig. 6 : Distribution of thickness after finished drawing operation for MILD Steel

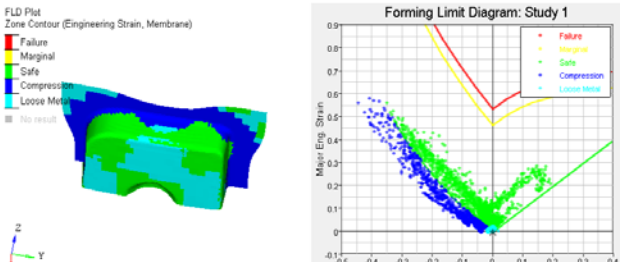

Fig. 7 : Forming limit Diagram for MILD Steel

Table – IV : Comparison of two materials

Properties	EDDQ		MS	
	Maximum	Minimum	Maximum	Minimum
THICKNESS [mm]	1.138	0.712	0.896	0.52
% THINNING	28.75	4	33.61	2
STRAIN	0.7186	0.08007	0.7339	0.08154
VON MISES STRESS [N/mm^2]	489.9	6.72	478.9	0

IV. CONCLUSION

In this paper, finite element analysis of rectangular cup for two materials EDDQ Steel and Mild Steel is carried out. The safe region for two materials is determined.By comparing EDDQ and MILD STEEL the stresses induced in EDDQ material is more as compare to mild steel but it is less than failure stresses, % thinning of EDDQ material is less, final thickness of component produced from EDDQ material is more.Therefore strength of component produced from EDDQ is more. Hence EDDQ is best material for deep drawing operation.

In material with high strain hardening coefficient (n) value, the flow stresses increases rapidly with strain, these results in the distribution of strain uniformly throughout the sheet and even in low strain area. As a consequence due to uniform deformation, formability increases. Therefore EDDQ Steel has more formability than MILD Steel.

REFERENCES

[1]. Dr.Sc. AmraTalić – ČikmišMuamerTrako, MladenKarivan(11-18 September 2010), Finite element analysis of deep drawing, 14th International Research/Expert Conference ”Trends in the Development of Machinery and Associated Technology”TMT 2010, Mediterranean Cruise.

[2]. A C Sekhara Reddy, Anoop Kumar Sukla, PavanKumar(December 2004), Optimization of blank shape in Square cup deep drawing process, Parametric finite element analysis of deep drawing-Hyderabad(AP).

[3]. F.Ayari, E.Bayraktar (2011.), Parametric finite element analysis of deep drawing September

[4]. Altair Hyper Works Students Manual

◈◈◈

To Improve Productivity By Using Work Study & Design A Fixture In Small Scale Industry

Mayank Dev Singh, Shah Saurabh K, Patel Sachin B, Patel Rahul B & Pansuria Ankit P

Abstract – The purpose of this research is to improve production capabilities for small scale industry and this research focused on the company, which produce Stay vane of Francis turbine. This research used work study technique to improve work process in company, and the research objectives towards accomplished this study is to identify problems in the production work process and improved it in terms of production time, number of process and production rate by proposing an efficient work process to company. This research used systematic observation, flow process and stopwatch time study as research methodology. Pro-E model software used for model testing and develop new model. The improvement of work process was executed by eliminating and combining of work process, which reduces production time, number of process and space utilization.

Field of research: *Production time, Productivity, Work study, Work measurement, Design of model.*

I. INTRODUCTION

1.1 Background of study

Industry consists of small numbers of employees and annual turnover. They can categorize into three criteria – primary agriculture, manufacturing and services. The company produces Stay Vane on vertical machining center. The small of its enterprise caused difficult for them to competing with other firmed companies. Thus, this research takes initiative to used work study technique to improve the work process in order to permit them to compete with international rivalry. The work study will examine the work process and eliminate nonproductive process, which can reduce number of process, space utilization and production and operation time. Time is important in production industry because according Fred (1992), time is money and time tells us exactly how much money was used. Besides that, this research was conducted based on industry development strategies and encouragement.

1.2 Scope of study

The scopes of this research are:

- This study concentrates on small scale industry, which is the company produced Stay vane of Francis turbine.
- The research is focused on time and the flow of work process in production department from the start until it produces finish products, which it will concentrate on production time and number of work process.

The data that needs to be carried out in this study is flow process of the work, the details for each process, the required time for specific process, number of stay vane that they produced in specific time

II. LITERATURE REVIEW

According to Abdul Talib Bon and Aliza Ariffin they are working on “An impact of time and motion study on small medium enterprise”.The purpose of this research to improve work process in small medium enterprise industries. In that they use time and motion study to improve work process in small medium enterprise industries. The improvement of work process was executed by eliminating and combining of work process, which reduces production time, number of process and space utilization.

They conclude that these modeling techniques are not designed to facilitate productivity measurement and analysis as they focus on the availability of the unit/equipment, which is only one aspect of the system performance. Among all the continuous improvement methodologies surveyed, no single methodology can be crowned as the best. The approach would help factory professionals to systematically perform factory diagnostics by quantitatively focusing on critical areas constraining manufacturing system productivity.

According to Charles F. Keberdle set up reduction is to reduce machine down time. Reducing setup time will boost your company's capacity, increase your manufacturing flexibility, and help increase overall output. A simple saying I often use is, "*If the machine is not running, you are not making money"*.

They conclude that there are several benefits of reduction of machine setup and changeover time which are listed below:

1. Shorter lead time and increased capacity
2. Better quality/more-consistent processes
3. Lower manufacturing costs
4. Fewer inventories
5. Increased flexibility
6. Better workforce utilization
7. Less process variability

2.1 Productivity

According to Eatwell and Newman (1991) defined productivity as a ratio of some measure of output to some index of input use. Put differently, productivity is nothing more than the arithmetic ratio between the amount produced and the amount of any resources used in the course of production.

Productivity = total output/total input which is identical to total results achieved/total resources consumed or effectiveness or efficiency.

2.2 Time study

According to Frederick W. Taylor (1880) they are working on time study by using a stopwatch to study and measure work content with his purpose to define "a fair day's work." Among his study is 'Taylor Shovelling Experiment' which they studied between 400and 600 men that using their own shovel from home to moving material from mountains of coal, coke and iron ore in around two mile-long yards. Purposes of Taylor to identify that there have different size of shovels and which shovel was the most efficient. Thus analyzing it using stopwatch the results were fantastic which it reduced time, saving numbers of workers and budgeting for every year.

2.2.1 Stop-watch time study

This method involves making direct observation by means of a stop-watch.the main steps that are required to be taken under this method are:

1. Check that the prescribed method is being followed in doing the job.
2. Divide the job observable and distinct element.
3. Choosing an appropriate operator, record the timing for each the work elements.
4. Rate the performance of the operator in each element and repeat measurement through a statistically, determined number of cycles of the job.
5. Based on the observations, compute the normal time for a unit of out.

III. PROBLEM STATEMENT AND OBJECTIVE

3.1 Problem statement

The company use vertical machining center in producing their stay vanes, where most of their work process was done manually by their workers. Sometimes, the production takes extra time in producing the stay vane. Moreover, the production department does not have any fixed or standard time for each process. They just decide and estimate the time for each process. Because of that, they often take longer than the time estimated. Also they have not proper methods for setting up the job on the machine bad. So the position of job may change at every cycle of production. This will affect the total job setup time at every cycle of machining, overall number of production of stay vane and also affect the overall production rate. Thus, it might be difficult for them to increase productivity and competes with other rivals.

The production method used currently in the company is time consuming as well as cumbersome. In order to reduce time and make the process simple, we applied various methodologies (Work study) and designed the new fixture accordingly. The new fixture so designed reduced the overall time period from job set up time to final dispatch.

3.2 Objectives

1. Identify the proposed methodology which reduces manufacturing lead time.
2. To design the template fixture in pro-e for vertical machining center.
3. Compare time study of both method and analyses on production.
4. Improve productivity by implementing new method.
5. Cost analysis of fixture components and analysis of net profit to the company.

IV. DATA COLLECTION

4.1 Plant layout

Plant layout refers to the arrangement of physical facilities such as machines, equipment, tools, furniture etc. in such a manner so as to have quickest flow of material at the lowest cost and with the least amount of handling in processing the product from the receipt of raw material to the delivery of the final product.

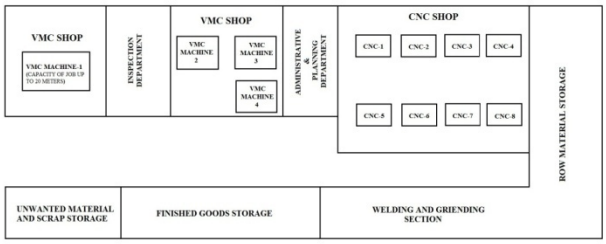

Figure 4.1 Plant layout

4.2 Details of job (Stay vane)

4.2.1 Final stay vane after machining

After machining of stay vane there are four welded road are attached to the stay vane which are used for the job setup on the bed of the VMC machine. This welded rod is required to remove and then final grinding require for final finishing of the stay vane

BEFORE GRINDING AFTER GRINDING

Figure 4.2 Final stay vane

4.3 Flow process of raw material to finished stay vane

Chart 4.1 Flow process of raw material to finished stay vane

4.4 Actual job setup used before implementation

This is the actual position the job setup in the machine in which four welded rod is used to setup the job on the bed with the help of some clamps and metal blocks.

Figure 4.3 Actual job setup

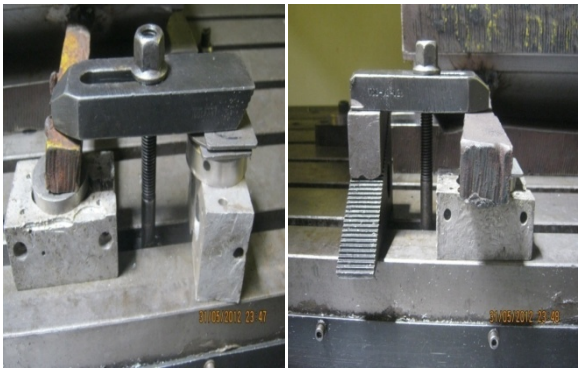

Figure 4.4 Clamps used for holding the job

V. DATA ANALYSIS

5.1 Comparison of new designed machining setup with company setup

5.1.1 For first side machining setup

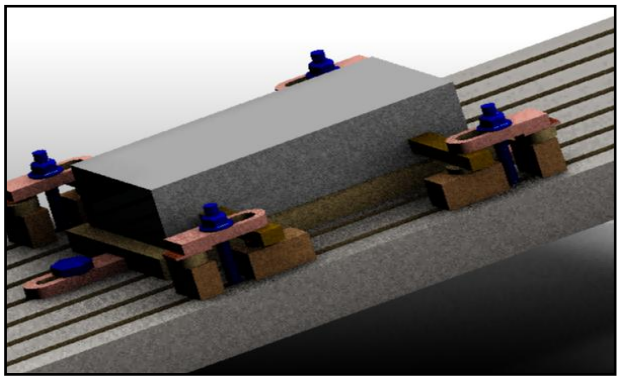

Figure 5.1 Company setup

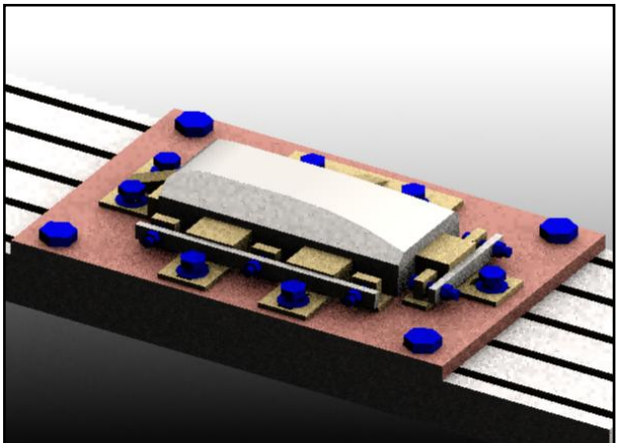

Figure 5.2 : New designed setup

5.1.2 For second side machining setup

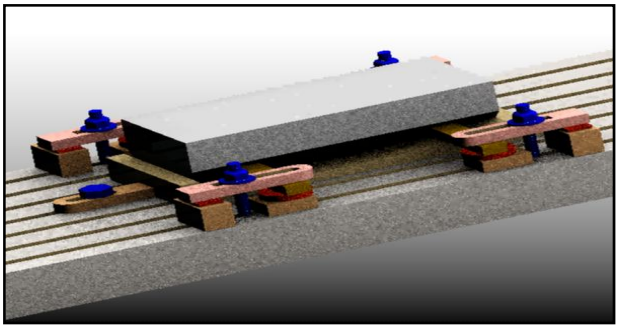

Figure 5.3 : Company setup

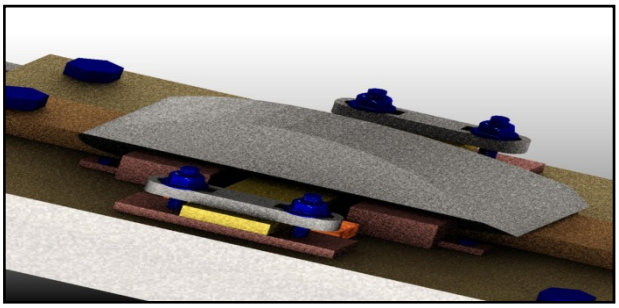

Figure 5.4 New designed setup

5.2 Difference between company setup and new design setup

First side setup		**Second side setup**	
Company setup	**New design setup**	**Company setup**	**New design setup**
Required four welded rod	No requirement of welded rod	Required four welded rod	Required two welded rod
Requirement of job positioning at every cycle	No requirement of job positioning at every cycle	Requirement of job positioning at every cycle	No requirement of job positioning at every cycle
Possibility of failure is more	Possibility of failure is less	Possibility of failure is more	Possibility of failure is less

5.3 Time study comparison

This table shows the comparisons of times which was reduced according to new implementation.

Sr no	**Activity**	**Time study comparison (hr: min: sec)**	
		Before	**After**
1	Transfer material from storage to welding section	00:10:00	00:10:00
2	Welding time	00:45:00	00:00:00
3	Transfer material from welding section to vmc machine-3	00:10:00	00:10:00
4	Job loading time	00:10:00	00:10:00
5	Setup time	00:35:00	00:30:00
6	Giving position of job to machine	00:20:00	00:00:00
7	Machining for one side	10:15:32	10:15:32
8	Job unloading time	00:10:00	00:10:00
9	Job travel from vmc-3 to welding section	00:10:00	00:10:00
10	Welding time	00:45:00	00:30:00
11	Transfer from welding section to vmc-4	00:10:00	00:10:00
12	Job loading time	00:10:00	00:10:00
13	Setup time	00:35:00	00:20:00
14	Giving position of job to machine	00:20:00	00:00:00
15	Machining for second side	12:15:25	12:15:25
16	Job unloading time	00:10:00	00:10:00
17	Job transfer to grinding section	00:10:00	00:10:00
18	Grinding time	00:45:00	00:30:00
19	Transfer job to grinding section	00:10:00	00:10:00
20	Total time	**28:15:57**	**26:00:57**
21	Total reduced time	**02:15:00**	

Table 5.1 : Time study comparison

5.4 Analysis of monthly production of stay vane

Sr no	Description	Before	After
1	total time for complete stay vane	28:15::57(hr: min: sec)	26:00:57 (hr: min: sec)
2	number of job produced in one month	19(546/18=19)	21(546/26=21)
Here 546 is the total working hours in one month			

Table 5.2 Analysis of monthly production of stay vane

.

VI. COST AND PROFIT ANALYSIS

6.1 Cost of fixture

Sr No	Part name	No. of Part	Volume mm^3	Cost(Rs)				
				Raw material	Machining cost	Welding cost	Drilling and threading cost	Total cost
1	L-shape clamp-1(width 200 mm)	1	1300000	560	100	20	40	**770**
2	L-shape clamp-2(width 300 mm)	1	1950000	840	100	20	40	**1050**
3	L-shape clamp (without rib)	3	850000	370	100	-	40	**1530**
4	T-clamp	5	200000	90	50	-	20	**800**
5	Bright flat plate-1	1	225000	100	-	-	60	**160**
6	Bright flat plate-2	1	112500	50	-	-	40	**90**
7	Bright flat plate-3	1	191250	80	-	-	40	**120**
8	45° taper clamp	4	301000	130	100	-	-	**920**
9	45° taper plate use for welding	2	400000	180	20	-	-	**400**
10	Fixture base plate	2	16200000	7000	-	-	80	**14160**
Total cost of fixture =20,000								

Table 6.1 Cost of fixture

6.2 Profit analysis

Sr no	Detail	Before implementation	After implementation
1	No. of job per month	19	21
2	No. of job per year	19*12=228	21*12=252
3	Profit per year	228*6600 =15,04,800Rs	252*6600 =16,63,200Rs
Net profit per year :1663200-1504800=1,58,400Rs			
Here 6600 is the total machining cost of manufacturing of one stay vane in Rs			

Table 6.2 Profit analysis

.

6.3 Net profit analysis after deducting cost of fixture

Sr no	Detail	Net profit
1	Profit per year	158400-20000=**1,38,400Rs**
2	Profit per month	138400/12=**11,500Rs**

Table 6.3 Net profit analysis after deducting cost of fixture

VII.SUMMARY & CONCLUSION

7.1 Summary

1. After applying work study and making design of fixture for stay vane total time reduced for manufacturing one stay vane from 28:15:57(hr:min:sec) to 26:00:57(hr:min:sec) shown in table 5.1.
2. By analysis of working hour for month, improving method study of stay vane and applying time study total number of job increased per month 19 to 21 shown in table 5.2.
3. After calculating machining cost and deducting cost of fixture from profit then net profit for company for producing stay vane per year is 1,38,400 Rs as shown in table 6.3.

7.2 Conclusion

From the discussion of the above parameters, it can be concluded that this process can be improved based on the five parameters (work process, method study, time measurement, fixture design and cost analysis) it will improve the current work process. These modifications are made by eliminating the wasted time and reduction of the work contents. From the comparison between current and new work process shown in topic 5.2, it indicates that the best alternative towards this problem by new method. After implementing new method on this stay vane job production it will increase production (2 stay vanes) as compare to company method. (In company method it would produce 19 stay vanes and after applying new method they can produce 21 stay vanes per month see table 5.2). This improvement was successfully implemented and it achieves the project goals and objectives, which improve processes, production layout, economy in human effort and the reduction of unnecessary fatigue.

REFERENCES

[1] Iyaniwura, O. and Osoba, A.M. (1983) "Measuring Productivity; Conceptual and Statistical Problems: Improvement of Statistics" in Osoba A.M. (ed.) 'Productivity in Nigeria' Proceedings of a National Conference' NISER, Ibadan.

[2] Antle, M. J. and Capalbo, S.M. (l988) "An Introduction to Recent Development in Production Theory and Productivity Measurement" in Capalbo, S.M. and Antle, M.J. 'Agricultural Productivity: Measurement and Explanation' Resources For the Future, Inc., Washington, DC.

[3] Eatwell, J.M. and Newman, P. (1991) "The New Palgrave: A Dictionary of Economics" vols. 3, 4. & 12, Macmillan, Tokyo.

[4] Amadi, A.O. (1991) "Recipe for Productivity Improvement" in Umeh, P.O.C. et al (1991) "Increasing Productivity in Nigeria" Proceedings of the First National Conference on Productivity 1sty-3rd December 1987, National Productivity Centre, Macmillan, Nigeria. Pp. 98 -106.

[5] Concept and Measurement of Productivity By "Gboyega A. Oyeranti" NECA (1991), {page no 2 to 3} http://www.cenbank.org/ OUT/PUBLICATIONS/OCCASIONALPAPERS/RD/ 2000/ABE-00-1.PDF

[6] Gershwin, S.B. (2000) 'Design and operation of manufacturing systems: the control-point policy', IIE Transactions, Vol. 32, pp.891–906.

[7] Int. J. Industrial and Systems Engineering, Vol. 1, No. 4, 2006 By Kanthi M.N. Muthiah* and Samuel H. Huang, {page no 1} http://pqprc.org/ userfiles/groups/ A%20review% 20of%20literature% 20on%20manufacturing% 20systems.pdf

[8] Text book of Industrial Engineering, Tech max publication By Dr. Pradip Kumar Sinha, {page no 3-18, 3-19, 3-22,3-23}

[9] An Impact Time Motion Study on Small Medium Enterprise Organization By Abdul Talib Bon[1] , Aliza Ariffin, {page no 3} http://www.academia.edu/ 1277107/AN_IMPACT_TIME_MOTION_STUDY_ON_SMALL_MEDIUM_ENTERPRISE_ORGANIZATION

[10] Reducing Machine Setup & Changeover Times

By Charles F. Keberdle, CPIM, {page no 2 & 3}

http://www.leansolutionsgroup.com/images/Setup_Reduction_Master.pdf

[11] UNIT- 4 Jigs and Fixtures, manufacturing process-III, {page no 47, 48 & 49} http://www.ignou.ac.in/ upload/jig.pdf

◈◈◈

Enhance Production Rate of Braiding Machine Using Speed Reduction Technique

[1]Manoj A. Kumbhalkar, [2]Sachin V. Mate, [3]Sushama Dhote & [4]Mudra Gondane

[1,2]Department of Mechanical Engineering, B.C.Y.R.C's Umrer college of Engineering, Umrer, Dist Nagpur, Maharashtra (India)
[3]Department of Mechanical Engineering, Bhagwati Chaturvedi College of Engineering, Nagpur, Maharashtra (India)
[4]Department of Mechanical Engineering, Priyadarshini College of Engineering, Nagpur, Maharashtra (India)
E-mail : manoj.kumbhalkar@rediffmail.com[1], sushama170888@gmail.com[3]

Abstract – Textile designing is a technical process which includes different methods for production of textile, surface design and structural design of a textile. Braid is the textile product having various types like round and flat braid made by using textile threads or wires which are alternatively interwoven in braiding machine. A small scale industry in Nagpur produces each type of cotton braids using 16 spindle braiding machines on the single line shaft acquired power from 0.50 HP motor runs at 1440 rpm with the production rate of 87.5 m/hr. This paper discusses about to increase production of braids and design parameters of braiding machine. The production rate has been improved by modifying the some parameters by maintaining quality of braid as per the today's market is concerned.

Keywords:- *braid, braiding machine, drives, production rate, spur gear, speed reduction*

.

I. INTRODUCTION

There is lot of textile products in market one of them is braided products like coated wire, yarns, plastic coatings etc. Braids are textile compositions made with yarn thread crossing in diagonal direction. Each thread intertwines the diagonal threads it crosses one from above and one from below. Braiding machines are used for such type of constructions. Braiding machines are used for producing wide range of articles viz. Round braid(cords, laces, cables or ropes) and flat braid (decorative objects, and hairstyles) shown in figure 1 and figure 2 using textile threads or wires which are alternatively interwoven.

Figure 1 Round Braid

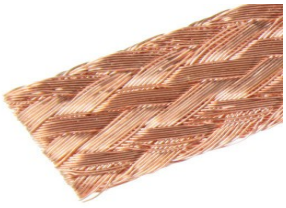

Figure 2 Flat Braid

The small scale industry in Nagpur produces round and flat braids of cotton and nylon material using 16 spindle braiding machines focus on to improve the production rate. 10-15 machines operate on single line shaft acquired power of 0.5 HP from electric motor and rotate at 1440 rpm with the capacity of 700 meter per day. The machine is constructed with the arrangements of spur gear, bevel gear, worm gear, horn gear, top plate and belt drives. Thread bundles (bobbins) has been mounted on the each spindle on the top plate having path for spindle carrier and the threads from each bobbins collected and carried by thread carrier on the top of the machine to form the braid as final product used for the laces of shoes, coating on electric wire, small size ropes.

A. *Observation*

During study in the industry about the production of braid, following points were observed:

1. Capacity of braiding machine to produce braid is about 700 meter per day from each machine.
2. Multiple machines operate on power of single motor (0.5HP) using line shaft.

3. On increasing the number of bobbins, thickness of final product is increases.
4. Total 60 machines are used for the continuous production of 4200-4500 meter per day for 8-10 hours.
5. For increasing the thickness of thread, the additional thread is provided from the centre of top plate as a central cord.

II. WORKING PRINCIPLE OF BRAIDING MACHINE

Braiding machine consist of component like electric motor, flat belt pulley, gears (bevel gear, horn gear, spur gear), rig-pick arrangement, thread carrier, spindles, top plate etc. Horn gears are mounted on the spur gears rotated below the top plate to drive yarn bobbins mounted over it. Each horn gear consists of four 'wings' that can accommodate one bobbin and the bobbin motion is prescribed through the groves in the top plate. The motion of yarns on one track is clockwise and the other is counter clockwise causing the yarns to interlace. The track plate consists of two separate paths: each path 180 degrees out of phase from the other. One path motion is clockwise, while the other path is counter clockwise; at the point where the paths converge, the yarns interact as one yarn travels over and the other yarn under. The over-under interaction causes an interlacing of the two yarns and is the chief mechanism responsible for the formation of the braided structure. The braid is formed as a continuous process by interlacing the yarns and drawing them through a 'braiding point'. The mounting of bobbins on spindle and rotation of horn gears are shown in figure 3.

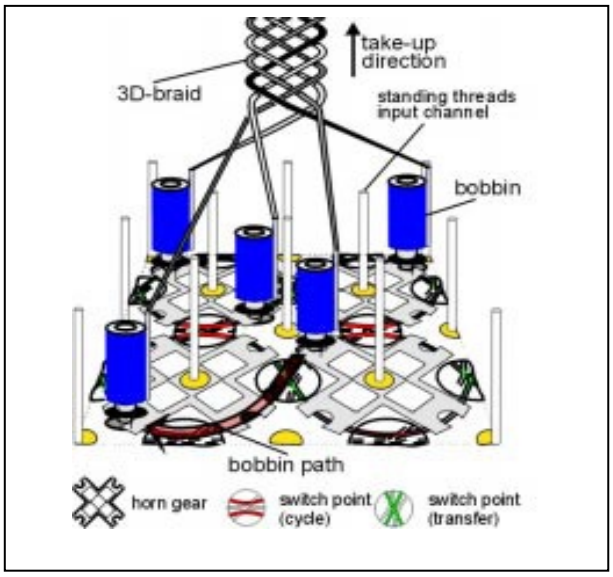

Figure 3 Rotation of bobbins due to horn gear

Groves in the top plate also guide the bobbins; however, switch points are located between each pair of horn gears that can be activated to transfer the bobbin to an adjacent horn gear. In braiding machine the top plate is intended with the path of spindle carrier as through which the spindle followed forward and reversed motion. The interlocked threads pulled up with the help of rig-pick arrangement. M. Schneider et al[4] explain the motion of bobbins due to rotation of horn gears. Figure 4 shows the driving path of bobbins on the top plate and figure 5 explain the driving mechanism.

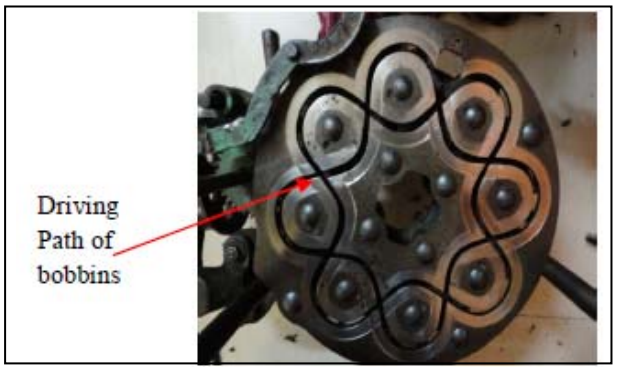

Figure 4 : Photo of Top plate showing driving path of bobbins

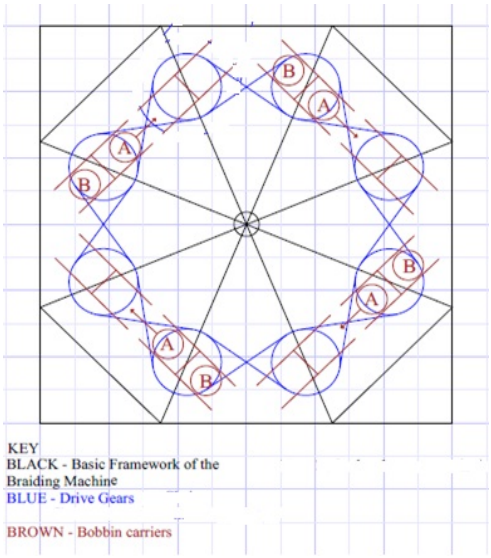

Figure 5 : Driving Mechanism of machine

The power of 0.5 horse power is first transmitted by the electric motor with the speed of 1440 rpm to the line shaft via V-belt drive which tansfer the power to the horizontal shaft of braiding machine via flat belt drive. Bevel gear is mounted on the same shaft of larger flat belt pulley rotates with same speed and transmitted power to the vertical shaft where the spur gear is fitted with bevel gear which rotates the horn gears and provide

motion to bobbins mounted on the top plate by transmitting the power to the gear train assembled below the top plate. The vertical shaft is attached with the worm and worm gear from which the power is transmitted to the rig-pick arrangement (spur gear drive) which plays an important role in production of braiding machine. The braid carries by the thread carrier (Spur gear drive) at the top depend on the speed of rig-pick arrangement. Therefore by incresing the speed of shaft between thread carrier and rig-pick arrangement the production of machine can be increased by maintaining the speed ratio to maintain the quality of braid. Figure 6 and 7 shows the actual photo and schematic diagram of braiding machine.

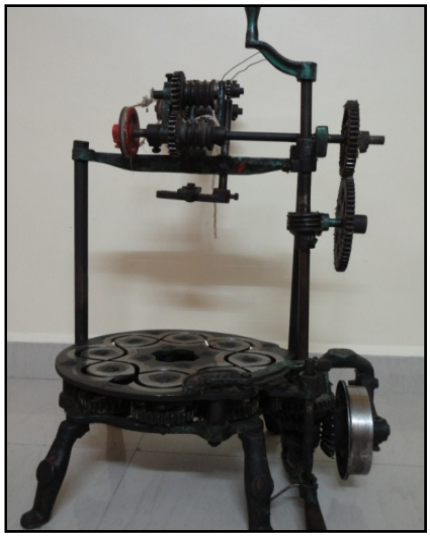

Figure 6 : Photograph of Braiding machine

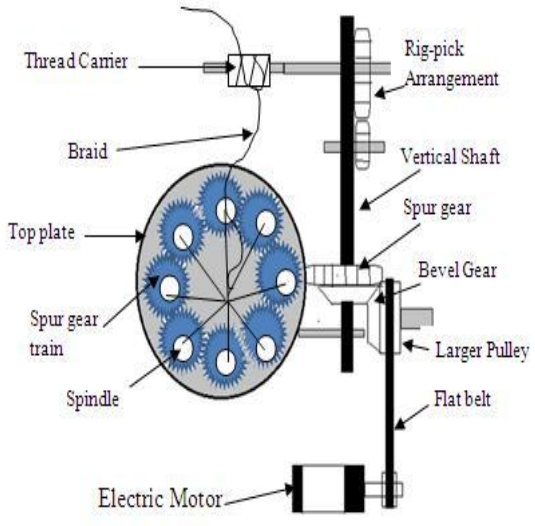

Figure 7 : Schematic diagram of Braiding machine

III. SPEED REDUCTION IN BRAIDING MACHINE

By study of the components and working of braiding machine it is observed that speed (in rpm) is main factor responsible for the production of braid. The speed is reduced from electric motor to thread carrier by the various arrangements of drives in the machine as per the requirements which is responsible for the production of braid. Table 1 shows the technical specification of the components of braiding machine.

Table 1 Technical specifications of components of braiding machine

Particulars	Unit	Dimensions
Spindle	-	16
Pitch Size	mm	3
Motor Power	HP	0.5
Weight	Kg	650
Length	mm	1650
Width	mm	1000
Height	mm	1600
Diameter of V- Belt Driver pulley	mm	50.8
Diameter of V- Belt Driven pulley	mm	457.2
Diameter of Flat belt driver and driven pulley	mm	127
Teeth on Spur Gear drive of top plate	-	32
Teeth on Bevel Gear	-	21
No. of teeth on worm and worm gear	-	4 & 24
Teeth on Spur Gear of rig-pick arrangement (larger& smaller)	-	60 & 45

With the help of technical specification of the components of braiding machine, speed in rpm of each components has been calculated using relation $N_1D_1=N_2D_2$ or $N_1T_1=N_2T_2$which finds the speed ratio of 4.45. Where N_1 & N_2 are the speed of driver and driven shaft, D_1 & D_2 are the diameter of driver and driven pulley and T_1 & T_2 are the number of teeth on driver and driven gear.

By maintaining the same speed ratio production of machine has been increased by replacing the spur gear of rig-pick arrangement as per the availability. The speed in whole arrangement is reduced from 1440 rpm to 36 rpm which gives the production of 700 m/day for each machine. The calculated value of speed of each component of the braiding machine is shown in table 2.

Table 2 : Speed Reduction in Braiding Machine

Sr. No.	Drives	Speed (rpm)	
		Driver	Driven
1	V-belt drive	1440	160
2	Flat belt drive	160	160
3	Bevel gear drive	160	160
4	Spur gear drive (Top plate)	160	160
5	Worm & worm gear drive	160	27
6	Spur gear drive (rig-pick arrangement)	27	36

The speed is varies from top plate to rig-pick arrangement (or pulling system) which gets the speed ratio of machine.

$$\text{Speed Ratio} = \frac{\text{Speed of top plate gear}}{\text{Speed of rig-pick gear arrangement}} = 4.45$$

A. *Analytical modification of machine parameter to increase production*

As the speed of shaft between pulling system and rig-pick arrangement is mainly responsible for the production, it is necessary to increase speed of that shaft to improve production by maintaining the quality of braid which has been obtained by maintaining the same speed ratio and calculate or redesign other parameters of braiding machine. Accordingly, the speed of top plate also increased which relieves thread to pulling system. To increase speed, the small gear with 45 teeth in the rig-pick arrangement has been replaced with the gear of 35 or 24 teeth as per the availability for the machine in industry. Accordingly the size of worm gear and flat belt pulley has been modified. To check the production of single braiding machine V-belt and flat belt drive is replaced with only flat belt drive. The calculations for 35 and 24 number of teeth are as follows:

For the power of 0.5 HP with motor speed N_1=1440 rpm, modify the parameter of components of braiding machine for two cases considered for rig-pick spur gear arrangement.

Case I: If T_g = 60, N_g = 27 keep unchanged & T_p = 35 from 45

$N_g T_g = N_p T_p$

N_p = 47 rpm

With respect to velocity ratio=4.45& speed of smaller spur gear= 47 rpm

Speed of top plate spur gear, $N_2 = 47 \times 4.45$

N_2=209 rpm

To enrich the speed of 27 rpm to driver rig-pick spur gear, the worm gear has to be replaced with 31 numbers of teeth.

From table 2, it is cleared that the speed of larger flat belt pulley is equal to the speed of top plate spur gear, therefore the diameter of the larger flat belt pulley can be modified and calculated using relation,

$N_1 \times D_1 = N_2 \times D_2$ (D_1= 50.8mm, from table 1)

D_2=350 mm (14 inch)

Accordingly, the production rate has been changed as the speed of pinion is increased from 36 rpm to 47 rpm. For N_p=36 rpm , production rate is 87.5 m/hr. So for N_p=47 rpm,

Production rate = (87.5/36) × 47 = 114.24 m/hr.

By replacing the spur gear of 45 teeth with 35 teeth the production rate has been increased to 114.24 m/hr

Case II: If T_g = 60, N_g = 27 keep unchanged & T_p = 24 from 45

$N_g T_g = N_p T_p$

N_p = 67.5 rpm

With respect to velocity ratio=4.45& speed of smaller spur gear= 67.5 rpm

.

Table 3 comparison between existing and modified machine

Braiding machine	Speed of motor (rpm)	V-belt Pulley Diameter (mm)		Flat-belt Pulley Diameter (mm)		Teeth on Worm & Worm Gear		Teeth on spur gear of rig-pick arrangement		Production rate (m/hr)
		Driver	Driven	Driver	Driven	Worm	Worm gear	Gear	Pinion	
Current machine	1440	50.8	457.2	127	127	4	24	60	45	87.5
Modified machine	1440	-	-	50.8	350	4	31	60	35	114.24
		-	-	50.8	244	4	45	60	24	164

. Speed of top plate spur gear, $N_2 = 67.5 \times 4.45$

$N_2 = 300$ rpm

To enrich the speed of 27 rpm to driver rig-pick spur gear, the worm gear has to be replaced with 45 numbers of teeth.

Similarly the diameter of larger gear and production rate for the speed of 67.5 rpm is calculated and compared with previous one.

$N_1 \times D_1 = N_2 \times D_2$ (D_1= 50.8mm, from table 1)

D_2= 244 mm (9.6 inch)

For N_p=36 rpm , production rate is 87.5 m/hr. So for N_p=67.5 rpm,

Production rate = $(87.5/36) \times 67.5 = 164$ m/hr.

By replacing the spur gear of 45 teeth with 24 teeth the production rate has been increased to 164 m/hr.

From the calculation it is observed that the production rate is increased by replacing the smaller spur gear of rig-pick arrangement and modifying some parameters of components of braiding machine. The comparison of production rate and other technical design parameter of existing and new machine is shown in table 2.

IV. CONCLUSION

After the Study of company profile, braiding machine and its components and company profile, it is observed that the braid plays an important role in textile engineering and useful for the laces, coating on wires etc. From company profile and market demand it is necessary to improve the production rate to achieve the demand. Each component of braiding machine and it's principle of working is studied well in order to get technical logic to improve the production rate. After analytical study of each component and its technical parameters it is conclude that the speed reduction is the main factor affecting the production rate. The current braiding machine gives the production of 87.5 m/hr for 8 hours per day which is increased to the level of 164 m/hr after the modification of some parameters analytically.

To increase the production rate, the smaller spur gear of rig-pick arrangement has been replaced from 45 number of teeth to 35 and 24 number of teeth. The production rate has been calculated for both the cases and it is observed that it is more in the replacement with 24 teeth gives the production rate of 164 m/hr by maintaining the quality of braid. Accordingly, the other parameters also affected and changed as per the details mentioned in table 3. After the modification production rate is increased and satisfies today's market demand.

REFERENCES

[1] Juha-Pekkanuutinen, Claude Clerc, Raija Reinikainen and Pertti tormala, "Mechanical properties and in vitro degradation of bioabsorbable self-expanding braided stents", J. Biomater. Sci. Polymer Edn, Vol. 14, No. 3, pp. 255–266, 2003.

[2] David John Branscomb, Royall M. Broughton, David G. Beale, "A machine vision and sensing system for braid defect detection, diagnosis and prevention during manufacture".

[3] Tadashi Uozum and Masao Hirukawa, "Braiding technologies for commercial applications", 6th Japan International SAMPE Symposium & Exhibition (JISSE-6) Tokyo Big Sight, Tokyo, Japan, 1999.

[4] M. Schneider, A. K. Pickett and B. Wulfhorst, "New rotary braiding machine and CAE procedure to produce efficient 3-d textiles for composite" 45th SAMPE international symposium, Long Beach CA, USA. 2000.

[5] J.H. van Ravenhorst and R. Akkerman, "A spool pattern tool for circular braiding", 18th international conference on composite materials.

[6] B. C. Giltgren and A. Kashem, "Experiences with manually operated net-braiding machine in Bangladesh", Development of Small-Scale Fisheries in the Bay of Bengal. BOB P/WP/50, 1986.

[7] P. Potluri, A. Rawal, M. Rivaldi, I. Porat, "Geometrical modelling and control of a triaxial braiding machine for producing 3D performs", Composites part- A: applied science and manufacturing, science direct, Composites: Part A 34 (2003) 481–492, 2003.

◈◈◈

Optimization of Blank Holding Force in Deep Drawing Process Using Friction Property of Steel Blank

Prasad S. Pandhare[1], Vipul U. Mehunkar[2], Ashish S. Joshi[3], Amruta M. Kirde[4] & V. M. Nandedkar[5]

[1-4] S.G.G.S.I.E & T. Vishnupuri, Nanded-431606 (MS)
[5] Department of Production Engineering, SGGSIE&T, Nanded (India)
Email: ppandhare38@gmail.com, vipulmehunkar@gmail.com, joshiashish024@gmail.com, amrutakirde@gmail.com, vilas.nandedkar@gmail.com

Abstract – Majority of automobile and appliances component are made by deep drawing sheet metal process. So these growing need demands a new design methodology based on metal forming simulation. With the help of metal forming simulation we can identify the problem areas and solutions can be validated in computers without any expensive shop floor operations prior to any tool construction. Metal forming simulation is also helpful at the product and tool design stage to decide various parameters. Problem and improvements in each area of the SDF technology and their interactions should be considered. In the product and process design phases in order to optimize Blank Holding Force which is one of the important parameters in Deep Drawing process. Sometimes accuracies of frictional values have more effect on the simulation results than most of the material properties. So that friction plays a major role during optimization of Blank Holding Force. In this paper, the friction is varied in six different values. CRDQ Steel is used as a material. For each value of friction and its corresponding B.H.F., Forming Limit Diagrams are drawn by using hyper mesh module of Hyper Form Solver software. Also the effect of these two parameters on occurrence of wrinkling during the process is studied. Thus, optimized range of coefficient of friction in which product is safe as well as having minimized wrinkles along with optimized B.H.F. is calculated

Keywords: *Blank Holding Force, Friction, Optimization, Hyper Mesh.*

I. INTRODUCTION

Metal forming involves plastically deforming a piece of material to obtain the desired product. A special class of metal forming where thickness of the work piece is small compared to the other dimension is called sheet metal forming. It is the process of converting a flat sheet metal into a part of desired shape without defects (fracture or excessive thinning, wrinkling etc.). Formability is the ability of a sheet metal to be formed without failure. [3] The formability of sheet metal is significantly affected by the sheet metal properties (work hardening, anisotropy ratio), the processing parameters (blank holder force and interface friction coefficient) and forming procedures. The formability of an isotropic material is described by its flow curve and the ductility is the measure of the forming limits.

II. FORMABILITY:

Formability is the ability of sheet metal to be stamped or formed successfully into useful components without developing any failure. The common failures encountered during sheet metal forming are fractures, wrinkling, puckering, snap distortion, loose metal etc. Formability is not easily quantified, as it depends on several interacting factors. Material flow properties, ductility, die geometry, die material, lubrication conditions and press feed contribute to the success or failure of the formed sheet metal component to varying degrees in an interdependent manner. Formability, unlike tensile properties, is not a simple and well defined material property. In fact, formability should be viewed more as "system" parameters, involving the sheet metal that is being formed, the stamping process conditions, and the forming press. i.e.:-

Formability = f (sheet metal, process conditions, sheet metal component shape, machine tools and Equipment) [5]

It is conceivable that a given sheet metal could be formed successfully into a particular component or lead to failure, depending upon the process conditions and

the tooling used. In other words, the same sheet metal can have "good" or"bad" formability depending upon the remaining components of the forming "system" conditions, i.e.

UTS = f (sheet metal); UTS ≠f (sheet thickness, process conditions, surface finish, etc.).

The sheet metal properties, such as the UTS, are usually referred to as intrinsic material properties.

III. FACTORS AFFECTING FORMABILITY:

Formability of sheet metal depends on both the material and process variables. Material properties on which the formability of sheet metal depends are the

1. Strain hardening exponent (n)
2. The strain rate hardening exponent (m)
3. Anisotropy ratio(r).

Various process Parameters influencing the formability are the blank holding force, the interfacial friction condition, the tooling geometry i.e. Punch and Die. [5]

IV. BLANK HOLDING:

Even though the thickness of work metal and the die radius offer some restraint to the flow of metal into the die, some additional constraint is usually required to control the flow of metal. This additional restraint is obtained by the use of blank holding plate. The purpose of blank holding is to suppress wrinkling and puckering, and to control the flow of the work metal into the die. [5]

When the draw progress, compressive force developed in the blank causing a reduction in the blank diameter and thickening of the blank. Correspondingly, the blank holder pressure increases as the draw progress due to increase in thickness. Now there is possibility for the cup to tear at the weakest point because instead of drawing, the punch stretches the metal into the die.

So an ideal blank holder would be the one capable of proportionately varying the blank holding the pressure as the draw depth increases and the thickness of the flange increases, to maintain constant uniform blank restraint.

Normally blank holding pressure is assumed to be one third of maximum force. It is clear that the blank holder force must be sufficient large to prevent excessive wrinkling but not too large to cause tearing.

V. FRICTION:

Friction is the one of the most important factors that eliminates the plastic deformation in sheet forming operation. Friction between sheet and tool play an important role. The frictional force plays an active role in affecting the material flow, the strain distribution and the forming force. Hence an accurate simulation requires a detailed understanding of friction behavior under actual forming condition. Any attempt to simulate sheet metal forming without a detailed understanding of friction cannot be successful [2]. It is known that Sometimes inaccuracies of frictional values have more effect on the simulation results than most of the material properties. [2]

The main difficulty in comparing the simulations and experiment is the largely unknown friction law, Even if the coulomb friction is assumed, the friction coefficient plays a critical role in determining strains and performance. During sheet forming, high friction condition raises the stresses in the sheet and promotes strain localization and split type failures.

This effect must be modeled accurately in order to obtain realistic FEM simulations. Friction and contact condition controls the development of non-uniform strain distribution.

For most forming operation maintaining a stable level of friction is more important than a low friction level. Use of the oiling conditions of the sheet permits to realize differential values on different area of the blank. In general, a low level of friction offers greater possibilities to press highly stressed parts with more complex shape.[2]

V. MODEL OF STANDARD DEEP DRAWING COMPONENT

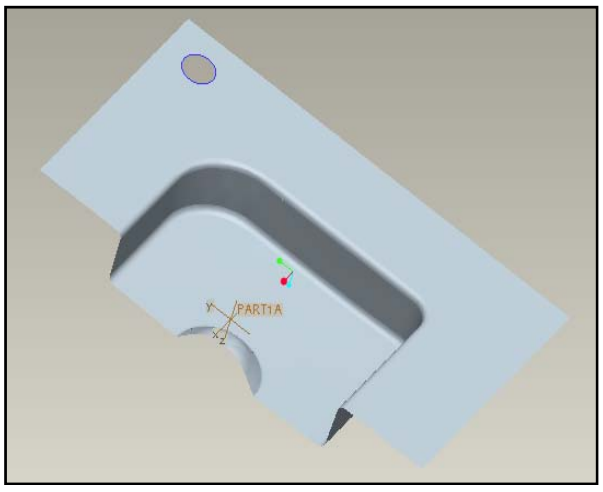

Fig.1. Part drawing in Pro-E software

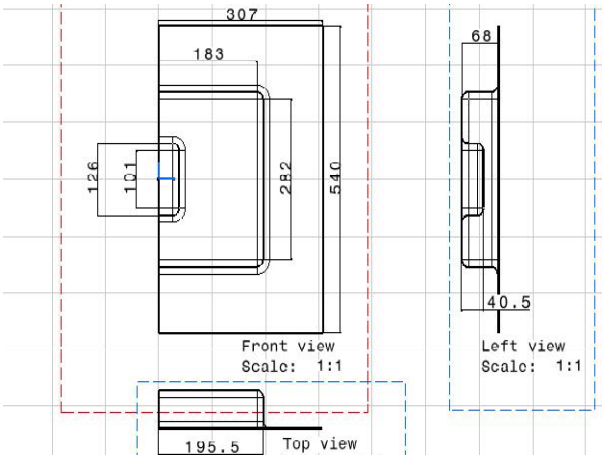

Fig.2. Detail drawing in Pro-E software

Meshing size: 07

Meshing Type: Triangular & rectangular (mixed).

Initial Blank Shape:

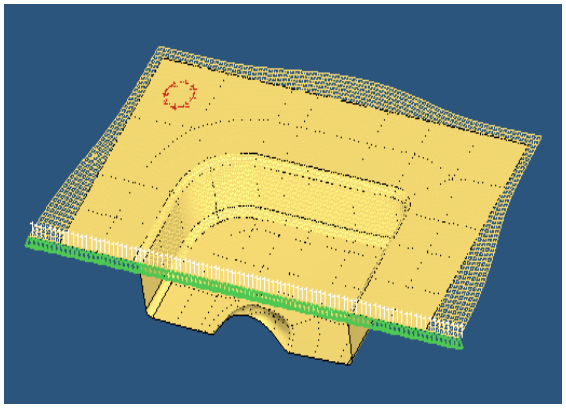

Final Blank Shape:

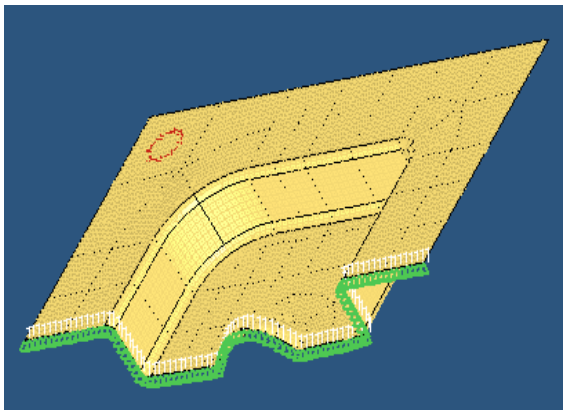

Fig.4. Deformed blank into the die cavity

VI. RESULT:

By taking number of iterations we plot the Forming Limit Diagram (FLD) for different coefficient of frictions (μ). Following are the FLDs

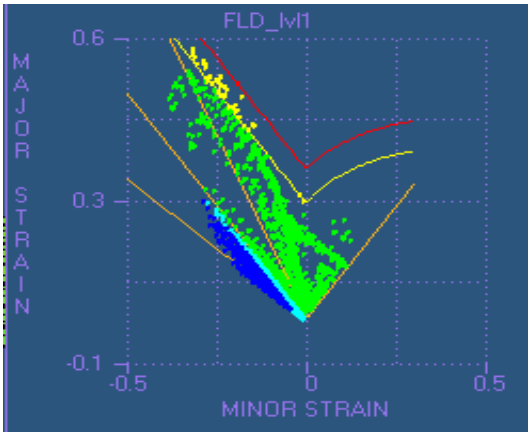

Fig.5. FLD when μ = 0.1

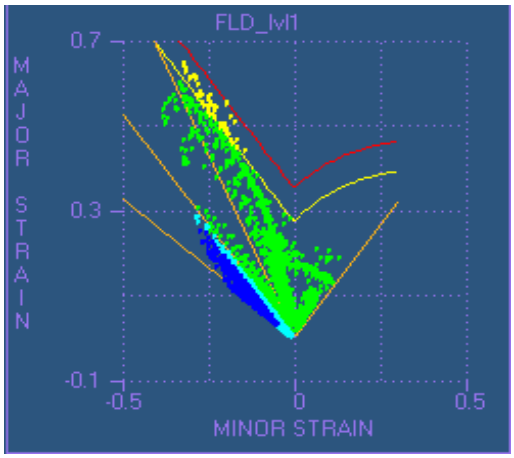

Fig.6. FLD when μ = 0.125

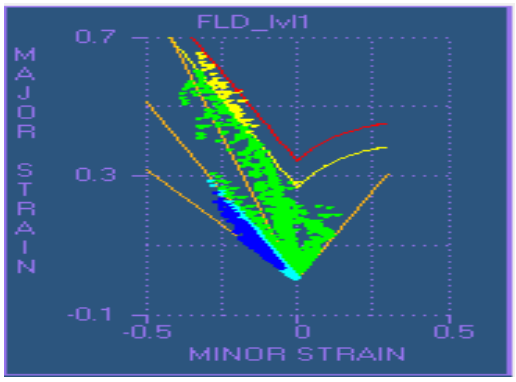

Fig.7. FLD when μ= 0.15

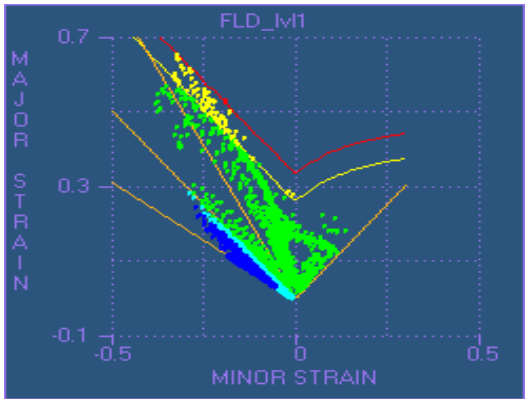

Fig.8. FLD when μ= 0.175

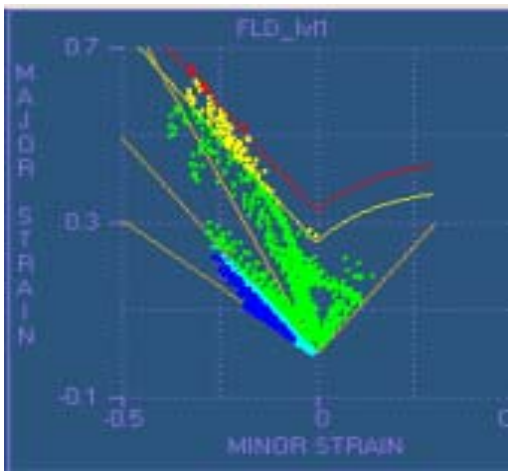

Fig.9. FLD when μ= 0.2

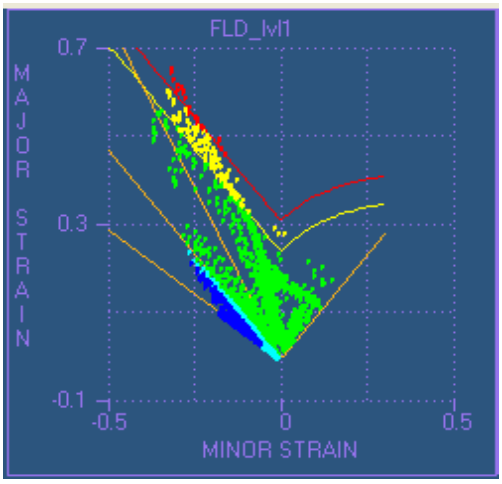

Fig.10. FLD when μ= 0.25

VII. Optimization Study:

Following are the graphs of friction and blank holding force with respect toprobability of formation of the wrinkle obtained after optimization study of the component.

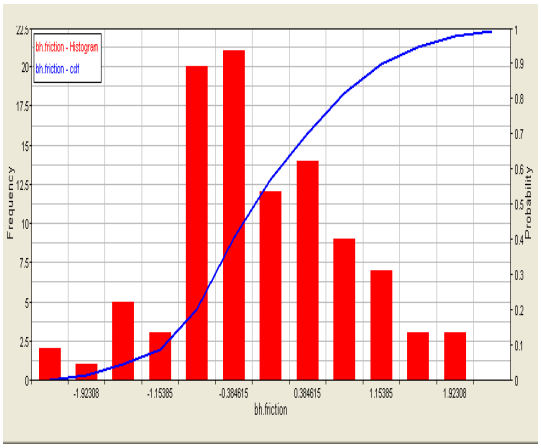

Fig.11. Coefficient of friction Vs. Probabilityof wrinkling

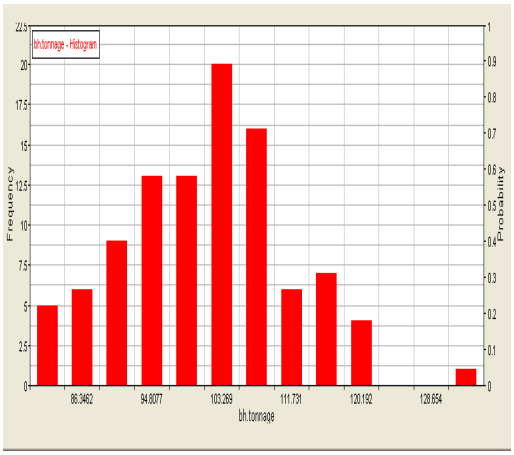

Fig.12. Blank Holding Force vs. Prob. Of wrinkling

Table.1. Relation between friction and blank holding force = (1/3)rd[Tonnage Force] [2]:

Sr. No.	Friction	Blank holding force (Tonne)	Conclusion
1	0.1	0.1290 E+02	More Wrinkles
2	0.125	0.1303 E+02	More Wrinkles
3	0.150	0.1323 E+02	Less Wrinkles
4	0.175	0.1346 E+02	Optimized
5	0.2	0.1370 E+02	Failure
6	0.25	0.1413 E+02	Failure

VIII. CONCLUSION

In this paper, we have studied effect of material properties i.e. n, m, r value. Also one of the important parameter, we consider is friction. Sometimes accuracies of frictional values have more effect on the simulation results than most of the material properties. By controlling it, we can be able to optimize Blank Holding Force up to certain range. For CRDQ Steel, the range of coefficient of friction is 0.125 to 0.175.

We conclude that, in the range of coefficient of friction. B.H.F. first start to decrease as coefficient of friction increases up to certain limit, then increases after certain value of μ.So we have taken number of iterations & found out range of μ for CRDQ Steel. By controlling μ in between 0.125 to 0.175, we can optimize B.H.F. for CRDQ Steel.

REFERENCES

[1] Ganesh M. Kakandikar, Design optimization of Deep Drawing process for circular components using genetic algorithm, Dept. of Prod. Engg.SGGSIE&T, Vishnupuri, Nanded (M.S.) 431 606.

[2] Sheet Metal forming and Blanking" in metal forming handbook/ Schuler.ISBN 3-540-61185-1, Chapter no.4, pp.174-182.

[3] P.N. Rao,Manufacturing Technology, 2nd Edition, Tata McGraw-Hill Publishing Company Limited, New Delhi.2004, Chapter No. 21, pp. 309- 311.

[4] Altair Hyper Works Students Manual..

[5] Dr. V.M. Nandedkar,"Formability and its Effects" private circulation

Passive Control Systems for Tall Structures

Shreyas Kulkarni[1], Dattatray Jadhav[2] & Pravin Khadke[3]

[1&2]Department of Mechanical Engineering, Sardar Patel College of Engineering, Mumbai
[3]HTAT Department, Toyo Technology Centre, Mumbai
E-mail : [1] shreyaskulkarni2006@yahoo.com , [2] d_jadhav@spce.ac.in , [3] pdkhadke@gmail.com

Abstract – Current trends in construction industry demands taller and lighter structures, which are also more flexible and having quite low damping value. This increases failure possibilities and also problems from serviceability point of view. This paper describes about different types of passive energy dissipating devices which helps to damp the vibration within a structural systems up to certain extent.

Keywords – *passive control, energy dissipation, damping, vibration, dynamic response.*

I. INTRODUCTION

A number of passive control systems are currently in use for protection of structures against seismic or wind excitation. The term "passive" is used to indicate that the operation of these systems does not require an external power source. Typically, the mechanical properties of these systems cannot be modified. Furthermore, a passive damping system utilizes the motion of the structure to produce relative motion within damping devices which, in turn, dissipate energy. Passive damping systems dissipate energy through a variety of mechanisms[1]. Unlike the mass and stiffness characteristics of the structural system, damping does not relate to a unique physical phenomenon, and it is often difficult to engineer without the addition of external damping systems. Furthermore, the amount of inherent damping cannot be estimated with certainty; however known level of damping may be introduced through an auxiliary source[2][3]. Such sources come in the form of both active and passive system. Focus of this paper is on the passive systems. Classification of passive dampers is shown in fig. 1

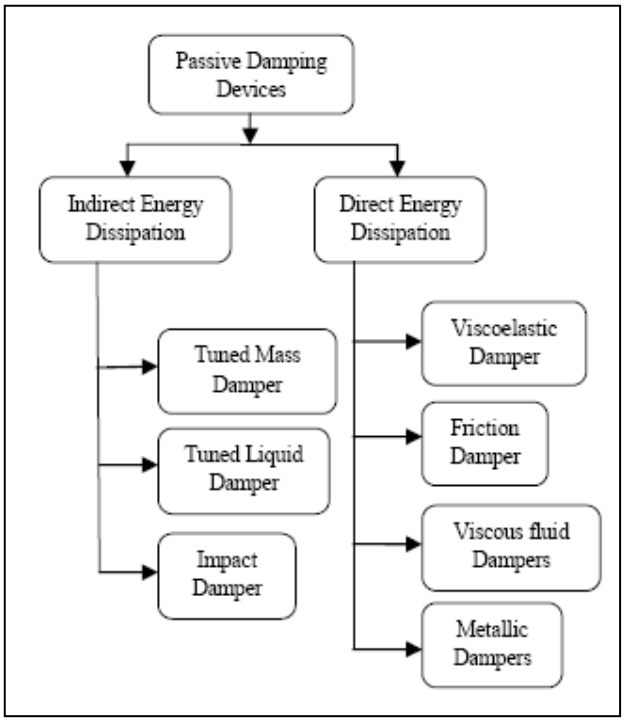

Fig. 1 : Classification of passive dampers

II. PASSIVE DAMPING DEVICES WITH INDIRECT ENERGY DISSIPATION

Auxiliary damping is commonly supplied through the incorporation of some secondary system capable of passive energy dissipation. Of the passive devices that impart indirect damping through modifications of the system characteristics, the damped inertial system is most popular. These systems, which will be discussed below, impart indirect damping to the structure by modifying its frequency response[4].

A. Tuned Mass Damper

Tuned mass dampers (TMD) have been widely used for vibration control in mechanical engineering systems. In recent years, TMD theory has been adopted to reduce vibrations of tall buildings and other civil engineering structures. Dynamic absorbers and tuned mass dampers

are the realizations of tuned absorbers and tuned dampers for structural vibration control applications. The inertial, resilient, and dissipative elements in such devices are: mass, spring and dashpot (or material damping) for linear applications and their rotary counterparts in rotational applications. Depending on the application, these devices are sized from a few ounces (grams) to many tons. Other configurations such as pendulum absorbers/dampers, and sloshing liquid absorbers/dampers have also been realized for vibration mitigation applications.

TMD is attached to a structure in order to reduce the dynamic response of the structure. The frequency of the damper is tuned to a particular structural frequency so that when that frequency is excited, the damper will resonate out of phase with the structural motion. The mass is usually attached to the building via a spring-dashpot system and energy is dissipated by the dashpot as relative motion develops between the mass and the structure[5]. A TMD typically consist of an inertial mass attached to the building at location where the response is maximum, generally near the top[6]. Although TMDs are often effective better performance has been noted through the use of multiple-damper configurations (MDCs) which consist of several dampers placed in parallel with natural frequencies distributed around the optimal frequency[7].

The modern concept of tuned mass dampers for structural applications has its roots in dynamic vibration absorbers studied as early as 1909 by Frahm[8][9]. A schematic representation of Frahm's absorber is shown in Fig. 2, which consists of a small mass m and a spring with spring stiffness *k* attached to the main mass *M* with spring stiffness *K*. Under a simple harmonic load, one can show that the main mass *M* can be kept completely stationary when the natural frequency of the attached absorber is chosen to be (or tuned to) the excitation frequency.

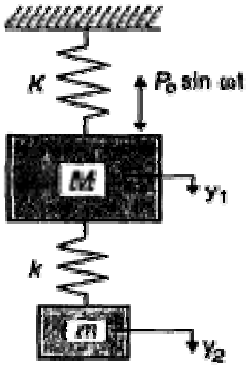

Fig.2 : Undamped Absorber and Main Mass Subject to Harmonic Excitation (Frahm's Absorber)

B. Tuned Liquid Dampers

In tuned mass dampers (TMD), typically a solid concrete or metal block acts as the secondary mass, although in some cases a deep tank filled with water serves the same purpose. Additional springs and dampers are used to attach this secondary mass to the primary structure, and to provide the restoring and dissipative mechanisms needed to tune the system for near-optimal response under various types of dynamic excitations[10]. The TLD absorbs vibration energy by the sloshing motion of liquid contained in a vessel & dissipates it through intrinsic friction of the liquid, friction at surface of walls or floating particles, collision of the particles, etc. There are some advantages in the TLD such as: low initial cost, free maintenance, ease of frequency tuning, no limit of vibration amplitude and applicability for existing buildings by dispersed installation of vessels[11].

The idea of applying tuned liquid dampers to reduce vibrations in civil engineering structures began in the mid-1980s. Bauer suggested the use of a rectangular container completely filled with two immiscible fluids to dampen response through the motion of the interface[12][13]. This concept is depicted in Fig. 3 for reduction of wind-induced motion. Welt and Modi were also among the first to suggest the use of a TLD in buildings to reduce overall response during strong wind or earthquakes[14].

A properly designed partially filled water tank can be utilized as a vibration absorber to reduce the dynamic motion of a structure and is referred to as a tuned liquid damper (TLD). It can be further divide into Tuned Sloshing Damper (TSD) and Tuned Column Damper (TCD). Tuned Liquid Damper (TLD) and Tuned Liquid Column Damper (TLCD) impart indirect damping to the system and thus improve structural performance[15]. A tuned liquid damper absorbs structural energy by means of viscous actions of the fluid and wave breaking.

Tuned liquid column dampers (TLCDs) are a special type of tuned liquid damper (TLD) that rely on the motion of the liquid column in a U-shaped tube to counter act the action of external forces acting on the structure. The inherent damping is introduced in the oscillating liquid column through an orifice.

The performance of a single-degree-of-freedom structure with a TLD subjected to sinusoidal excitations was investigated by Sun, along with its application to the suppression of wind induced vibration by Wakahara[5]

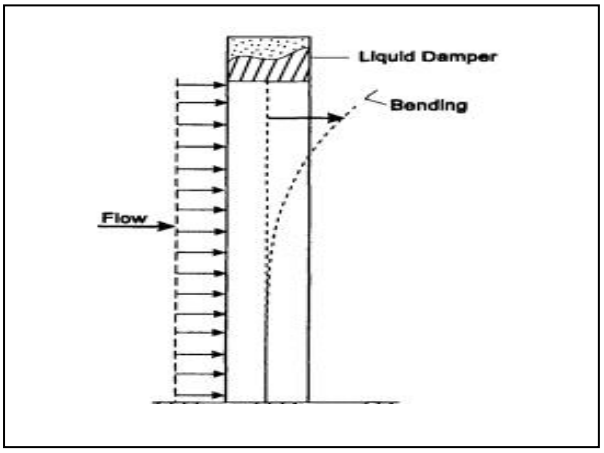

Fig. 3: Tuned Liquid Dampers for Structural Applications: Immiscible Fluids Damper[13]

C. Impact Dampers

An Impact Vibration Absorber (IVA), which is also referred to as an impact damper, consists of a free mass moving between the motion limiting stops of a primary system. When the amplitude of vibration of the primary system exceeds the gap between the stops, the absorber mass collides with the stop. Under sufficient excitation, the IVA undergoes cyclic motion, colliding intermittently with the stops. By this mechanism, the IVA reduces the vibration of the primary system through momentum transfer by collision and dissipation of kinetic energy as acoustic and heat energy[16].

III. PASSIVE DAMPING DEVICES WITH DIRECT ENERGY DISSIPATION

Passive systems also help to increase the level of damping in a structure through a direct energy dissipation mechanism. Various passive systems with Viscoelastic Dampers, Friction Dampers, Viscous Fluid Dampers, Metallic Dampers.

A. Viscoelastic Dampers

Viscoelastic materials used in structural application dissipate energy when subjected to shear deformation. Viscoelastic dampers, made of bonded viscoelastic layers (acrylic polymers), have been developed by 3M company and used in wind vibration control applications[17]. Its application to civil engineering structures appears to have begun in 1969 when 10,000 viscoelastic dampers were installed in each of the twin towers of the World Trade Center in New York to help resist wind loads[18][19][20]. Further studies on the dynamic response of viscoelastic dampers have been carried out, and the results show that they can also be effectively used in reducing structural response due to large range of intensity levels of earthquake.

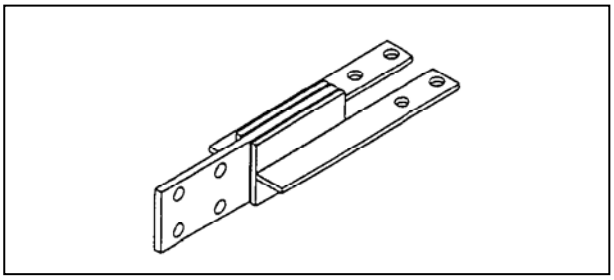

Fig. 4 : Viscoelastic Damper[17]

Viscoelastic materials used in structural application are typically copolymers or glassy substances which dissipate energy when subjected to shear deformation. A typical viscoelastic (VE) damper is shown in fig.4 which consists of viscoelastic layers bonded with steel plates. When mounted in a structure, shear deformation and hence energy dissipation takes place when the structural vibration induces relative motion between the outer steel flanges and the center plate[10].

B. Friction Dampers

The dampers that utilize the mechanism of solid friction to provide the desired energy dissipation are called as friction dampers. Process of the friction that develops between two solid bodies sliding relative to one another is prevalent in nature and have also been employed in many engineered systems[10]. Friction provides another excellent mechanism for energy dissipation, and has been used for many years in automotive brakes to dissipate kinetic energy of motion. In the development of friction dampers, it is important to minimize stick-slip phenomena to avoid introducing high frequency excitation. Furthermore, compatible materials must be employed to maintain a consistent coefficient of friction over the intended life of the device[5]. The Pall device is one of the damper elements utilizing the friction principle, which can be installed in a structure in an X-braced frame as illustrated in the Fig. 5.

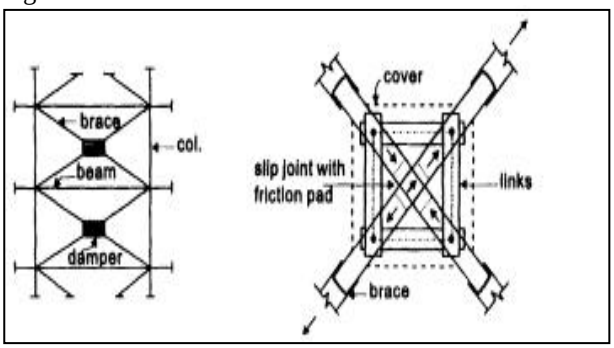

Fig. 5 : X-braced Friction Damper[21]

Several different types of friction dampers are such as Limited Slip Bolted (LSB) joint originated by Pall[22], Sumitomo Friction Damper[23], Energy Dissipating Restraint[24], Slotted Bolted Connection[25].

C. Viscous Fluid Dampers

All the dampers such as viscoelastic, friction and metallic all utilize the action of solids to enhance the performance of structures subjected to transient environmental disturbances. Fluids can also be effectively employed in order to achieve the desired level of passive control[10]. Viscous fluid dampers, are widely used in aerospace and military applications, and have recently been adapted for structural applications[26]. Characteristics of these devices which are of primary interest in structural applications, are the linear viscous response achieved over a broad frequency range, insensitivity to temperature, and compactness in comparison to stroke and output force. The viscous nature of the device is obtained through the use of specially configured orifices, and is responsible for generating damper forces that are out of phase with displacement. A viscous fluid damper generally consists of a piston in the damper housing filled with a compound of silicone or oil[27]. A typical damper of this type is shown in Fig. 6.

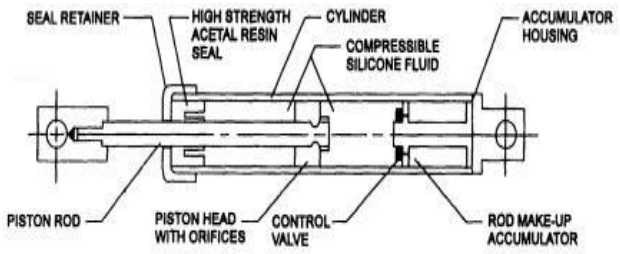

Fig. 6 : Taylor Devices Fluid Damper[26]

By incorporating fluid viscous dampers to control wind induced vibrations, structures may be built with reduced lateral stiffness, as the fluid dampers alone reduce the wind deflection by a factor of 2 to 3, which greatly improves occupant comfort without creating localized stiff sections[28].

D. Metallic Dampers

One of the most effective mechanisms available for the dissipation of energy, input to a structure during an earthquake, is through the inelastic deformation of metallic substances. In traditional steel structures, aseismic design relies upon the post-yield ductility of structural members to provide the required dissipation. However, the idea of utilizing separate metallic hysteretic dampers within a structure to absorb a large portion of the seismic energy began with the conceptual and experimental work by Kelly[29] and Skinner[30]. Many of these devices use mild steel plates with triangular or hourglass shapes so that yielding is spread almost uniformly throughout the material. A typical X-shaped plate damper or added damping and stiffness (ADAS) device is shown in Fig. 7.

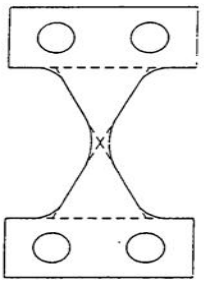

Fig. 7 : (ADAS) Device[31]

IV. CONCLUSION

In order to reduce dynamic response of tall structure or buildings, we have to develop the techniques to control the structural vibrations produced by earthquake or wind by various means such as modifying rigidities, masses, damping, or shape, and by providing passive or active counter forces A discussion of various passive control systems used to mitigate structure motion was presented. Device that have most commonly been used for seismic protection of structures include viscous fluid dampers, viscoelastic solid dampers, friction dampers, and metallic dampers. Other devices that could be classified as passive energy dissipation devices (or, more generally, passive control devices) include tuned mass and tuned liquid dampers, both of which are primarily applicable to wind vibration control.

REFERENCES

[1] M. D. Symans, , M. C. Constantinou, D. P. Taylor and K. D. Garnjost, "Semi-Active Fluid Viscous Dampers For Seismic Response Control"

[2] Housner, G.W., Bergman, L.A., Caughey, T.K., Chassiakos, A.G., Claus, R.O., Masri, S.F., Skeleton, R.E., Soong, T.T., Spencer, B.F. and Yao, J.T.P. 1997, "Structural Control : past, present and future", J. Eng. Mech., 123(9)

[3] Kijewski, T., Kareem, A. and Tamura, Y. (1998), "Overview of the methods to mitigate the response of wind-sensitive structures," Proceedings of Structural Engineers World Congress, San Francisco, July.

[4] Kareem, A. (1983), "Mitigation of wind induced motion of tall buildings," J. Wind. Eng. and Ind. 11(1-3), 273-284.

[5] Rashmi Mishra (2011), National Institute of Technology, Rourkela, " Application of Tuned Mass Damper for vibration control of frame structure under seismic excitations".

[6] Kareem, A., Kijewski, T. and Tamura, Y. (1999), "Mitigation of motions of tall buildings with specific examples of recent applications," Wind and Structure, Vol. 2, No. 3, 201-251.

[7] Kareem, A. and Kline, S. (1995), "Performance of multiple mass dampers under random loading," Structural Engineering, 121(2), 348-361.

[8] Frahm, H. (1909), Device for Damped Vibrations of Bodies, U.S. Patent No. 989958, Oct. 30, 1909.

[9] Den Hartog, J. P. (1956), Mechanical Vibrations, 4th Edition, McGraw-Hill, NY.

[10] T. T. Soong, G. F. Dargush, "Passive Energy Dissipation Systems in Structural Engineering" , State University of New York at Buffalo, USA, John Wiley & Sons.

[11] Tamura Y., Fujii K., Ohtuski T., Wakahara T., Kohsaka R. (1995), "Effectiveness of tuned liquid dampers under wind excitation", Engineering Structures, Vol. 17, No. 9, 609-621.

[12] Bauer, H.F. (1984), Oscillations of Immiscible Liquids in a Rectangular Container: A New Damper for Excited structures, Journal of Sound and Vibration, 93(1), 117-133.

[13] Bauer, H.F. (1984), New Proposed Dynamic Vibration Absorbers for Excited Structure, Vibration Damping Workshop Proceedings, Lynn Rogers (ed.) DD1-DD27.

[14] Modi, V. J. and Welt, F. (1987), Vibration Control Using Nutation Dampers, International Conference on Flow Induced Vibrations , R.King (ed.), BHRA, London, 369-376.

[15] Kareem, A. (1994), "The next generation of tuned liquid dampers" , Proceedings of the First World Conference on Structural Control, Los Angeles.

[16] Ihsan Cem Desen (2000), B.S.M.E, Texas Tech University, "Experimental Study Onan Impact Vibration Absorber" (Master Thesis).

[17] T.T. Soong and M.C. Constantinou (1994), "Passive And Active Structural Vibration Control In Civil Engineering" , State University Of New York At Buffalo Buffalo, NY.

[18] Mahmoodi, P. (1969), Structural Dampers, ASCE J. of the Structural Division, 95(8), 1661-1672

[19] Mahmoodi, P., Robertson, L. E., Yontar, M., Moy, C. and Feld, I. (1987), Performance of Viscoelastic Dampers in World Trade Center Towers, Dynamic of Structures Congress '87, Orlando, FL.

[20] Caldwell, D. B. (1986), Viscoelastic Damping Devices Proving Effective in Tall Buildings, AISC Engineering Journal, 23(4), 148-150.

[21] Pall, A. S. and Marsh, C. (1982), Response of Friction Damped Braced Frames, J. Struct. Div.,ASCE,108(ST6), 1313-1323.

[22] Pall, A. S., Marsh, C. and Fazio, P. (1980), Friction Joints for Seismic Control of Large Panel Structures, J. Prestressed Concrete Inst., 25(6), 38-61

[23] Aiken, I.D. and Kelly, J. M. (1990), Earthquake Simulator Testing and Analytical Studies of Two Energy Absorbing Systems for Multistory Structures, Report No. UCB/EERC- 90/03, University of California, Berkeley, CA.

[24] Nims, D. K., Richter, P. J. and Bachman, R. E. (1993), The Use of the Energy Dissipating Restraint for Seismic Hazard Mitigation, Earthquake Spectra, 9(3), 467-489.

[25] FitzGerald, T. F., Anagnos, T., Goodson, M., and Zsutty, T. (1989), Slotted Bolted Connections in Aseismic Design for Concentrically Braced Connections, Earthquake Spectra, 5(2), 383-391.

[26] Constantinou, M. C., Symans, M.D., Tsopelas, P. and Taylor, D. P. (1993), Fluid Viscous Dampers in Applications of Seismic Energy Dissipation and Seismic Isolation, Proc. ATC 17-1 on Seismic Isolation, Energy Dissipation and Active Control, 2, 581-591.

[27] Makris, N. and Constantinou, M. C. (1990), Viscous Dampers: Testing, Modeling and Application in Vibration and Seismic Isolation, Technical Report NCEER-90-0028, National Center for Earthquake Engineering Research, Buffalo, NY.

[28] Taylor, D. P. and Constantinou, M. C. (1996), Fluid Dampers for Applications of Seismic Energy Dissipation and Seismic Isolation, Proceedings of the Eleventh World Conference on Earthquake Engineering, Acapulco, Mexico.

[29] Kelly, J. M., Skinner, R. I. and Heine, A. J. (1972), Mechanisms of Energy Absorption in Special Devices for Use in Earthquake Resistant Structures, Bull. N.Z. Soc. Earthquake Engineering, 5(3), 63-88.

[30] Skinner, R. I., Kelly, J. M. and Heine, A. J. (1975), Hysteresis Dampers for Earthquake-Resistant Structures, Earthquake Engineering and Structural Dynamics, 3, 287-296.

[31] Whittaker, A.S., Bertero,V.V., Alonso, J.L., and Thompson, C.L. (1989), "Earthquake simulator testing of steel plate added damping and stiffness elements" , Report No. UCB/EERC- 89/02. University of California, Berkeley.

◈◈◈

Trouble Shooting in Vertical Fire Hydrant Pump by Vibration Analysis - A Case Study

V. G. Arajpure & H. G. Patil

Department of Mechanical Engineering, BDCOE Sewagram, Wardha, Maharashtra – 442001, India
E-mail : vgarajpure07@rediffmail.com, hgpatil4285@gmail.com

Abstract – The vertically mounted fire fighting pump used in pump house generally subjected to mechanical, structural and hydraulic problems. This generates dynamic load and produces vibrations of high frequencies and stresses which affects the pump performance and increases the maintenance cost. These problems leading to failure and damage of the costly components of pump houses. In this regard vibration analysis is necessary, to detect and diagnose faults of the fire fighting pumping house, to avoid any failure and efficient operation of pump system.

This paper presents, the vibration analysis of different components of pump by actual measurement and performance testing at test rig. The vibrations are measured at no load as well as at full load condition. The defects in different components are identified and balanced. The balancing of the unbalanced motor fan enhances dynamic performance greatly due to decreased vibrations. The two different case studies of old as well as new pump are discussed here. The study becomes the benchmark for erection, commissioning and provides guidelines for fault diagnose of fire fighting pumps.

Keywords – *Dynamic balancing, vibration analysis, fault diagnosis, Vertical fire fighting pump.*

I. INTRODUCTION

In the high speed Vertical fire fighting pumping house the most common problems are due to wrong installation and operation, resulting in increasing the vibration problems. This has increased the necessity of doing vibration analysis of pump to detect faults early. There are many causes of vibration in the Vertical fire fighting pumping house which include mechanical, structural and hydraulic causes etc. These reduce the performance of pump and decrease the operating life. Flow induced vibration in pumping system is mainly dependent on operating conditions, inlet distortion, cavitations, surge etc. In cases of such flow induced vibration in pumps, periodic vibration monitoring is widely recognized as a reliable method of dynamically determining the health of pump. Analysis on the overall vibration levels and associated vibration frequency spectra can result into early detection and isolation of common pump problems. The early detection allows corrective actions to be scheduled in the suitable time resulting in increased pump productivity economically and efficiently **[7].**

II. METHODOLOGIES:

The objective of the analysis is to determine the sources of high vibration. Knowing dynamic characteristics of the pumping system is the primary step to solve any structural weakness leading to resonance problems. Each faulty element has its exciting frequencies to the pump system. It is very important to identify all the exciting frequencies for the motor fan, thrust bearing, coupling etc. in the beginning before doing vibration analysis in addition to modal analysis to easily relate each exciting frequency and high vibration level to its source**[7].**

Vibration in Vertical fire fighting pump may be the results of several phenomena and may affect various pump parts. Most vibration failures are caused by dynamic overloads; wear, bearing damages, shaft coupling misaligned etc. and performance loss occurs due to internal trans bearing clearance rubs. Vibration measurements and dynamic balancing were done for the different components of the pump by measuring overall vibration levels and vibration echo. Overall vibration levels indicate severity of vibration and are compared

with ISO 10816-1. Also, vibration echo is the relation of vibration amplitude with frequency and is measured to determine the excitation frequencies and the source of high vibration. According to ISO 10816-1, class III was used as a guide limit for the pump. The good vibration limit is up to 1.80mm/s rms vibration velocity, acceptable limit is up to 4.50mm/s, just tolerable limit is up to 11.2 mm/s. Vibration readings were recorded along the different parts of the pump system axially, horizontally and vertically **[7].**

1. Pump Vibration Analysis:

Vertical fire fighting pump can exhibit high vibration levels than other mounted pumps. These pumps often operate with unstable operation conditions, misalignments and vibration condition that cause immediate stops in the pump. There are many problems affecting dynamic performance of pumps. These problems include misalignment of shaft, unbalance of motor, bearing, pump flow, discharge pipe in tension, piping support, coupling misalignment and civil structural fracture. These problems generate vibration of high levels which may damage the pump components. The most common problem that can be found in any Vertical fire fighting pump is unbalance and misalignment **[7].**

2. Case Study:

Six different case studies are tested in the field and machinery workshop representing the problems leading to vibration in pump. A new Vertical fire fighting pump, showed high vibration and noise in the pump operation, was measured with and without load.

III. VIBRATION PROBLEMS OF DEFECTIVE VERTICAL FIRE FIGHTING PUMP:-

Vibration measurements were done on a vertical mounted fire fighting hydrant pump in the field at fire fighting pump house. The pump house was in the.

Fig. 1 : Measurement locations for vibration of fire hydrant pump.

commissioning stage where high level of vibration and noise was observed. Measurements were done on fire hydrant pump at no load condition where the motor was disconnected completely from the pump via the coupling and at full load condition. For no load condition, vibration data was taken on 9 locations on the motor, pump, thrust bearing and foundation axially, horizontally and vertically as shown Figure1

Overall vibration measurements were done on the fire hydrant pump during the normal operating conditions and it was observed that vibration level was not permissible on some locations at pump. The motor was disconnected from the pump system. After the motor was operated at this condition and vibration level was measured. The vibration source was observed from the motor itself, whether connected to a load or not. Vibration levels at no load condition are maximum at motor non drive end in the horizontal direction on both sides of motor at locations **[7].** Maximum vibration for no load condition occurs at vertical direction is of 15.4 mm/sec. However, maximum vibration level measured horizontal for fire hydrant pump is of 19.3 mm/sec.

Overall vibration levels measured at full load condition are larger than that no load condition at the corresponding locations. However, maximum vibration level measured at vertical direction is of 53 mm/sec and horizontal direction is of 50 mm/sec. Moreover, full load condition observed high vibration level from the pump itself. Frequency analyses were done on the fire hydrant pump at no load and full load conditions to define the causes of high level of vibration. In the overall vibration measured, the maximum vibration levels were found on the motor non drive end and on the pump itself.

3.1 DEVIATION CHECKING OF A FIRE HYDRANT PUMP PARTS:-

Inspection Report of Fire Hydrant Pump -

Deviations found in discharge head stool, motor stool, line shafts, thrust bearing housing, gun metal bush housing and pump coupling are replace it.

1) Discharge head Stool – With reference to the Motor Stool radial location, radial location of impeller housing shows 0.8 mm deviation and also surface variation of top surface shows 0.14 mm.

2) Motor Stool –With reference to the discharge stool radial location counter, motor radial location counter shows 0.45mm deviation.

3) Line Shafts - Shaft number one- 0.15 mm max deviation, Shaft number two-0.2 mm max deviation and Shaft number three-0.06 mm max deviation.

4) Thrust bearing housing - With reference to Housing locations step outer diameter and face Thrust Bearing radial location shows 0.32 deviation and Ratchet flange seating surfaces shows 0.18 mm of face run out.

5) Gun Metal Bush Housing – Bore location faces show 0.15 mm variation and location step in radial direction shows 0.2mm deviation.

6) Pump Coupling - With reference to outer diameter bore shows 0.18 deviations and PCD Variation shows 0.3 mm.

The manufacturing defects in the various components of fire hydrant pump that create enormous vibration are identified during commissioning and operation of pump in fire pumping house and have been discussed in Table 1 as follows.

PART NAME	PART PHOTO	OBSERVATION
1.Discharge head stool		• Radial deviation at bottom side is 0.8 mm. • The variation at top surface is 0.14 mm.
2.Motor stool		• Radial deviation at motor seating area is 0.45 mm. • Radial Joviality at discharge top seating area is 0.40 mm.
3.Line shaft		• Top shaft radial run out of 0.15mm. • Line shaft radial run out of 0.20 mm. • Bottom shaft radial run out of 0.06mm.
4.Thrust bearing Housing		• Thrust bearing radial deviation is 0.32 mm. • Thrust bearing housing radial deviation is 0.11 mm. • Thrust bearing housing axial deviation is 0.18mm.
5.Gun metal bush Housing		• Bore location face deviation is 0.15mm. • Bore location step radial deviation is 0.2mm.
6.Pump coupling		• Outer diameter bore deviation is 0.18 mm. • PCD deviation is 0.3mm.

Table 1 Pump Component Deviations

3.2. VIBRATION PROBLEM OF A NEW FIRE HYDRANT PUMP:-

Replacement of old fire hydrant pump part was done due to deviation that created a very high vibration in pump and foundation. After replacements of parts the pump was started and reassembly of long coupled fire hydrant pump was done again and very high vibration level and noise observed at motor non drive end and motor coupling. Measurements were done on fire hydrant pump at no load condition, vibration measurements were done on 8 locations on the motor and motor stool. For full load condition, vibration data were recorded on 18 locations on the motor, pump, thrust bearing and foundation in the axial and radial direction. Connecting the motor to the fire hydrant pump has little effect on vibration level measured on the motor. So, the vibration source was from the motor itself

whether connecting to a load or not. Maximum vibration for no load condition occurs at vertical direction is of 26.8mm/sec. However, maximum vibration level measured horizontal for fire hydrant pump is of 40.1 mm/sec.

3.2 UNBALANCE PROBLEM OF NEW FIRE HYDRANT PUMP:-

Summary of the results show that there was a problem of unbalanced motor at non drive end and motor coupling. Dynamic balancing analysis was done in the axial and radial direction to determine exciting frequencies and evaluate sources of high vibration. This situation indicated server unbalance problem for the motor fan and motor coupling, simulated by adding different weights in different planes by using trial error method.

The reading which were noted during measuring vibration have been tabulated in the Table-2 and plotted in Figure2(a)and(b),as given below

Vibration in fire hydrant pump	Balancing weight in fire hydrant pump	
Velocity in mm/sec	Weight added in Motor fan	Weight added in Motor coupling
40.1 mm/sec	85.64 gm	------
26.8 mm/sec	81.3 gm	------
7 mm/sec	24.51 gm	112 gm
5.1 mm/sec	16.24 gm	119.5 gm

Table 2 Pump Component Deviations

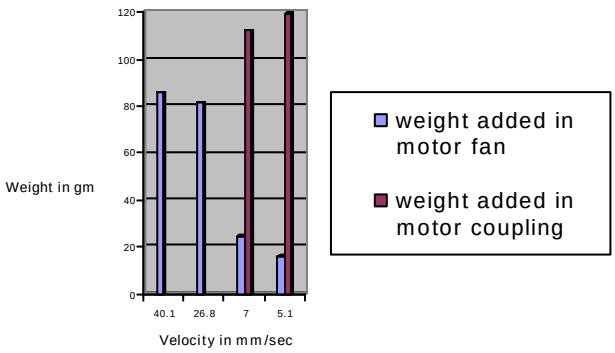

Fig. 2(a) : Balancing of Pump

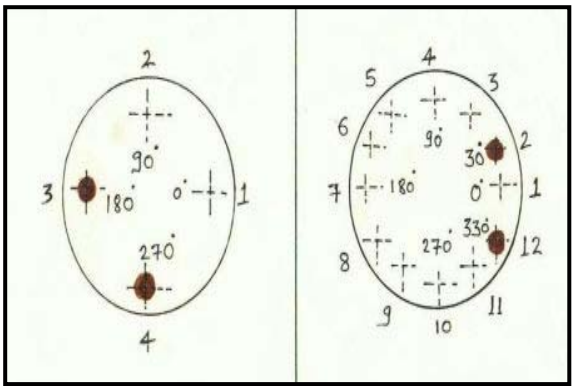

Fig. 2(b) : Balancing weight added in motor coupling and motor fan.

Balancing was done to the motor fan- motor coupling and vibration level was measured and analyzed. Vibration amplitude had decreased greatly vertically to 5.1mm/sec and horizontally to 5.4mm/sec and axially to 1.7 mm/sec. All reading were in allowable zone according to the ISO 10816-1 class III and dynamic performance enhanced greatly as vibration level decreased.

IV. RESULT AND DISSCUSSION-

Replacement of old fire hydrant pump part was done due to deviation that created a very high vibration in pump and foundation. After replacements of parts the pump was started and reassembly of long coupled fire hydrant pump was done again and very high vibration level and noise observed at motor non drive end and motor coupling. It was observed that unbalanced problem was in motor itself. The same was simulated by adding different weights in different planes, by using trial error method. Results of vibration levels then measured at normal condition were well within allowable limit in the order of 5.1 mm/sec.

V. CONCLUSION:

Vibration level generated from fire hydrant pump is high, dangerous and not in permissible limit according to the standards ISO 10186-1 class III. Maximum vibration level measured at no load is of 50 mm/sec at the motor non drive end. However, maximum vibration level that increases at full load is of 53 mm/sec at the motor non drive end. Pump loading creates other sources of high vibration of 12.0 mm/sec due to misalignment and thrust bearing housing problems. Unbalance problem of a fire hydrant pump produces high vibration of 40.1 mm/sec; however, balancing of the unbalanced motor fan enhances dynamic balancing performance greatly as vibration level decreases at 5.1 mm/sec.

Vibration analysis should be done regularly to bring the pumps to a good condition capable of performing their duty in safe operation and minimum maintenance costs. Special care should be taken to monitor operational health of vertical fire hydrant pump. Assembly and disassembly for heavy vertical pumps should be done precisely.

REFERENCES:

[1] Walter, T., Marchonie, M., and Shugars, H., “Diagnosis Vibration Problems in Vertical Mounted Pumps,” Transactions of the ASME, Vol. 110, PP. 172-177, April, 1988.

[2] Hancock, W., “How to Control Pump Vibration”, Hydrocarbon Processing, pp. 107-113, 1974.

[3] Nasser, M. A., “Mechanical Vibration problem and solutions in Large scale Pumping station”, Engineering Research Journal, Vol. 50, University of Helwan, Faculty Of Eng. Tech., Mataria, Cairo, Nov., 1996.

[4] Smith, R., and Woodward, G., “Vibration Analysis of Vertical Pumps”, Sound and Vibration, Vol. 22, No.6, pp. 24-30, 1988.

[5] ISO 10816-1, 1995, “Mechanical Vibration-Evaluation of Machine Vibration By Measurements on Non-Rotating Parts”, part 1, General Guidelines.

[6] Awasthi, J., “Vibration Problem Of Large Capacity Pumps- A Case Study”, Journal of Indian Water Works Association, Vol.19, pp. 287-294, 1987.

[7] Abdel-Rahman, S. M. and Sami A. A. EI-Shaikh., “Diagnosis Vibration Problems Of Pumping Stations : Case Studies”, Thirteenth International Water Technology Conference, IWTC 13, 2009, Hurghada, Egypt.

[8] Lees, A. W., “Fault Diagnosis in Rotating Machinery”, 18 th International Modal Analysis Conf.(IMAC), San Antonio, Texas, pp, 313-319, Feb 2000.

[9] Abdel- Rahman, S. M., and Hela, M. A., “Measurements and Analysis of Mechanical Vibration of Awlad Tuke No-2 Pumping Station, Tech. Report, Mech & Elect. Research Institute, National Water Research Center, Delta Barrage Egypt, 1997.

◈◈◈

LEFM Analysis of Edged Crack Plate by Analytical and FEA Approach

Swapnil Marwadi[1], Dattatray Jadhav[2] & Nikhil Patil[3]

[1&2]Department of Mechanical Engineering, Sardar Patel College of Engineering, Mumbai,
[3]R&D Centre, Larsen & Toubro, Mumbai
E-mail : [1]swapnilmech777@gmail.com, [2]d_jadhav@spce.ac.in, [3]nikhil_patil@lntenc.com

Abstract – This paper describes results obtained by analyzing cracked plates by means of FEA based on the procedures of ANSYS 13. The numerical results are compared with their analytical solution. Same problem is considered half crack symmetric model (2d) and half crack symmetric model (3d) are considered and analysed analytically and with FEA approach. Stress intensity factor (SIF) and J-integral is calculated both analytically and by FEA software. The results obtained from both approaches have been compared and are in agreement with more than 99% accuracy.

Keywords – *FEA, ANSYS, CINT, Linear elastic fracture mechanics (LEFM), Stress Intensity Factor (SIF), J-Integral*

I. INTRODUCTION

Linear Elastic Fracture Mechanics (LEFM) assumes that the material is elastic and plastic zone around the crack tip is very small compared to crack length, the influence of plastic zone in elastic analysis may be neglected. [2]The modelling of linear elastic fracture mechanics problem requires singular elements at the crack tip. The use of FEA for solving tasks in the field of LEFM is the development of "quarter-point" (¼) of the final element by Henshell, Shaw and Barsoum [1]. They proved that the correct fields of displacements, stresses and deformations at the crack tip could be numerically modelled (for linear environment) by moving the node (position ½) to the crack tip (position ¼) and introduces singularities (infinite stresses at crack tip) in the stress field [1]. The determination of linear elastic fracture mechanics parameters – Stress Intensity Factors (SIF) [1] and J-integral plays an important role in fracture analysis. The brittle failure state of structures could be estimated by comparing these parameters with their particular critical values [1]. In order to compare the results from ANSYS a simple geometry is chosen because of the availability of its analytical solution in literature [1].

II. ANALYTICAL PART

A. The Model Specimen Geometry (Fig. 1): Plate with edge crack with crack length, a=10mm length. The plate dimensions are:
H = 75mm, W = 50mm

B. Crack: A crack is placed perpendicularly to the loading direction in the centre of the plate. The edged crack tension plate is assumed to be in the plane strain condition in the present analysis.

C. Material Model: Linear elastic isotropic with modulus of elasticity (E) = 2×10^5 N/mm^2 and Poisson ratio (ν) = 0.3.

D. Boundary conditions: The elastic plate is subjected to a uniform tensile stress in the longitudinal direction as much as σ= 40 N/mm^2.

The calculation procedure presented below is an analytical solution for centre cracked plates under tension (Fig. 1). According to Murakami, Y [3] SIF (K_I) is defined as:

$$K_I = f(\alpha) \times \sigma \times \sqrt{\pi \times a}$$

Where, f (α) is a function of geometry of the plate. Given by,

$$f(\alpha) = 1.12 - 0.23\alpha + 10.55\alpha^2 - 21.72\alpha^3 + 30.39\alpha^4$$

$$\alpha = (a/w)[2]$$

Also,J-integral is defined as,

$$J = \frac{{K_I}^2 \times (1 - \nu^2)}{E}$$

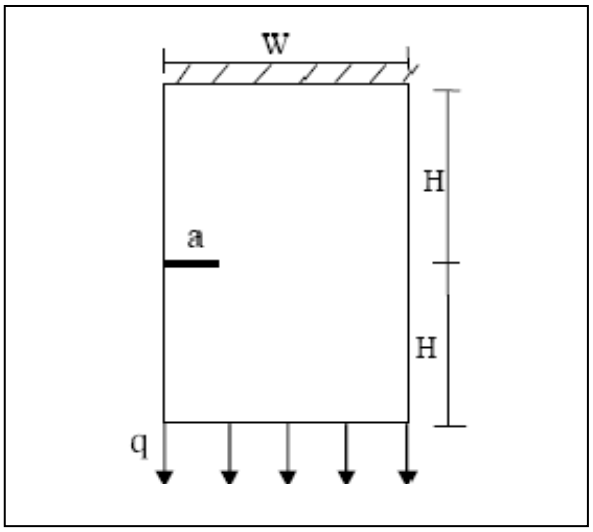

Fig. 1 : A schematic showing plate parameters used for analytical solution.

For numerical solution a, PLANE183 a higher order 2-D, 8-node is used. This element is defined by 8 nodes having two degrees of freedom at each node: translations in the nodal x and y directions. The element may be used as a plane element (plane stress, plane strain and generalized plane strain) or as an axisymmetric element. It has nodes at the corners and also at the midpoint on its each side [1].

Another similar element (Fig. 2) has midpoints which are moved one- node - placed at the crack tip position. Such a ¼ point element is also called "a singular element" [1]. The elements designed for numerical computation of SIF in two-dimensional space are elements: a quadrilateral 8 node point element (Fig 2) and a collapsed ¼ point element (Fig 3).

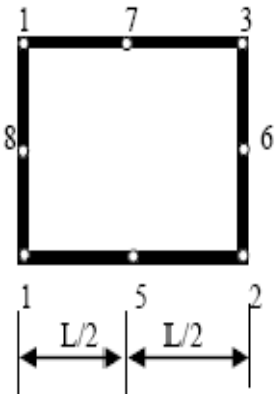

Fig 2: A conception of a quadrilateral 8 node element in the two-dimensional space [1].

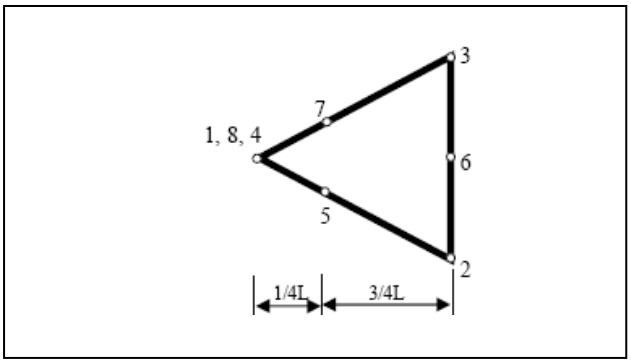

Fig. 3: A conception of a collapsed (triangular) ¼ point (singular) element in the two-dimensional space [1].

Displacement, stress and strain fields are modelled by moving of the mid-side node of the element to the position of ¼ nearer to the crack tip – as it is shown on Fig. 3 (points 5 and 7).

Around the node at the crack tip, a circular area is created and it is divided into a designated number of triangular singular elements by an option of concentrated key points in ANSYS. These are precisely the elements which can interpolate the stress distribution in the vicinity of the crack tip. [1] They introduce $1/\sqrt{r}$ singularity where r is the distance from the crack tip ($r/a \ll 1$) [1]. These elements are implemented for FEA calculations of the SIF – K_I and J-integral.

III. NUMERICAL SIMULATION

The computation of SIF is performed using ANSYS software. The general steps are:

1. Inputs are material, geometry, the boundary and loading conditions for FEA analysis of the plate.
2. The crack parameters are crack points, the length of the crack, the crack position and the sides of the crack are input data.
3. Assigning a concentrated key point at crack tip using KSCON command.
4. Meshing the structures. The local FE mesh is refined at the crack tip.
5. Using operators KCALC for linear problems to obtain SIF [1].
6. Using CINT command for computing J-integral.

J-Integral Calculation with CINT command requires following steps:

Step 1: Initiate a New J-Integral Calculation

Step 2: Define Crack Information

Step 3: Specify the Number of Contours to Calculate

Step 4: Define a Crack Symmetry Condition

Step 5: Specify Output Controls.

CINT macro:

CINT, NEW, <CRACK ID>

CINT, CTNC, <CRACKTIP COMPONENT>, < ANY NODE ON OPEN SIDE>

CINT, CENC, <CRACK EXTENSION DIRECTION COMPONENT>, <CRACKTIP NODE>,,, <COORDINATE SYSTEM NUMBER>,,

CINT, TYPE, JINT

CINT, NCON, <NUMBER OF COUNTERS>

CINT, SYMMETICITY, <ON OR OFF>

CINT, NORM, <COORDINATE SYSTEM NUMBER>, <AXIS OF COORDINATE SYSTEM NUMBER>

IV. ANALYTICAL SOLUTION

The data presented above allow us to calculate the values α=(a/w).

α=10/50=0.2.

$$f(\alpha) = 1.12 - 0.23(0.2) + 10.55(0.2)^2 - 21.72(0.2)^3 + 30.39(0.2)^4 = 1.37,$$

$$K_I = 1.37 \times 40 \times \sqrt{\pi \times 10} = 306.15\ N/mm^{\frac{3}{2}}$$

$$J = \frac{{K_I}^2 \times (1 - \nu^2)}{E}$$

$$J = \frac{306.15^2 \times (1 - 0.3^2)}{2 \times 10^5} = 0.429\ N - mm$$

This K_I and J-integral value will be used as reference to the results obtained from FEA method.

V. NUMERICAL SOLUTION WITH ANSYS.

The results from a numerical investigation are compared with the analytical fracture mechanics parameters. They refer to plates with transversal to the loading force cracks.

CASE1: Two dimensional half crack model:

The mesh (Fig.6) is generated according to [4]. To obtain reliable results ¼ finite elements are used. The radius of the first row of elements, generated in the vicinity of the crack tip, is:

r=a/8=10/8=1.25mm.

Where a is the length of the crack. Every one of these elements is positioned at 18° in the circumferential direction. Due to symmetricity half model is considered and symmetric boundary condition is applied. The mesh generated contains contains 10 elements around the crack tip, total 445 elements and 1378 nodes (Fig.6). Due to symmetricity half model is considered and symmetric boundary condition is applied in line.

SIF is calculated by nodal results during post-processing after definition of the path along the crack face.

J-integral is calculated by CINT command during the post processing defining the crack tip node, any node on open side of crack, number of counters and crack plane as mentioned in above CINT macro.

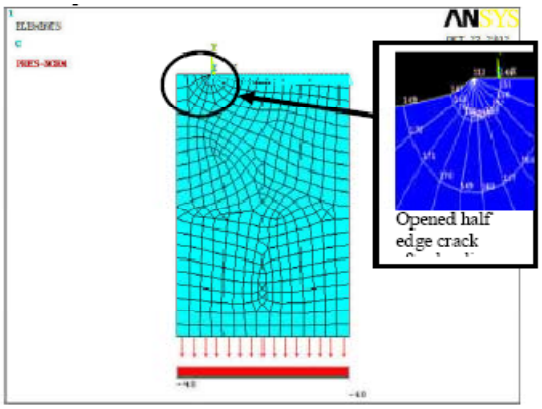

Fig 6 : FEA ANSYS half model with boundary conditions.

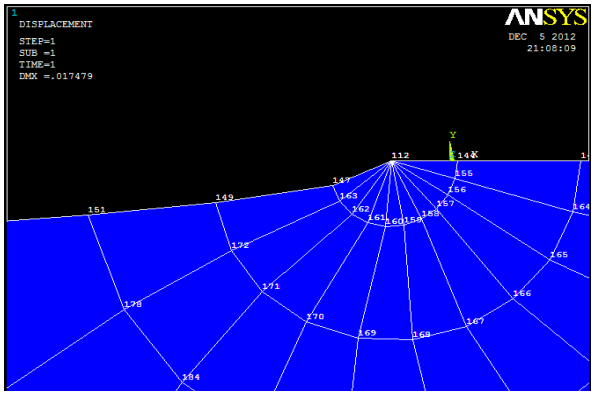

Fig. 7 : FEA ANSYS half model with node numbering for calculation purpose

CINT output:

POST1 J-INTEGRAL RESULT LISTING

Crack ID = 1

Crack Front Node = 112

Contour Values =0.42840 0.42647 0.42754 0.42757 0.42757

KCAL output: 306.67

CASE2: Three dimensional half crack model:

The mesh (Fig.8) is generated according to [4]. To obtain reliable results ¼ finite elements are used. The radius of the first row of elements, generated in the vicinity of the crack tip, is:

r=a/8=10/8=1.25mm.

Where a is the length of the crack. Every one of these elements is positioned at 18° in the circumferential direction. Due to symmetricity half model is considered and symmetric boundary condition is applied. The mesh generated contains contains 30 elements along crack length, total 2665 elements and 11662 nodes (Fig.8). Due to symmetricity three dimensional half model is considered and symmetric boundary condition is applied on symmetric area.

J-integral is calculated by CINT command during the post processing defining the crack tip node, any node on open side of crack, number of counters and crack plane as mentioned in above CINT macro.

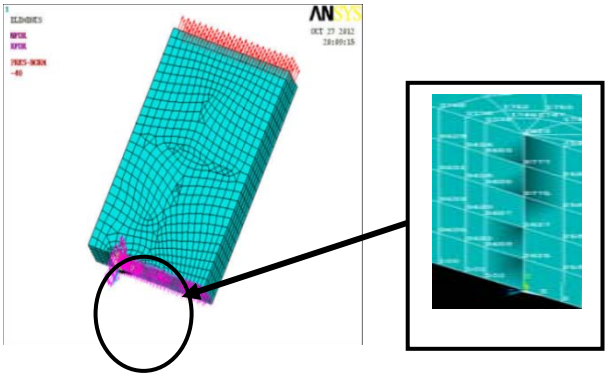

Fig 8 FEA ANSYS 3d half model with boundary conditions.

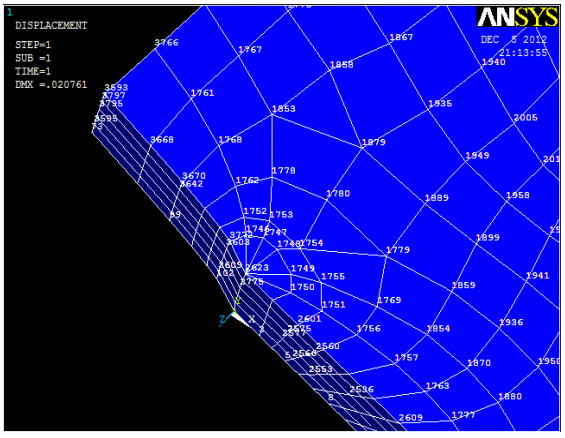

Fig 9: FEA ANSYS 3d half model with node numbering for calculation purpose.

TABLE I.

CINT output: VALUES OF J-INTEGRAL ALONG CRACK FRONT

Crack D = 1					
Crack Front Node	=	1			
Contour Values =	-1.59E02	1.1332	1.1332	1.1332	1.1332
Crack Front Node	=	2624			
Contour Values =	0.15652	0.1565	0.1565	0.1565	0.1565
Crack Front Node	=	2625			
Contour Values =	0.35725	0.5266	0.5266	0.5266	0.5266
Crack Front Node	=	2626			
Contour Values =	0.42932	0.4641	0.4648	0.4647	0.4644
Crack Front Node	=	2627			
Contour Values =	0.47621	0.4746	0.4744	0.4748	0.4747
Crack Front Node	=	3774			
Contour Values =	0.42802	0.4734	0.473	0.4735	0.4734
Crack Front Node	=	3775			
Contour Values =	0.47518	0.4737	0.4735	0.4739	0.4739
Crack Front Node	=	3776			
Contour Values =	0.43016	0.4735	0.4729	0.4734	0.4733
Crack Front Node	=	3777			
Contour Values =	0.46874	0.4673	0.4671	0.4677	0.4676
Crack Front Node	=	3778			
Contour Values =	0.41177	0.4553	0.456	0.4563	0.4561
Crack Front Node	=	2623			
Contour Values =	0.4345	0.4338	0.4339	0.4344	0.4344

Calculation Of SIF:

Here we will consider the values of j-integral along the countours of last node 2623 given by ansys.

J-integral value is 0.433,

Putting $J=0.433$ in below equation,we calculate K_I ,

$$J = \frac{K_I{}^2 \times (1-\nu^2)}{E}$$

$$K_I = 308.48$$

VI. RESULTS AND DISCUSSIONS

TABLE II.

RESULTS COMPARISON TABLE

Parameter	Analytical results	ANSYS	
		2d half	3d half
J-integral (N/mm)	0.429	0.426	0.433
Variation in J (%)		-0.699	0.932
SIF (N/mm$^{3/2}$)	306.150	306.670	308.480
Variation in SIF (%)		0.169	0.755

VII. CONCLUSION

A numerical simulation for cracked plates with two different cases is accomplished by means of ANSYS. The reduction of model to its half symmetry reduces the computation time and requires less storage space on disk. Symmetric boundary conditions are to be applied for half model. The Stress Intensity Factor and J-integral is received for plates with an edge transverse crack and under uniaxial loading. The comparison Table II above between numerical results and analytical solution shows excellent agreement (more than 99% accuracy) for K_I and J-integral. ANSYS gives fictitious results about K_{II} and these results must be neglected. As the plane of loading symmetry coincides with the plane of the geometrical symmetry, then in this plane - tangential stresses are zero.[1]

VIII. ACKNOWLEDGMENT

Authors are thankful to Mechanical Engineering Department, Sardar Patel College of Engineering and L&T Management. Special thanks to Mechanical Engineering Group, Research and Development Centre, L&T Hydrocarbon-IC, Mumbai, for their valuable support.

REFERENCES

[1] Galina Todorova., Valentin Dikov.: Reliability of the FEN calculations of the fracture mechanics parameters, International Conference on Economic Engineering and Manufacturing Systems, Brasov, Vol. 10, no.3(27), November, 2009

[2] Kumar.P, Fracture Mechanics, chap 4, appendix 4B, pg-96-97.

[3] Murakami, Y (1987).Stress Intensity Factors Handbook,Pergamon Press,Oxford.

[4] ***_Documentation for ANSYS-Release 13.0

◈◈◈